

# ON THE SET OF NORMALIZED DILATATIONS OF FULLY-PUNCTURED PSEUDO-ANOSOV MAPS

CHI CHEUK TSANG

ABSTRACT. We improve the bound on the number of tetrahedra in the veering triangulation of a fully-punctured pseudo-Anosov mapping torus in terms of the normalized dilatation. When the mapping torus has only one boundary component, we employ various techniques to improve the bound further. Together with the author's work with Hironaka in the case when the mapping torus has at least two boundary components, this allows us to understand small elements of the set  $\mathcal{D}$  of normalized dilatations of fully-punctured pseudo-Anosov maps using computational means. In particular, we certify that the minimum element of  $\mathcal{D}$  is  $\mu^2$  and the minimum accumulation point of  $\mathcal{D}$  is  $\mu^4$ , where  $\mu = \frac{1+\sqrt{5}}{2} \approx 1.618$  is the golden ratio.

## 1. INTRODUCTION

An orientation preserving surface homeomorphism  $f : S \rightarrow S$  is *pseudo-Anosov* if there exists a transverse pair of singular measured foliations  $\ell^s$  and  $\ell^u$  such that  $f$  contracts the leaves of  $\ell^s$  and expands the leaves of  $\ell^u$  by a factor of  $\lambda(f) > 1$ . The number  $\lambda(f)$  is called the *dilatation* of  $f$ .

In this case,  $\ell^s$  and  $\ell^u$  determine a conformal structure on  $S$ . Contracting and expanding the leaves of the two foliations deforms the conformal structure and determines a geodesic path on the *Teichmüller space* of  $S$  (with the *Teichmüller metric*). In particular,  $f$  determines a closed geodesic of length  $\log \lambda(f)$  on the *moduli space*  $\mathcal{M}(S)$ . Conversely, every closed geodesic on  $\mathcal{M}(S)$  comes from a pseudo-Anosov map on  $S$ . See [Abi80] for details.

This gives a natural motivation for the

**Minimum dilatation problem.** What is the minimum dilatation  $\delta_{g,s}$  among all pseudo-Anosov maps defined on a given surface  $S_{g,s}$  with genus  $g$  and  $s$  punctures?

This problem has been studied since at least [Pen91], but so far it has only been solved for a handful of surfaces with small values of  $g$  and  $s$ . We refer to [LT11b] and [LT11a] for details and references. We remark that between these known values and some upper bounds (see, for example, [Hir10], [AD10], [KT13]), the pattern of these minimum dilatations seem to be very erratic, and it is not even clear what a good set of conjectural values should be.

The situation becomes simpler if instead of asking for the minimum dilatation on specific surfaces, one considers the asymptotics of these minimum dilatations. In particular we have the following well-known conjecture by Hironaka. See also [McM00, P.44 Question].

---

Chi Cheuk Tsang was partially supported by a grant from the Simons Foundation #376200.

**Golden ratio conjecture (Hironaka, [Hir10, Question 1.12]).** The minimum dilatations  $\delta_{g,0}$  on the closed surfaces of genus  $g$  grow as

$$\lim_{g \rightarrow \infty} \delta_{g,0}^g = \mu^2 \approx 2.618.$$

where  $\mu = \frac{1+\sqrt{5}}{2} \approx 1.618$  is the golden ratio.

This simplification is in part due to the fact that pseudo-Anosov maps naturally come in *flow equivalence classes*. Given a pseudo-Anosov map  $f : S \rightarrow S$ , its *mapping torus* is a 3-manifold with a fibration over  $S^1$  and a transverse *suspension flow*. Two pseudo-Anosov maps  $f_1 : S_1 \rightarrow S_1$  and  $f_2 : S_2 \rightarrow S_2$  are *flow equivalent* if their mapping torus is the same 3-manifold  $M$  and their suspension flows are the same.

Thurston [Thu86] showed that for every orientable, irreducible, atoroidal 3-manifold  $M$ , there is a norm  $\|\cdot\|$  defined on  $H_2(M, \partial M)$  with a polyhedral unit ball  $B$ . The elements of a flow equivalence class with mapping tori  $M$  correspond to the rational points on some top-dimensional *fibred face*  $F$  of  $B$ . More precisely, a map  $f : S \rightarrow S$  corresponds to the normalized homology class  $\frac{[S_t]}{|\chi(S)|}$  of the fibers  $S_t$  of the associated fibration.

**Remark 1.1.** Strictly speaking, our exposition is not the most accurate here: The mapping torus  $M$  of a map  $f$  on a punctured surface has no boundary components but is instead non-compact with the set of ends in one-to-one correspondence with the *puncture orbits* of  $f$ . However,  $M$  is clearly the interior of a compact 3-manifold with torus boundary components  $\overline{M}$ . In this paper we will often abuse notation and conflate  $M$  and  $\overline{M}$ .

Meanwhile, Fried [Fri85] showed that the function assigning a map  $f : S \rightarrow S$  to the *normalized dilatation*  $\lambda(f)^{|\chi(S)|}$  extends to a continuous convex function on  $F$  that goes to infinity at  $\partial F$ . In particular, this function attains a minimum  $\lambda_F$  in the interior of  $F$ . A consequence of this is if  $\dim F \geq 1$ , then there will be infinitely many pseudo-Anosov maps with normalized dilatation accumulating from above onto  $\lambda_F$ . Thus the topological invariants  $\lambda_F$  of 3-manifolds gives information about the asymptotics of minimum dilatations.

However, one must take care in unpiecing this information. Specifically, it is a nontrivial task to recover the type of the surface  $S_a$  for which the map corresponding to a point  $a \in F$  is defined on. While it is true that the Euler characteristic of  $S_a$  can be recovered from the Thurston norm, the number of punctures, thus the genus of  $S_a$ , depends on the greatest common divisors between certain coordinates of  $a$ , and these could behave wildly even along nice families of  $a$ . Indeed, the erratic nature of the original minimum dilatation problem can at least in part be credited to these number theoretical intricacies.

One way to eliminate the number theoretical part of the problem and focus on the surface dynamical aspects is to restrict to *fully-punctured* pseudo-Anosov maps. These are pseudo-Anosov maps where all the singularities of the foliations  $\ell^s$  and  $\ell^u$  are at the punctures of the surface  $S$ .

Given any pseudo-Anosov map, one can always puncture the surface at all the singularities to get a fully-punctured map with the same dilatation. On the level of mapping tori, this is equivalent to drilling out the singular orbits of the suspension flow. Consequently, every

flow equivalence class is contained in a fully-punctured flow equivalence class. The hope is that if one understands the fully-punctured flow equivalence classes which give small dilatations, then one can recover information about general flow equivalence classes by Dehn filling the corresponding 3-manifolds and performing an analysis as in [KKT13].

This motivates the

**Fully-punctured normalized dilatation problem.** Let  $\mathcal{D}$  be the set of normalized dilatations of fully-punctured pseudo-Anosov maps. What are the smallest elements of  $\mathcal{D}$  and what are the maps that attain them?

This paper aims to provide some progress on this problem. In particular, we will show that the minimum element of  $\mathcal{D}$  is  $\mu^2$  and the minimum accumulation point of  $\mathcal{D}$  is  $\mu^4$ . See [Theorem 1.6](#) for the full statement of our results.

Our strategy is to combine the results of [HT22] and a new veering triangulation argument, the latter of which comprises the main part of this paper. For the rest of this introduction, we will give some ideas of both of these ingredients, before stating our full results.

As mentioned above, restricting to fully-punctured maps isolates out the dynamical part of the problem. More specifically, one can encode the dynamics of a fully-punctured pseudo-Anosov map  $f$  using the combinatorial tool of *train tracks*. The general idea is to approximate the stable foliation  $\ell^s$  using a train track  $\tau$ . The fact that  $f$  contracts along  $\ell^s$  and expands along  $\ell^u$  translates to the fact that  $f(\tau)$  can be obtained by folding  $\tau$ . One can then compute the dilatation of  $f$  from the *transition matrix* recording how the weights on the branches of  $\tau$  add up to those of  $f(\tau)$ .

In [Ago11], Agol showed that one can choose  $\tau$  above such that there is a canonical periodic splitting sequence from  $f(\tau)$  to  $\tau$ . The dual triangulations of this splitting sequence determines an ideal triangulation of the mapping torus, which we refer to as the *layered veering triangulation* associated to  $f$ .

As the name suggests, there is a definition of *veering triangulations* in general, for which these layered veering triangulations is a subclass of. We will defer this general definition to [Section 2.1](#). Here it suffices to know that these are ideal triangulations satisfying certain combinatorial conditions which impose strong constraints on the local structure. This makes it possible to enumerate veering triangulations up to 16 tetrahedra [GSS] whereas the census for general triangulations is currently only available up to 9 tetrahedra.

In [AT22], by studying the Perron-Frobenius components of the transition matrix associated to the splitting sequence, Agol and the author proved the following theorem.

**Theorem 1.2** ([AT22]). *Let  $f : S \rightarrow S$  be a fully-punctured pseudo-Anosov map with normalized dilatation  $\lambda^{-x} \leq P$ , then the mapping torus of  $f$  admits a veering triangulation with  $\leq \frac{P^3-1}{2} \left( \frac{2 \log P^3}{\log(2P^{-3}+1)} - 1 \right)$  tetrahedra.*

Here we remark that a non-quantitative version of this result was proved by Farb, Leininger, and Margalit [FLM11] earlier. In [Ago11], Agol showed a quantitative version but the proof contained a gap; the work in [AT22] fixes that gap.

Notice that the fully-punctured normalized dilatation problem is theoretically solved by [Theorem 1.2](#): Suppose one is interested in the elements of  $\mathcal{D}$  smaller than some number  $P$ . Then one can look at all veering triangulations with  $\leq \frac{P^3-1}{2} \left( \frac{2 \log P^3}{\log(2P^{-3}+1)} - 1 \right)$  tetrahedra, and for each of them compute the normalized dilatations of the maps associated to the triangulation, using, for example, the machinery developed by McMullen in [[McM00](#)], then read off those maps whose normalized dilatations are less than  $P$ .

However, this strategy using [Theorem 1.2](#) is not actually feasible in practice. For example, if one puts in  $P = \mu^2$ , which we will show is the minimum element of  $\mathcal{D}$ , then one has to look at all veering triangulations with  $\leq 454$  tetrahedra, which is much larger than the census of veering triangulations we can possibly generate currently.

A different idea was explored in [[HT22](#)] by Hironaka and the author. We showed that if  $f : S \rightarrow S$  is a fully-punctured pseudo-Anosov map with at least two puncture orbits, then one can take  $\tau$  to be a *standardly embedded train track*. Then by applying the theory of Perron-Frobenius digraphs, developed by McMullen in [[McM15](#)], on the real edges of  $\tau$ , we showed [Theorem 1.3](#) below. Here we write  $|LT_{a,b}|$  for the largest real root of the *Lanneau-Thiffeault polynomial*  $t^{2b} - t^{b+a} - t^b - t^{b-a} + 1$ .

**Theorem 1.3** ([[HT22](#)]). *Let  $f : S \rightarrow S$  be a fully-punctured pseudo-Anosov map with at least two puncture orbits. Then the normalized dilatation  $\lambda^{-x}$  of  $f$  satisfies the inequality*

$$\lambda^{-x} \geq \begin{cases} \mu^4 \approx 6.854 & \text{if } |\chi(S)| = 2 \\ \left| LT_{1, \frac{|\chi(S)|}{2}} \right|^{|\chi(S)|} > \mu^4 & \text{if } |\chi(S)| \text{ is even and } \geq 4 \\ 8 > \mu^4 & \text{if } |\chi(S)| \text{ is odd} \end{cases}$$

Moreover, for each  $k \geq 1$ , equality for the first two cases is achieved by a fully-punctured pseudo-Anosov map with  $|\chi(S)| = 2k$ .

In particular, if we let  $\mathcal{D}^*$  be the set of normalized dilatations of fully-punctured pseudo-Anosov maps with at least two puncture orbits, then the minimum element of  $\mathcal{D}^*$  is  $\mu^4$ . We remind the reader that the condition of  $f$  having at least two puncture orbits is equivalent to its mapping torus having at least two boundary components.

Now, a mapping torus with at least two torus boundary components must have Betti number at least two. The converse is not true, but is empirically true for ‘sufficiently simple’ maps. From Thurston-Fried fibered face theory, this strongly suggests that the minimum accumulation point of  $\mathcal{D}$  should be  $\mu^4$ . In fact, given [Theorem 1.3](#), the remaining case for showing this is the case when the mapping torus has only one boundary component.

Motivated by this, the author revisited the idea of veering triangulations, in the hopes that one could improve [Theorem 1.2](#) in the one boundary component case. What we were able to come up with is in fact a general argument that drastically improves the bound.

**Theorem 1.4.** *Let  $f : S \rightarrow S$  be a fully-punctured pseudo-Anosov map with normalized dilatation  $\lambda^{-x} \leq P$ . Then the mapping torus of  $f$  admits a veering triangulation with less than or equal to  $\frac{1}{2}P^2$  tetrahedra.*

We outline the idea behind the proof of [Theorem 1.4](#) for the reader who is familiar with veering triangulations. Let  $B$  be the *stable branched surface* of the associated layered veering triangulation, obtained by suspending the periodic splitting sequence. One can lift  $B$  to a branched surface  $\widehat{B}$  in the infinite cyclic cover corresponding to the fibration associated to  $f$ . Notice that  $\widehat{B}$  is a measured branched surface.

Meanwhile, the branch locus of  $B$ , also known as the *dual graph*  $\Gamma$ , is a finite directed graph that is  $(2, 2)$ -valent. In particular, there are many Eulerian circuits of  $\Gamma$ . Each Eulerian circuit can be lifted to a branch path of  $\widehat{B}$ , which can be perturbed (and reversed) into a *descending path*  $\alpha$ . The fact that the circuit is Eulerian means that the difference in weights between the starting and ending sectors of  $\alpha$  can be expressed in terms of the normalized dilatation, while the number of times  $\alpha$  intersects the branch locus of  $\widehat{B}$  can be expressed in terms of the number of tetrahedra.

We define a special type of circuit, called a *hook circuit*, that allows one to bound the former in terms of the latter from below. When worked out precisely, this gives the bound stated in [Theorem 1.4](#). Finally, we demonstrate that in all but one instance of layered veering triangulations, one can pick an Eulerian circuit that is a hook circuit. This last part makes heavy use of the knowledge of the local combinatorics of veering triangulations. We introduce the tool of *A- and B-quads* to translate the combinatorial information back and forth between edge colors of the triangulation and *resolutions* of the dual graph  $\Gamma$ . We refer to [Section 3](#) for details.

Now repeating the strategy with [Theorem 1.4](#) replacing [Theorem 1.2](#), when one puts in  $P = \mu^2$ , one only has to look at all veering triangulations with  $\leq 3$  tetrahedra. However, for the purposes of determining the minimum accumulation point of  $\mathcal{D}$ , one has to put in  $P = \mu^4$ , for which [Theorem 1.4](#) gives  $\leq 23$  tetrahedra. Unfortunately, this is still out of reach of the current veering triangulation census.

But recall that [Theorem 1.3](#) already takes care of the case with at least two boundary components, so if we can sharpen the bound of [Theorem 1.4](#) in the one boundary component case (when  $P = \mu^4$ ) from 23 to 16, then we can still use the current census for our goal of determining the minimum accumulation point of  $\mathcal{D}$ .

The good news is that the estimates used in the argument of [Theorem 1.4](#) are quite loose, so there are many possible sources of improvement. The bad news is that these sources of improvement don't tend to exist at the same time. For example, certain arguments only work when  $B$  has many branch cycles, and others only work when  $B$  has few branch cycles. What we managed at the end is a technical patchwork of ideas, the individual domains in which they work cover all the cases and lowers the 23 to 16. (The curious reader can take a glimpse at [Figure 31](#) for a sense of the patchwork involved here.)

**Theorem 1.5.** *Let  $f : S \rightarrow S$  be a fully-punctured pseudo-Anosov map with normalized dilatation  $\lambda^{-x} \leq 6.86$ . Suppose the mapping torus of  $f$  has only one boundary component, then the mapping torus of  $f$  admits a veering triangulation with less than or equal to 16 tetrahedra.*

We point out that more elegant approaches may exist here. In fact, one of the techniques we use has particular potential. The idea is to essentially locate two hook circuits instead of a single hook circuit. We conjecture that such double hook circuits always exist, which, if true, would improve [Theorem 1.4](#) by roughly a factor of 2, in particular simplifying the proof, as well as improving the statement of [Theorem 1.5](#). See [Section 4](#) for details.

In any case, [Theorem 1.5](#) implies that we can finally complete our goal of determining the minimum accumulation point of  $\mathcal{D}$  by going through the current census [[GSS](#)].

Now, this in itself is still a nontrivial task since there are 51766 layered veering triangulations in the census. To carry out the computation, we wrote up SageMath scripts which integrate the Veering code of Parlak, Schleimer, and Segerman ([[PSS23](#)]), to compute normalized dilatations. We include these scripts in the auxiliary files and provide a brief rundown of the code in [Appendix B](#). Running this code certifies that  $\mu^4$  is indeed the minimum accumulation point of  $\mathcal{D}$ , and furthermore determines the isolated points beneath it.

The full results obtained by this computation is recorded in the theorem below.

**Theorem 1.6.** *The set  $\mathcal{D}$  of normalized dilatations of fully-punctured pseudo-Anosov maps is the union of the isolated points*

$$\begin{aligned} \frac{3+\sqrt{5}}{2} \approx 2.618, \quad \frac{4+\sqrt{12}}{2} \approx 3.732, \quad (\text{Lehmer's number})^9 \approx 4.311, \\ \frac{5+\sqrt{21}}{2} \approx 4.791, \quad |LT_{1,2}|^3 \approx 5.107, \quad \frac{6+\sqrt{32}}{2} \approx 5.828, \end{aligned}$$

and a dense subset of  $[\mu^4, \infty)$ . In particular the minimum element of  $\mathcal{D}$  is  $\mu^2 = \frac{3+\sqrt{5}}{2}$  and the minimum accumulation point of  $\mathcal{D}$  is  $\mu^4 = \frac{7+\sqrt{45}}{2}$ .

Moreover, the fully-punctured pseudo-Anosov maps whose normalized dilatations attain the isolated points are those listed in [Table 1](#). The fully-punctured pseudo-Anosov maps whose normalized dilatations attain the minimum accumulation point are those listed in [Table 2](#).

Here *Lehmer's number* is the largest real root of  $t^{10} + t^9 - t^7 - t^6 - t^5 - t^4 - t^3 + t + 1$ , which is approximately 1.176.

We provide some explanations for the descriptions of maps in [Table 1](#) and [Table 2](#).

As before, we denote by  $S_{g,s}$  the orientable surface with genus  $g$  and  $s$  punctures.

In particular  $S_{1,0}$  is the torus, which can be regarded as  $\mathbb{R}^2/\mathbb{Z}^2$ . Under this description, every element of  $\text{SL}_2\mathbb{Z}$  induces a map on  $S_{1,0}$ . Each of these maps fixes the point  $(0,0)$ . Unless otherwise specified, by the map on  $S_{1,1}$  induced by an element of  $\text{SL}_2\mathbb{Z}$ , we mean the map induced on  $S_{1,0}$  with a puncture at  $(0,0)$ .

Up to a sign, every element of  $\text{SL}_2\mathbb{Z}$  can be uniquely written as a word in  $R = \begin{bmatrix} 1 & 1 \\ 0 & 1 \end{bmatrix}$  and  $L = \begin{bmatrix} 1 & 0 \\ 1 & 1 \end{bmatrix}$ . There is a neat way of understanding the layered veering triangulation associated to the induced map on  $S_{1,1}$  from this factorization. We refer to [[Gué06](#)] for



TABLE 1. The isolated points of  $\mathcal{D}$ , the fully-punctured pseudo-Anosov maps  $f$  that attain them, and the veering triangulations of the corresponding mapping tori.

Normalized dilatation	Pseudo-Anosov maps	Veering triangulations
$\frac{3+\sqrt{5}}{2}$	Map on $S_{1,1}$ induced by $\begin{vmatrix} 2 & 1 \\ 1 & 1 \end{vmatrix} = RL$	cPcbbbiht_12
	Map on $S_{1,1}$ induced by $\begin{vmatrix} -2 & -1 \\ -1 & -1 \end{vmatrix} = -RL$	cPcbbbdxm_10
$\frac{4+\sqrt{12}}{2}$	Map on $S_{1,1}$ induced by $\begin{vmatrix} 3 & 2 \\ 1 & 1 \end{vmatrix} = R^2L$	dLQbccchhf_122
	Map on $S_{1,1}$ induced by $\begin{vmatrix} -3 & -2 \\ -1 & -1 \end{vmatrix} = -R^2L$	dLQbccchhsj_122
(Lehmer's number) <sup>9</sup>	Map on $S_{5,1}$ induced by quotient of geodesic flow on $P(-2, 3, 7)$	dLQaccjsnk_200
$\frac{5+\sqrt{21}}{2}$	Map on $S_{1,1}$ induced by $\begin{vmatrix} 4 & 3 \\ 1 & 1 \end{vmatrix} = R^3L$	eLMkbcdddhhhm1_1221
	Map on $S_{1,1}$ induced by $\begin{vmatrix} -4 & -3 \\ -1 & -1 \end{vmatrix} = -R^3L$	eLMkbcdddhhhd_1221
$ LT_{1,2} ^3$	Map on $S_{2,1}$ lifted from minimum dilatation 5-braid	eLPkaccddjnka_j_2002
	Map on $S_{2,1}$ lifted from minimum dilatation 5-braid	eLPkbcdddhrvcv_1200
$\frac{6+\sqrt{32}}{2}$	Map on $S_{1,1}$ induced by $\begin{vmatrix} 5 & 2 \\ 2 & 1 \end{vmatrix} = R^2L^2$	eLMkbcdddhhqqa_1220
	Map on $S_{1,1}$ induced by $\begin{vmatrix} -5 & -2 \\ -2 & -1 \end{vmatrix} = -R^2L^2$	eLMkbcdddhhqxh_1220
	Map on $S_{1,1}$ induced by $\begin{vmatrix} 5 & 4 \\ 1 & 1 \end{vmatrix} = R^4L$	fLMPcbcdeeehhhhkn_12211
	Map on $S_{1,1}$ induced by $\begin{vmatrix} -5 & -4 \\ -1 & -1 \end{vmatrix} = -R^4L$	fLMPcbcdeeehhhhvc_12211

details. Here we have included this factorization for the maps on  $S_{1,1}$  in hopes that the experts would find it easier to comprehend the examples.

Similarly, we can regard  $S_{0,4}$  as  $(\mathbb{R}^2 \setminus \mathbb{Z}^2) / (\pm(2\mathbb{Z})^2)$ . From this description, every element of  $SL_2\mathbb{Z}$  induces a map on  $S_{0,4}$ , and one can understand the associated veering triangulations from the factorization into words in  $R$  and  $L$ . We again refer to [Gué06] for details.

We now move on to the more sporadic examples. For the map defined on  $S_{5,1}$  in Table 1, recall that the double branched cover of  $S^3$  over the pretzel knot  $P(-2, 3, 7)$  is the unit tangent bundle over the orbifold  $S^2(2, 3, 7)$ . The deck transformation is the map induced by reflection of  $S^2(2, 3, 7)$  across a curve  $c$  dividing the orbifold into two triangles. See for example [BS09]. The union of fibers lying over  $c$  (with the full lift of  $c$  removed) is a (Birkhoff) section to the geodesic flow on  $T^1S^2(2, 3, 7)$ . The monodromy on the quotient of this section is the described map.

For the two maps defined on  $S_{2,1}$  in Table 1, recall from [HS07] that  $\sigma_1\sigma_2\sigma_3\sigma_4\sigma_1\sigma_2$  is the fully-punctured 5-braid with minimum dilatation  $|LT_{1,2}|$ . The braid points are 1-pronged

TABLE 2. The fully-punctured pseudo-Anosov maps with normalized dilatation  $\mu^4$ , and the veering triangulations and Betti number of the corresponding mapping tori.

Pseudo-Anosov maps	Veering triangulations	Betti number
Map on $S_{1,1}$ induced by $\begin{bmatrix} 5 & 3 \\ 3 & 2 \end{bmatrix} = RLRL$	eLMkbcdddhxqdu_1200	1
Map on $S_{1,1}$ induced by $\begin{bmatrix} -5 & -3 \\ -3 & -2 \end{bmatrix} = -RLRL$	eLMkbcdddhxqlm_1200	1
Map on $S_{1,2}$ induced by $\begin{bmatrix} 2 & 1 \\ 1 & 1 \end{bmatrix}$ punctured at a period 2 point	fLLQcbeddeehhkhkh_21112	1
Map on $S_{1,1}$ induced by $\begin{bmatrix} 6 & 5 \\ 1 & 1 \end{bmatrix} = R^5L$	gLMzQbcdeffhkhkhhit_122112	1
Map on $S_{1,1}$ induced by $\begin{bmatrix} -6 & -5 \\ -1 & -1 \end{bmatrix} = -R^5L$	gLMzQbcdeffhkhkhpe_122112	1
Map on $S_{0,4}$ induced by $\begin{bmatrix} 2 & 1 \\ 1 & 1 \end{bmatrix} = RL$	eLMkbcdddhxqlm_1200	2
Map on $S_{1,2}$ induced by $\begin{bmatrix} -2 & -1 \\ -1 & -1 \end{bmatrix}$ punctured at two fixed points	fLLQcbeddeehhbghh_01110	2

singularities while the point at infinity is 3-pronged. Consider the double cover  $S_{2,6} \rightarrow S_{0,6}$  with degree two over each of the punctures. Lift the braid monodromy to a map on  $S_{2,6}$ . There are two choices here, which differ by the deck transformation of the double cover. For either choice, 5 of the 6 punctures of  $S_{2,6}$  are 2-pronged hence can be filled in. Together these give the described maps.

For the first map defined on  $S_{1,2}$  in [Table 2](#), we puncture the map induced by  $\begin{bmatrix} 2 & 1 \\ 1 & 1 \end{bmatrix}$  on  $S_{1,0}$  at a pair of points of period 2. There are two choices here for which pair of points to puncture but they give conjugate maps.

For the other map defined on  $S_{1,2}$  in [Table 2](#), we puncture the map induced by  $\begin{bmatrix} -2 & -1 \\ -1 & -1 \end{bmatrix}$  on  $S_{1,0}$  at two fixed points. Again, there are a number of choices here, but the resulting maps are all conjugate.

[Theorem 1.6](#) has the following corollaries:

**Corollary 1.7.** *Let  $f$  be a fully-punctured pseudo-Anosov map. Then the normalized dilatation of  $f$  is  $\geq \mu^2$ .*

**Corollary 1.8.** *Let  $(f_i)$  be an infinite sequence of distinct fully-punctured pseudo-Anosov maps. Then the normalized dilatation of  $f_i$  is  $\geq \mu^4$  for large enough  $i$ .*

**Corollary 1.9.** *Let  $f$  be a fully-punctured pseudo-Anosov map whose mapping torus has first Betti number at least two. Then the normalized dilatation of  $f$  is  $\geq \mu^4$ .*



To our understanding, [Corollary 1.7](#) has been a folklore theorem but no proof of it exists in the literature. As mentioned above, [Corollary 1.9](#) is an upgrade to [Theorem 1.3](#).

**Outline of paper.** In [Section 2](#) we provide some background for (layered) veering triangulations and set up some terminology. In [Section 3](#) we explain the proof of [Theorem 1.4](#).

In [Section 4](#) and [Section 5](#) we explain many ways to sharpen the argument in [Section 3](#), which will result in an improved bound in the one boundary case, as recorded in [Theorem 5.16](#). There are some calculus computations that needs to be performed in the course of proving [Theorem 5.16](#) and deducing [Theorem 1.5](#) from [Theorem 5.16](#). We defer these to [Appendix A](#) so that the reader can focus on the main ideas.

In [Section 6](#) we explain how to use results from computations to arrive at [Theorem 1.6](#). Explanations for the code used for the computation are deferred to [Appendix B](#). Finally, in [Section 7](#), we discuss some future directions.

**Acknowledgements.** A very special thanks to my PhD advisor Ian Agol for his guidance, support, and patience with me during my time as his student. I would like to thank Eriko Hironaka for her collaboration on the paper [[HT22](#)] which directly inspired this one, and for many helpful conversations about pseudo-Anosov maps and dynamics in general. I would also like to thank Anna Parlak, Saul Schleimer, and Henry Segerman for writing and maintaining the Veering code, as well as their advice on coding. I would like to thank Chris Leininger for comments on an earlier version of this paper.

**Notational conventions.** Throughout this paper,

- $X \parallel Y$  will denote the metric completion of  $X \setminus Y$  with respect to the induced path metric from  $X$ . In addition, we will call the components of  $X \parallel Y$  the complementary regions of  $Y$  in  $X$ .
- If  $G$  is a directed graph, we will denote an edge path as the sequence of edges  $(e_1, \dots, e_n)$  that it traverses.
- Suppose  $\alpha$  is a path, then  $-\alpha$  will denote the path traversed in the opposite direction.

## 2. BACKGROUND

**2.1. Veering triangulations.** We recall the definition of a veering triangulation.

An *ideal tetrahedron* is a tetrahedon with its 4 vertices removed. The removed vertices are called the *ideal vertices*. An *ideal triangulation* of a 3-manifold  $M$  is a decomposition of  $M$  into ideal tetrahedra glued along pairs of faces.

A *taut structure* on an ideal triangulation is a labelling of the dihedral angles by 0 or  $\pi$ , such that

- Each tetrahedron has exactly two dihedral angles labelled  $\pi$ , and they are opposite to each other.
- The angle sum around each edge in the triangulation is  $2\pi$ .

A *transverse taut structure* is a taut structure along with a coorientation on each face, such that for any 0-labelled edge in a tetrahedron, exactly one of the faces adjacent to it is cooriented inwards. A *transverse taut ideal triangulation* is an ideal triangulation with a transverse taut structure.

In this paper, we will take the convention that coorientations point upwards.

**Definition 2.1.** A *veering structure* on a transverse taut ideal triangulation of an oriented 3-manifold is a coloring of the edges by red or blue, so that if we look at each tetrahedron with a  $\pi$ -labelled edge in front, the four outer 0-labelled edges, starting from an end of the front edge and going counter-clockwise, are colored red, blue, red, blue, respectively. See [Figure 1](#).

A *veering triangulation* is a transverse taut ideal triangulation with a veering structure.

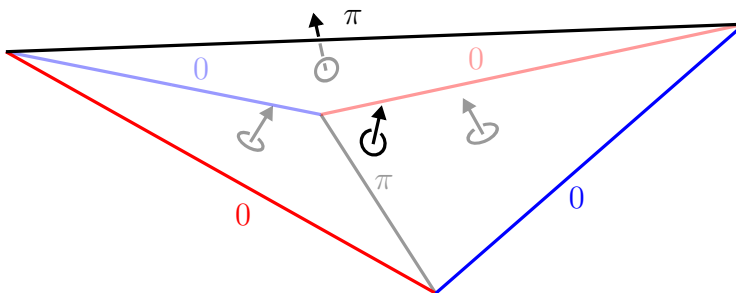


FIGURE 1. A tetrahedron in a veering triangulation. There are no restrictions on the colors of the top and bottom edges.

The local structure of a veering triangulation is fairly restricted. To be more precise, we have [Proposition 2.3](#) below, which describes how a veering triangulation can look like around each edge.

**Definition 2.2.** Let  $\Delta$  be a veering triangulation. A tetrahedron in  $\Delta$  is called a *toggle tetrahedron* if the colors on its top and bottom edges differ. It is called a *red/blue fan tetrahedron* if both its top and bottom edges are red/blue respectively.

Note that some authors call toggle and fan tetrahedra *hinge* and *non-hinge* respectively.

**Proposition 2.3** ([\[FG13, Observation 2.6\]](#)). *Every edge  $e$  in  $\Delta$  has one tetrahedron above it, one tetrahedron below it, and two stacks of tetrahedra, in between the tetrahedra above and below, on either of its sides.*

*Each stack must be nonempty. Suppose  $e$  is blue/red. If there is exactly one tetrahedron in one stack, then that tetrahedron is a blue/red fan tetrahedron respectively. If there are  $n > 1$  tetrahedron in one stack, then going from bottom to top in that stack, the tetrahedra are: one toggle tetrahedron,  $n - 2$  red/blue fan tetrahedra, and one toggle tetrahedron, respectively.*

**Definition 2.4.** A side of an edge in  $\Delta$  is said to be *short* if the stack of tetrahedra to that side has exactly one tetrahedron, otherwise it is said to be *long*.

In [Figure 2](#), we illustrate a blue edge whose left side is short and right side is long.

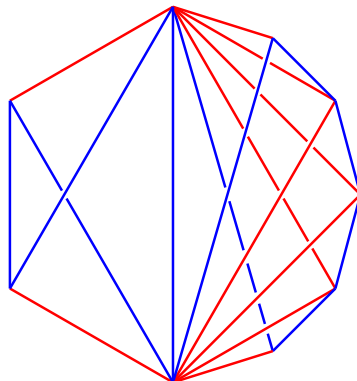


FIGURE 2. A blue edge whose left side is short and right side is long.

Associated to a veering triangulation are its *stable branched surface* and *dual graph*. We recall their definitions in [Definition 2.6](#) below.

**Definition 2.5.** Let  $M$  be a 3-manifold. A *branched surface*  $B$  is a subset of  $M$  locally of the form of one of the pictures in [Figure 3](#).

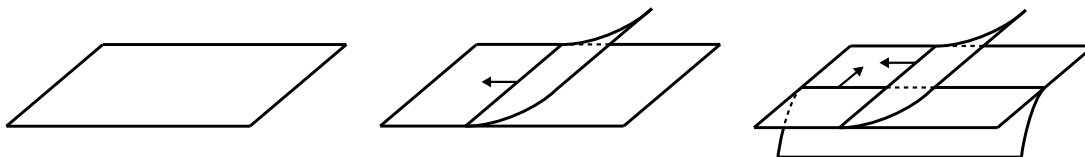


FIGURE 3. The local models for branched surfaces. The arrows indicate the *maw coorientation* of the branch locus.

The set of points where  $B$  is locally of the form of [Figure 3](#) middle and right is called the *branch locus* of  $B$ . The points where  $B$  is locally of the form of [Figure 3](#) right are called the *vertices* of  $B$ . The complementary regions of the branch locus in  $B$  are called the *sectors*.

The branch locus can be naturally considered as a 4-valent graph by taking the set of vertices to be the set of vertices of  $B$  and taking the set of edges to be the complementary regions of the vertices. Each edge of the branch locus has a canonical coorientation on  $B$ , which we call the *maw coorientation*, given locally by the direction from the side with more sectors to the side with less sectors.

Near a vertex  $v$ ,  $B$  can be considered as a disc with two sectors attached along two smooth arcs that intersect once at  $v$ . We call the two attached sectors the *fins* of  $B$  at  $v$ . In [Figure 3](#) right these would be the topmost and bottommost sectors.

**Definition 2.6.** Let  $\Delta$  be a veering triangulation on a 3-manifold  $M$ . We define the *stable branched surface*  $B$  of  $\Delta$  to be the branched surface which, in each tetrahedron  $t$  in  $\Delta$ , consists of a quadrilateral with its 4 vertices on the top and bottom edges and the two side edges of the same color as the top edge of  $t$ , and a triangular fin for each side edge of the opposite color to the top edge, with a vertex on that side edge and attached to the quadrilateral along an arc going between the two faces adjacent to that side edge, the two arcs of attachment having downward maw coorientation and intersecting at a single vertex in  $t$ . See [Figure 4](#) left.

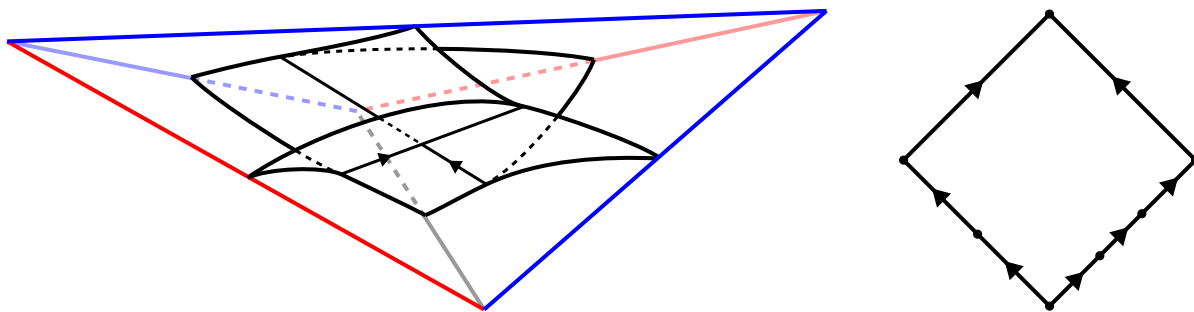


FIGURE 4. Left: The portion of the stable branched surface and the dual graph within each tetrahedron. Right: The form of each sector of the stable branched surface.

Consider the branch locus of the stable branched surface. We orient its edges to be positively transverse to the faces of  $\Delta$ . This defines a directed graph, which we call the *dual graph* of  $\Delta$  and denote by  $\Gamma$ .

**Definition 2.7.** Suppose  $c$  is an edge path of  $\Gamma$ , then at a vertex  $v$  of  $c$ , we say that  $c$  takes a *branching turn* at  $v$  if it is smooth near  $v$ , otherwise we say that  $c$  takes an *anti-branching turn* at  $v$ . A cycle of  $\Gamma$  that only takes branching turns is called a *branch cycle*. A cycle of  $\Gamma$  that only takes anti-branching turns is called an *AB cycle*.

We will in fact deal with the stable branched surface more than the triangulation itself in this paper, so we will spend some time describing its combinatorics.

Each sector of the stable branched surface  $B$  is dual to an edge of the triangulation  $\Delta$ , namely the one that passes through it. We define the *color* of a sector to be the color of its dual edge. Also, each vertex of  $\Gamma$  is dual to a tetrahedron of  $\Delta$ , namely the one that it sits inside of. In particular, the number of vertices of  $B$  is equal to the number of tetrahedra in  $\Delta$ .

Under these dual correspondences, the first part of [Proposition 2.3](#) translates to the following. See also [[SS19](#), Section 6.13].

**Proposition 2.8.** *Each sector  $s$  in  $B$  is a diamond with the two top sides each being an edge of  $\Gamma$  and the two bottom sides divided into edges of  $\Gamma$ . The number of edges a bottom side is divided into is equal to the number of tetrahedra to that side of the dual edge of  $\Delta$ . See [Figure 4](#) right.*

In particular we can talk about the *top vertex*, the *bottom vertex*, and the two *side vertices* of a sector, the last term meaning the two vertices where a top side meets a bottom side.

We then make some definitions that will allow us to translate the second part of [Proposition 2.3](#) cleanly.

**Definition 2.9.** A vertex of  $B$  is said to be *blue* if  $B$  is locally of the form as in [Figure 5](#) left, and is said to be *red* if  $B$  is locally of the form as in [Figure 5](#) right. Note that here we use the fact that the 3-manifold is oriented in order to distinguish the two pictures.

A useful mnemonic for this definition is to look at the fins of  $v$ . If they protrude out in a Left/Right-handed fashion then  $v$  is **bLue/Red**, respectively.

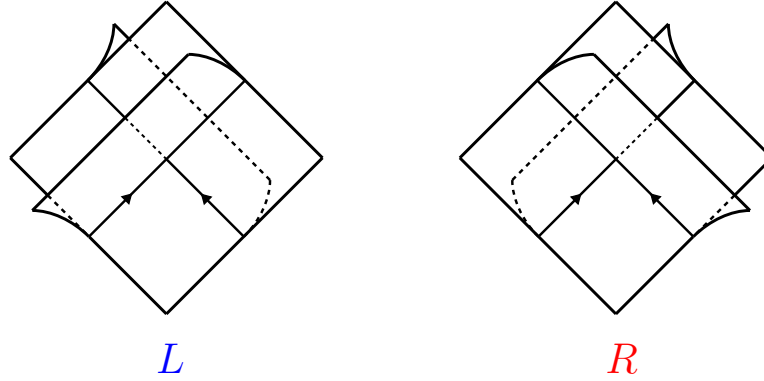


FIGURE 5. Defining the color of a vertex.

**Definition 2.10.** A sector of  $B$  is said to be a *toggle sector* if the colors on its top and bottom vertices differ. Otherwise it is called a *fan sector*.

With these definitions, an edge of  $\Delta$  is blue/red iff its dual sector is blue/red iff the bottom vertex of this dual sector is blue/red, respectively. A sector is toggle/fan iff the tetrahedron dual to its top vertex is toggle/fan respectively. Hence the second part of [Proposition 2.3](#) translates to the following.

**Proposition 2.11.** *Let  $s$  be a blue/red sector of  $B$ . On a bottom side of  $s$ , the vertices at the endpoints are colored blue/red while the vertices in the interior are colored red/blue, respectively.*

*Suppose a bottom side of  $s$  is divided into edges  $e_1, \dots, e_\delta$ , listed from bottom to top. Let  $s_i$  be the sector that has  $e_i$  as a top side. If  $\delta = 1$ , equivalently, that side of the dual edge in  $\Delta$  is short, then  $s_1$  is fan. If  $\delta \geq 2$ , equivalently, that side of the dual edge in  $\Delta$  is long, then  $s_1$  and  $s_\delta$  are toggle while  $s_i$  for  $i = 2, \dots, \delta - 1$  are fan, moreover a top side of  $s_i$  is equal to a bottom side of  $s_{i+1}$  for  $i = 2, \dots, \delta - 1$  and a top side of  $s_1$  is a proper subset of a bottom side of  $s_2$ .*

As an example, in [Figure 6](#), we draw the sector dual to the edge in [Figure 2](#) and some of the neighboring sectors. In the sequel our figures will only be drawn in the style of [Figure 6](#) left, but here we draw a 3-dimensional version of the figure in [Figure 6](#) right for the reader to familiarize themselves with the relevant notions.

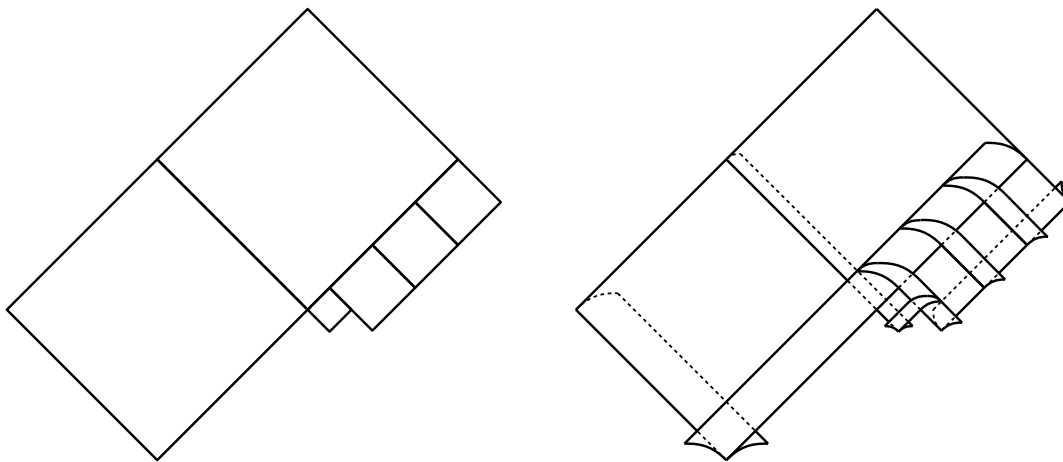


FIGURE 6. The sector dual to the edge in [Figure 2](#) and some of its neighboring sectors.

**Proposition 2.12.** *A branch cycle in  $B$  must meet vertices of both colors.*

*Proof.* Suppose otherwise, then there will be some sector that is a fin to every vertex on the branch cycle. That sector will contain the branch cycle as a boundary component. But this contradicts the fact that each sector is a diamond.  $\square$

**Remark 2.13.** There is another branched surface, called the *unstable branched surface*, that can be associated to a veering triangulation. This is the branched surface which, in each tetrahedron  $t$  in  $\Delta$ , consists of a quadrilateral with its 4 vertices on the top and bottom edges and the two side edges of the same color as the bottom edge of  $t$ , and a triangular fin for each side edge of the opposite color to the bottom edge, with a vertex on that side edge and attached to the quadrilateral along an arc going between the two faces adjacent to that side edge, the two arcs of attachment having upward maw coorientation and intersecting at a single vertex in  $t$ . Or more succinctly, the unstable branched surface is the stable branched surface associated to the veering triangulation obtained by reversing the coorientation on all the faces.

The branch locus of the unstable branched surface has the same underlying directed graph as the dual graph  $\Gamma$ , however the notions of branching and anti-branching turns becomes different if one defines them using the unstable, instead of the stable, branched surface.

To avoid confusion, we will not make use of the unstable branched surface in this paper. However, some of our arguments can be streamlined by observing the symmetry between the stable and unstable branched surface. The reader who is familiar with veering triangulations is invited to fill in these alternate arguments for themselves.



**2.2. Dynamic planes.** We recall the notion of a dynamic plane, which was introduced in [LMT21]. Technically we do not make use of these in this paper, but we will make use of the related notion of a descending path. We will also explain how dynamic planes provide the correct setting of understanding figures such as Figure 6 left.

**Definition 2.14.** A *descending path* on the stable branched surface  $B$  is a path that intersects the branch locus of  $B$  transversely and induces the maw coorientation at each intersection, that is, it goes from a side with more sectors to a side with less sectors.

Suppose  $c$  is an edge path of the dual graph  $\Gamma$ . By pushing  $c$  downwards slightly in  $B$  and reversing its orientation, we obtain a descending path  $\alpha$  on  $B$ . We illustrate a local picture of this procedure in Figure 7 left. In Figure 7 right, we show a bigger example, drawn in the style of the figures used in the rest of this paper.

The intersection points of  $\alpha$  with the branch locus of  $B$  are in one-to-one correspondence with the vertices of  $c$ . At such an intersection point  $x$ ,  $\alpha$  meets the boundary of exactly one sector  $s$  which it does not locally meet the interior of. We say that  $s$  *merges into*  $\alpha$  at  $x$ . In particular  $s$  is a fin of the vertex of  $c$  corresponding to  $x$ .

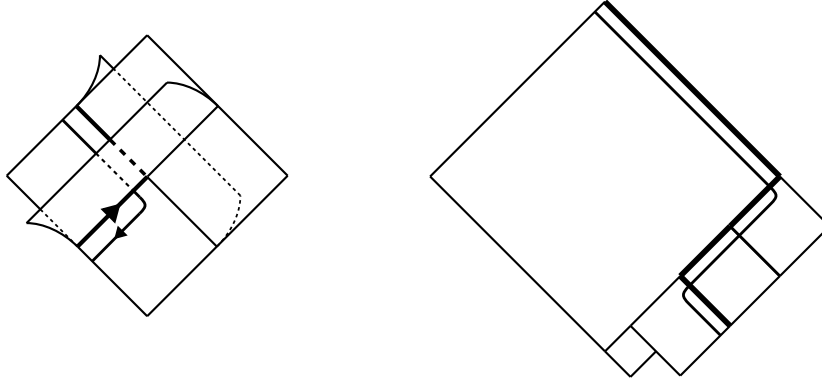


FIGURE 7. Pushing an edge path of the dual graph (thickened) downwards and reversing its orientation to get a descending path.

**Definition 2.15.** Let  $\Delta$  be a veering triangulation on a 3-manifold  $M$ . Let  $\tilde{\Delta}$  be the lift of the triangulation to the universal cover  $\tilde{M}$ . Let  $\tilde{B}$  and  $\tilde{\Gamma}$  be the stable branched surface and dual graph of  $\tilde{\Delta}$  respectively.

Let  $x$  be a point on  $\tilde{B}$ . The *descending set* of  $x$ , denoted by  $\Delta(x)$ , is the set of points on  $\tilde{B}$  that can be reached from  $x$  via a descending path. By [LMT21, Lemma 3.1], each descending set is a union of sectors that forms a quarter-plane.

Now let  $\tilde{c}$  be an infinite path of  $\tilde{\Gamma}$ . The *dynamic plane* associated to  $\tilde{c}$ , denoted by  $D(\tilde{c})$ , is the set of points on  $\tilde{B}$  that can be reached from a point on  $\tilde{c}$  via a descending path.  $D(\tilde{c})$  is a union of sectors that is homeomorphic to a plane if  $\tilde{c}$  does not eventually lie along a branch line, and is homeomorphic to a half-plane otherwise.

Although it would not be necessary for understanding this paper, the rigorous way to interpret figures such as [Figure 6](#) left, where we lay out sectors on a plane to show their relative placement, is that they illustrate a subset of some appropriate dynamic plane.

**2.3. Pseudo-Anosov mapping tori.** We recall the construction of the layered veering triangulation associated to a pseudo-Anosov mapping torus, and set up some terminology along the way.

**Definition 2.16.** A finite-type surface is an oriented closed surface with finitely many points, which we call the *punctures*, removed.

A homeomorphism  $f$  on a finite-type surface  $S$  is said to be *pseudo-Anosov* if there exists a pair of singular measured foliations  $(l^s, \mu^s)$  and  $(l^u, \mu^u)$  such that:

- (1) Away from a finite collection of *singular points*, which includes the punctures,  $(l^s, l^u)$  is locally conjugate to the foliations of  $\mathbb{R}^2$  by vertical and horizontal lines respectively.
- (2) Near a singular point,  $(l^s, l^u)$  is locally conjugate to either
  - the pull back of the foliations of  $\mathbb{R}^2$  by vertical and horizontal lines by the map  $z \mapsto z^{\frac{n}{2}}$  respectively, for some  $n \geq 3$ , or
  - the pull back of the foliations of  $\mathbb{R}^2 \setminus \{(0, 0)\}$  by vertical and horizontal lines by the map  $z \mapsto z^{\frac{n}{2}}$  respectively, for some  $n \geq 1$ .
- (3)  $f_*(l^s, \mu^s) = (l^s, \lambda^{-1}\mu^s)$  and  $f_*(l^u, \mu^u) = (l^u, \lambda\mu^u)$  for some  $\lambda > 1$ .

$f$  is said to be *fully-punctured* if the set of singular points is equal to the set of punctures and is nonempty.

Let  $f : S \rightarrow S$  be a fully-punctured pseudo-Anosov map. By blowing air into the leaves of the stable measured foliation that contain the punctures, we obtain a measured lamination, which we still denote by  $(l^s, \mu^s)$ .

Let  $T_f$  be the mapping torus of  $f$ . Recall this is constructed by taking  $S \times [0, 1]$  and gluing  $S \times \{1\}$  to  $S \times \{0\}$  by  $f$ . The suspension of the lamination  $l^s$ , that is, the image of  $l^s \times [0, 1]$ , is a lamination on  $T_f$ , which we call the *stable lamination* and denote by  $\Lambda^s$ .

**Theorem 2.17** ([\[Ago11\]](#)). *There is a veering triangulation on  $T_f$  whose stable branched surface carries  $\Lambda^s$ .*

Such a veering triangulation is in fact unique, see for example, [\[LT23, Theorem 9.1\]](#), but logically we will not need this fact in this paper. One can simply fix a veering triangulation  $\Delta$  on  $T_f$ , for example the canonical one defined in [\[Gué16\]](#). We let  $B$  be the stable branched surface and  $\Gamma$  be the dual graph of such a veering triangulation.

**Definition 2.18.** A *fiber surface* in  $T_f$  is a surface in the same isotopy class as  $S \times \{0\}$  that is positively transverse to the edges of  $\Gamma$  and does not pass through the vertices of  $\Gamma$ .

At the end of this section, we will recall the proof of [Theorem 2.17](#), which will also show that fiber surfaces exist. Before that, we set up some notation that we will use for the rest of this paper.

The homology class of  $S \times \{0\}$  determines a  $\mathbb{Z}$ -covering of  $T_f$ , which we denote by  $\widehat{T}_f$ .  $\Lambda^s$  lifts to a lamination  $\widehat{\Lambda}^s$  on  $\widehat{T}_f$ . Unlike  $\Lambda^s$ ,  $\widehat{\Lambda}^s$  has a natural transverse measure induced by  $\mu^s$ . We denote this measure as  $\widehat{\mu}^s$ . Let  $g$  be the generator of the deck transformation group of  $\widehat{T}_f$  for which  $g_*\widehat{\mu}^s = \lambda\widehat{\mu}^s$ , that is,  $g$  shifts  $\widehat{T}_f$  upwards.

Let  $\widehat{B}$  be the lift of  $B$  to  $\widehat{T}_f$ .  $\widehat{B}$  carries  $\widehat{\Lambda}^s$ , hence we can define the *weight* of a sector to be the total  $\widehat{\mu}^s$ -measure of the leaves that are carried by the sector.

Fix a fiber surface, which we denote by  $S$ . This slight abuse of notation is justified because a fiber surface must be homeomorphic to the surface  $f$  is defined on. The intersection of  $S$  with  $B$  determines a train track  $\tau$  on  $S$ . Meanwhile,  $S$  intersects each sector  $s$  of  $B$  in disjoint *arcs*. Each arc has endpoints on edges of  $\Gamma$  that lie on different sides of  $s$ . We order the arcs from bottom to top, using terms such as ‘the bottommost arc on  $s$ ’. Notice that these arcs, over all sectors, are exactly the branches of  $\tau$ . Similarly, the intersection points of  $S$  with  $B$  are exactly the switches of  $\tau$ . In particular, the number of such intersection points is equal to the number of switches of  $\tau$ . Now, each complementary region of  $\tau$  in  $S$  is a once-punctured polygon, hence by an index argument, we see that the number of intersection points of  $S$  with  $B$  is  $-2\chi(S)$ .

Fix a homeomorphic lift of  $S$  to  $\widehat{T}_f$ , which we denote by  $S_0$ . Write  $S_r = g^r \cdot S_0$ . Each  $S_r$  is a separating surface in  $\widehat{T}_f$ , hence it makes sense to say that a set lies above or below some  $S_r$ . For each sector  $\widehat{s}$  of  $\widehat{B}$ , suppose  $r$  is the smallest integer such that  $\widehat{s}$  lies above  $S_{r-1}$ . If  $\widehat{s}$  intersects any  $S_i$  at all, then  $r$  is also the smallest integer such that  $S_r$  intersects  $\widehat{s}$ . In this case we say that  $\widehat{s}$  is *at height*  $r$ . Notice that each sector  $s$  of  $B$  has a collection of lifts  $\{\widehat{s}_r\}_{r \in \mathbb{Z}}$  where each  $\widehat{s}_r$  is at height  $r$ . We define the *weight* of  $s$  to be the weight of  $\widehat{s}_0$ . We caution the reader that this does NOT make  $B$  a measured branched surface, since this measure may not be additive across the branch locus.

Finally, let  $\widehat{\Gamma}$  be the lift of  $\Gamma$  to  $\widehat{T}_f$ . We say that a vertex  $\widehat{v}$  of  $\widehat{\Gamma}$  is *at height*  $r$  if  $r$  is the smallest integer such that  $\widehat{v}$  lies above  $S_{r-1}$ . Notice that if a sector  $\widehat{s}$  of  $\widehat{B}$  has a vertex at height  $r$  on its boundary, then  $\widehat{s}$  is of height  $\leq r$ .

As promised, we recall the proof of [Theorem 2.17](#).

*Proof of [Theorem 2.17](#).* The following definition is the main insight of [[Ago11](#)].

**Definition 2.19.** A *periodic splitting sequence* for  $f$  is a sequence of train tracks  $(\tau_i)_{i \in \mathbb{Z}}$  such that:

- Each  $\tau_i$  carries the stable lamination  $l^s$ .
- Each complementary region of  $\tau_i$  contains exactly one puncture.
- $\tau_{i+1}$  is obtained by a *splitting move* on  $\tau_i$  for each  $i$ .

- There exists  $N$  such that  $f(\tau_{i+N}) = \tau_i$  for every  $i$ .

In [Ago11], it is shown that periodic splitting sequences exist.

Fix a periodic splitting sequence  $(\tau_i)$ . Consider the sequence of dual ideal triangulations  $(\delta_i)$  to the train tracks. Each  $\delta_{i+1}$  is related to  $\delta_i$  by a diagonal switch. See Figure 8. We can construct a triangulation  $\Delta$  on  $T_f$  by starting with  $\delta_0$ , then stacking  $N$  tetrahedra, one at a time, to effect the  $N$  diagonal switches from  $\delta_0$  to  $\delta_N$ , and finally gluing  $\delta_N$  at the top of the stack to  $\delta_0$  at the bottom of the stack using  $f$ .

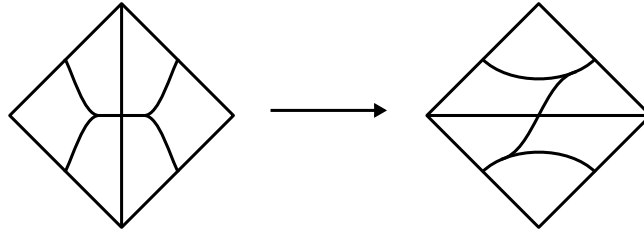


FIGURE 8. The layered veering triangulation on a mapping torus is constructed from the dual triangulations of a periodic splitting sequence.

Between each  $\delta_i$  and  $\delta_{i+1}$ , the train tracks  $\tau_i$  and  $\tau_{i+1}$  can be naturally interpolated by a portion of a branched surface containing one vertex. Color the edges of  $\Delta$  such that the union of these ends up being the stable branched surface of  $\Delta$ , that is, following Figure 5. It is straightforward to check that  $\Delta$  is then a veering triangulation and by definition,  $B$  carries the stable lamination  $\Lambda^s$ . Moreover, the underlying surface of each layer  $\delta_i$  is a fiber surface.  $\square$

Before we move on, we state one fact about veering triangulations on pseudo-Anosov mapping tori that we will use in Section 5.

**Proposition 2.20.** *Let  $S$  be a fiber surface and let  $c$  be a cycle of the dual graph  $\Gamma$ , then  $S$  and  $c$  must intersect.*

*Proof.* We show two ways of proving this proposition.

The more high-brow way is to use the results in [LMT20]. By [LMT20, Theorem 5.1], the cone over the fibered face that  $[S] \in H_2(T_f, \partial T_f)$  lies in is dual to the cone of all  $\Gamma$ -cycles in  $H_1(T_f)$ . By [LMT20, Theorem 5.15], none of the  $\Gamma$ -cycles are null-homologous, so since  $[S]$  lies in the interior of the cone,  $[S]$  has positive intersection number with all  $\Gamma$ -cycles.

The more straightforward proof is to consider the construction in the proof of Theorem 2.17. The collection of all the underlying surfaces of the  $\delta_i$  intersects every edge of  $\Gamma$  positively, so some fiber surface intersects the  $\Gamma$ -cycle  $c$  positively. Now use the fact that any two fiber surfaces are isotopic.  $\square$

### 3. SINGLE HOOK CIRCUITS

In this section we will show [Theorem 1.4](#). The proof uses a special type of circuit in the dual graph, which we call hook circuits. The title of the section comes from the fact that we only make use of a single hook circuit in this section, as opposed to [Section 4](#) where we use up to two hook circuits. The argument bounding the number of tetrahedra is not very difficult; the complicated part is showing that the hook circuits that we use exist. These two parts will occupy [Section 3.1](#) and [Section 3.3](#) respectively.

**3.1. Bounding the number of vertices using single hook circuits.** We fix the following setting. Let  $T_f$  be the mapping torus of a fully-punctured pseudo-Anosov map  $f$ . Let  $\Delta$  be the veering triangulation on  $T_f$  that carries  $\Lambda^s$ , let  $B$  be the stable branched surface of  $\Delta$ , and let  $\Gamma$  be the dual graph of  $\Delta$ . Finally, let  $S$  be a fiber surface. We use notation as in [Section 2.3](#).

**Definition 3.1.** An edge path in a directed graph is *simple* if it does not repeat edges (but it is allowed to repeat vertices). A *circuit* is a simple cycle. An *Eulerian circuit* is a circuit that traverses each edge exactly once.

**Definition 3.2.** Let  $s$  be a sector of  $B$ . Suppose the two bottom sides of  $s$  are divided into edges of  $\Gamma$  which we label, from bottom to top,  $e_1^1, \dots, e_{\delta_1}^1$  and  $e_1^2, \dots, e_{\delta_2}^2$  respectively. Label the edge of  $\Gamma$  that is the top side of  $s$  above  $e_{\delta_\beta}^\beta$  to be  $e_{\delta_\beta+1}^\beta$ . Suppose the bottommost arc on  $s$  has endpoints on  $e_{k_1}^1$  and  $e_{k_2}^2$ . The *hook* of  $s$  on the side  $\beta$ , which we denote by  $h_\beta$ , is the path  $(e_{k_\beta}^\beta, e_{k_\beta+1}^\beta, \dots, e_{\delta_\beta+1}^\beta)$ . If  $k_\beta = 1$  we say that the hook  $h_\beta$  is *deep*. We illustrate an example of a sector in [Figure 9](#) whose left hook is deep but right hook is not. If  $s$  does not have any arcs, we leave its hooks undefined.

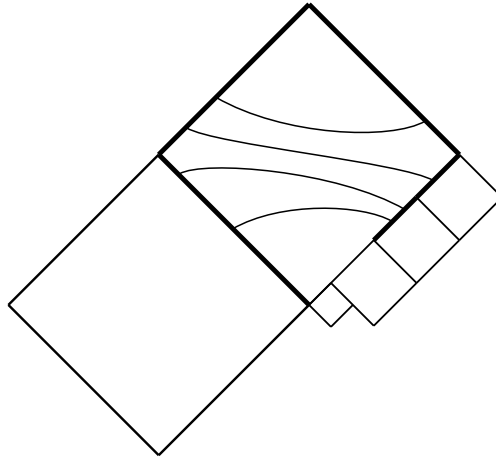


FIGURE 9. The two hooks (thickened) of a sector with the given placement of arcs. Here the left hook is deep but the right hook is not.

A circuit  $c$  in  $\Gamma$  is said to *hook around  $s$  on side  $\beta$*  if it contains  $h_\beta$  as a sub-path. When  $h_\beta$  is understood, we will refer to the vertices of  $c$  in the interior of  $h_\beta$  as the *hook vertices* of  $c$ .

There is a degenerate case here when  $k_\beta \neq \delta_\beta + 1$  and  $e_{\delta_\beta+1}^\beta = e_{k_\beta}^\beta$  (which forces  $k_\beta = 1$  by [Proposition 2.11](#)). In this case,  $h_\beta$  is not simple; we will say that the circuit  $(e_i^\beta)_{i \in \mathbb{Z}/\delta_\beta}$  *hooks around  $s$  on side  $\beta$* . In other words, we allow non-simple paths to be sub-paths of circuits if they traverse the same sequence of edges in the same order. In this case, all the vertices on  $(e_i^\beta)$  are hook vertices.

We refer to circuits that hook around a sector as *hook circuits* in general.

We will essentially only be interested in the case when  $s$  is a sector of minimum weight. In this case,  $s$  must contain arcs. One way to see this is to consider the lift  $\widehat{s}_0$  of  $s$  in  $\widehat{B}$  that is at height 0. If  $s$  does not contain arcs, the same is true for  $\widehat{s}_0$ , so the sector on top of  $\widehat{s}_0$  is at height 0 as well, but of smaller weight, implying that the sector of  $B$  it covers is of smaller weight than  $s$ .

Similarly, in this case one can see that  $k_1$  and  $k_2$  in [Definition 3.2](#) must be at most  $\delta_1$  and  $\delta_2$  respectively. Otherwise, say  $j_1 = \delta_1 + 1$ , then the two sectors with  $e_{\delta_1+1}$  along their bottom sides must have smaller weight by the same reasoning.

**Proposition 3.3.** *Let  $s$  be a sector of  $B$  of minimum weight. Suppose there exists an Eulerian circuit  $c$  of  $\Gamma$  which hooks around  $s$ . Then the number of tetrahedra in the veering triangulation is  $\leq \frac{1}{2}\lambda^{-2\chi}$ .*

*Proof.* Let the weight of  $s$  be  $w$ . Let  $\widehat{s}_0$  be the lift of  $s$  in  $\widehat{B}$  that is of height 0. Recall that the weight of  $\widehat{s}_0$  is  $w$ . Take the basepoint of  $c$  to be the top vertex of  $s$ . Lift  $c$  to a path  $\widehat{c}$  ending at the top vertex of  $\widehat{s}_0$ , reverse its orientation, then push it downwards to get a descending path  $\alpha$ .

Since  $c$  is Eulerian, it passes through each vertex of  $B$  two times, hence its length is two times the number of tetrahedra  $N$  in the triangulation. Meanwhile,  $\Gamma$  intersects the fiber surface  $S$  for  $-2\chi(S)$  times, hence  $c$  intersects  $S$  for  $-2\chi(S)$  times as well. These facts imply that the starting point of  $\alpha$  lies on a sector of weight  $w$ , the ending point of  $\alpha$  lies on a sector of weight  $\lambda^{-2\chi}w$ , and  $\alpha$  passes through the branch locus of  $\widehat{B}$  for  $2N$  times. Hence we get an equation

$$(3.1) \quad \lambda^{-2\chi}w = w + \sum_{j=1}^{2N} w_j$$

Here  $w_j$  is the weight of the  $j^{\text{th}}$  sector merging into  $\alpha$ . Our task is to show a lower bound for  $\sum_{j=1}^{2N} w_j$  in terms of  $w$  and  $N$ .

We first set up some notation. For each vertex  $v$ ,  $c$  either takes an anti-branching turn or a branching turn at  $v$  for the both times it visits  $v$ . We say that  $v$  is *A-resolved* or *B-resolved* respectively in those cases. This terminology is motivated from the perspective that we are ‘resolving’ the directed graph  $\Gamma$  at each vertex to produce a 1-manifold, and will be consistent with our future discussion on existence of hook circuits.



Recall that each intersection point of  $\alpha$  with  $\widehat{\Gamma}$  corresponds naturally to a vertex of  $\widehat{c}$ . Under this correspondence, the term in  $W = \sum_{j=1}^{2N} w_j$  that arises from an intersection point of  $\alpha$  with  $\widehat{\Gamma}$  is the weight of one of the fins of the corresponding vertex  $v$  of  $\widehat{c}$ . The height of this sector is bounded above by the height  $r_v$  of  $v$ , hence the weight of the sector is bounded below by  $\lambda^{-r_v} w$ . If  $v$  does not cover a hook vertex of  $c$ , then  $v$  will be at non-positive height, since  $-\widehat{c}$  will have gone through  $S_0$  after having traversed the hook at the start, hence the corresponding term is  $\geq w$ . This argument does not work if  $v$  does cover a hook vertex of  $c$  however, so we will need to modify our strategy a little bit.

What we will do is that for each B-resolved hook vertex  $u$ , we pair up the two terms in  $W$  that correspond to the two vertices of  $\widehat{c}$  covering the vertex of  $\Gamma$  that  $u$  lies at. See [Figure 10](#). Consider a lift  $\widehat{u}$  of  $u$ . Let  $d_u$  be the difference between the heights of the two fins of  $\widehat{u}$ . This quantity only depends on  $u$  since any other lift is  $g^r \cdot \widehat{u}$  for some  $r$ , and  $g^r$  changes the heights of both fins by  $r$ . For the two terms of  $W$  in such a pair, we can now bound their sum from below by  $\lambda^{-r_1+d_u} w + \lambda^{-r_2-d_u} w$  where  $r_i$  is the height of the fin opposite to the one whose weight is added (up to relabeling  $r_1, r_2$  or changing the sign of  $d_u$ ).

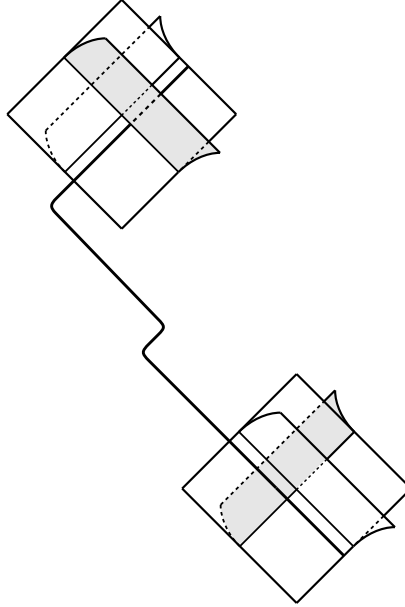


FIGURE 10. For each B-resolved hook vertex  $u$ , we pair up the two vertices of  $\widehat{c}$  covering the vertex of  $\Gamma$  that  $u$  lies at. The two corresponding terms are the weights of sectors (shaded) covering the two fins at  $u$ .

We claim that  $r_1$  and  $r_2$  must be non-positive. If the corresponding vertex of  $\widehat{c}$  covers a hook vertex, then this follows from the fact that  $\widehat{s}_0$  is at height 0, since in this case the fin opposite to the one whose weight is added is  $\widehat{s}_0$ . Otherwise, this follows from the fact that the corresponding vertex of  $\widehat{c}$  has non-positive height. Hence  $\lambda^{-r_1+d_u} w + \lambda^{-r_2-d_u} w \geq \lambda^{d_u} w + \lambda^{-d_u} w \geq 2w$ .

Now, there is only one A-resolved hook vertex, so by doing this grouping for each B-resolved hook vertex and using the original argument for the other vertices of  $\widehat{c}$  not covering a hook vertex, we see that  $W = \sum_{j=1}^{2N} w_j \geq (2N - 1)w$ . Hence from [Equation \(3.1\)](#), we get  $\lambda^{-2\chi} \geq 2N$  which implies the bound in the proposition.  $\square$

**3.2. Resolutions and Alexander duality.** To utilize [Proposition 3.3](#), we need to be able to find hook circuits. The way we will do so is to change our perspective and study the connectedness of the dual graph after resolutions. In turn, the way we study this connectedness will be to use a version of Alexander duality. In this subsection we will explain these ideas.

**Definition 3.4.** A  $(2,2)$ -valent directed graph is a directed graph for which every vertex has exactly two incoming edges and exactly two outgoing edges.

Let  $G$  be a  $(2,2)$ -valent directed graph. Let  $v$  be a vertex of  $G$ . Let  $i_1, i_2$  be the incoming edges and  $o_1, o_2$  be the outgoing edges at  $v$ . We define a *resolution at  $v$*  to be the operation of deleting  $v$  from  $G$  then joining  $i_\beta$  to  $o_{\sigma(\beta)}$  for some permutation  $\sigma$ , which returns another  $(2,2)$ -valent directed graph. Notice that any vertex can be resolved in two ways.

Suppose  $G'$  is obtained from  $G$  by repeated resolutions of vertices. Then  $G'$  is determined by a collection  $I = \{(v_i, \sigma_i)\}$  where the  $v_i$  are distinct vertices of  $G$  and  $\sigma_i$  are permutations dictating how the resolutions are performed at  $v_i$ . In this case we write  $G' = G(I)$ . Notice that there is a natural map  $G' \rightarrow G$  defined by gluing back the resolved vertices. Also, notice that the notation is set up such that  $G(I_1 \cup I_2)$  makes sense as long as  $I_1$  and  $I_2$  do not contain contradicting instructions on how to resolve a vertex.

A simple edge path or cycle  $c$  of  $G$  determines a resolution of  $G$  by resolving every vertex in the interior of  $c$  in a manner such that  $c$  lifts to a subset of an edge in the resolved graph  $G'$ . In this case we use  $c$  to denote the collection that determines the resolution, that is, we write  $G' = G(c)$ .

For a general  $(2,2)$ -valent directed graph, there is no good way of referring to the two ways of resolving a vertex. But for dual graphs of veering triangulations, we can use the following terminology, which was already hinted at in the proof of [Proposition 3.3](#).

**Definition 3.5.** Let  $v$  be a vertex of the dual graph of a veering triangulation. If in [Definition 3.4](#),  $(i_\beta, o_{\sigma(\beta)})$  takes an anti-branching turn at  $v$ , then we call the resolution an *A-resolution*. Otherwise,  $(i_\beta, o_{\sigma(\beta)})$  takes a branching turn at  $v$ , and we call the resolution a *B-resolution*.

With this notation, the existence of an Eulerian hook circuit can be rephrased as

**Proposition 3.6.** *There exists an Eulerian circuit that hooks around a sector  $s$  on side  $\beta$  if and only if  $\Gamma(h_\beta)$  is connected.*

*Proof.* For the forward direction, the Eulerian hook circuit  $c$  in  $\Gamma$  lifts to an Eulerian circuit in  $\Gamma(h_\beta)$ , hence  $\Gamma(h_\beta)$  is connected.

For the backward direction, since  $\Gamma(h_\beta)$  is a connected  $(2,2)$ -valent directed graph, by a classical theorem of Euler,  $\Gamma(h_\beta)$  has a Eulerian circuit  $c$ . The image of  $c$  in  $\Gamma$  is a Eulerian circuit that contains  $h_\beta$  as a sub-path.  $\square$

This shift in perspective to resolutions transfers the question that one must answer to apply [Proposition 3.3](#) into: how can one study the connectedness of resolutions of the dual graph? Here is where Alexander duality comes in.

Consider the general setting of having a cell complex  $X$ . For our purposes, this means that  $X$  is obtained by gluing  $n$ -balls along faces on their boundary that are homeomorphic to  $n - 1$ -balls by homeomorphisms. The *dual graph* of  $X$  is defined to be the graph with set of vertices equal to the set of  $n$ -balls and an edge between  $e_1$  and  $e_2$  for every pair of faces on  $e_1$  and  $e_2$  that are glued together. Then a general position argument shows that the number of components of  $X$  is equal to the number of components of its dual graph.

When  $\Delta$  is a veering triangulation, this definition of dual graph agrees with the definition in [Definition 2.6](#) that we have used so far, with the edge orientations forgotten. In particular this shows that the dual graph of a veering triangulation is always connected.

Suppose  $v$  is a vertex of the dual graph  $\Gamma$  of a veering triangulation  $\Delta$ . Recall that  $v$  is dual to a tetrahedron  $t$  of  $\Delta$ . We define the *A-quad* of  $t$  to be a properly embedded quadrilateral-with-4-ideal-vertices with edges along the top edge, the 2 side edges of the opposite color as the top edge, and the bottom edge of  $t$ . We define the *B-quad* of  $t$  to be a properly embedded quadrilateral-with-4-ideal-vertices with edges along the top edge, the 2 side edges of the same color as the top edge, and the bottom edge of  $t$ . We will only consider A/B-quads up to isotopy hence these are uniquely defined for each tetrahedron.

If we now define a new cell complex  $\Delta'$  by cutting  $\Delta$  along the A/B-quad of  $t$ , then the dual graph of  $\Delta'$  is exactly the A/B-resolution of  $\Gamma$  at  $v$ , respectively (again, with the edge orientations forgotten).

More generally, the graph  $\Gamma(I)$  obtained by resolving according to some collection  $I$  is the dual graph of the cell complex obtained by cutting  $\Delta$  along the union of A/B-quads in the corresponding collection of tetrahedra, where we take the A/B-quad in a tetrahedron if we A/B-resolve the corresponding vertex respectively.

At this point, it is convenient for our discussion to compactify the triangulation. That is, we cut away a neighborhood of each end of  $T_f$ , so that it has torus boundary components instead of torus ends. Correspondingly,  $\Delta$  becomes a triangulation by truncated tetrahedra, and each quad becomes an octagon with every other side lying along  $\partial T_f$ , however we will still refer to them as quads.

In the above scenario, we let  $Q = Q(I)$  be the union of A/B-quads, and let  $\partial_v Q = Q \cap \partial T_f$ . Here  $Q$  is a 2-complex and via a version of Alexander duality, we can compute the number of components of  $\Delta \setminus Q$  using the homology of  $Q$ . For concreteness, let us use homology with  $\mathbb{R}$ -coefficients.

**Proposition 3.7.** *We have  $\tilde{H}^0(\Delta \setminus Q) \cong \ker(H_2(Q, \partial_v Q) \rightarrow H_2(T_f, \partial T_f))$ . In particular, the number of components of  $\Gamma(I)$  is equal to  $1 + \dim \ker(H_2(Q, \partial_v Q) \rightarrow H_2(T_f, \partial T_f))$*

*Proof.* Let  $U$  be a regular neighborhood of  $Q$  in  $T_f$ . Let  $\partial_v U = U \cap \partial T_f$  and  $\partial_h U = \partial U \setminus \partial_v U$ .  $\partial_v U$  is a regular neighborhood of  $\partial_v Q$  on  $\partial T_f$ .

Consider the commutative diagram of long exact sequences

$$\begin{array}{ccccccccc}
0 & & \mathbb{R} & & & & H_2(Q, \partial_v Q) & & \\
\parallel & & \parallel & & & & \parallel & & \\
H_3(U, \partial_v U) & \longrightarrow & H_3(T_f, \partial T_f) & \longrightarrow & H_3(T_f, U \cup \partial T_f) & \longrightarrow & H_2(U, \partial_v U) & \longrightarrow & H_2(T_f, \partial T_f) \\
\downarrow & & \downarrow & & \parallel & & \downarrow & & \downarrow \\
& & & & H_3(T_f \setminus U, \partial(T_f \setminus U)) & & & & \\
& & & & \downarrow & & & & \\
H^0(U, \partial_h U) & \longrightarrow & H^0(T_f) & \longrightarrow & H^0(T_f \setminus U) & \longrightarrow & H^1(U, \partial_h U) & \longrightarrow & H^1(T_f) \\
\parallel & & \parallel & & \parallel & & & & \\
0 & & \mathbb{R} & & H^0(T_f \setminus Q) & & & & 
\end{array}$$

The vertical arrows are isomorphisms given by Poincare (or Poincare-Lefschetz) duality. Hence this shows that

$$\tilde{H}^0(T_f \setminus Q) \cong \ker(H_2(Q, \partial_v Q) \rightarrow H_2(T_f, \partial T_f))$$

□

In practice, we will need to know how the isomorphism in [Proposition 3.7](#) actually operates. For a given component  $C$  of  $\Delta \setminus Q$ , its boundary in  $\Delta$  will consist of a collection of quads. If we coorient each of these quads to point out of  $C$ , their sum will determine the corresponding 2-cycle in  $\ker(H_2(Q, \partial_v Q) \rightarrow H_2(T_f, \partial T_f))$ . Note that if both sides of a quad lie in  $C$ , then the quad will be included twice in the sum with opposite coorientations, hence end up not appearing in the 2-cycle. In general, the coefficient of each quad that appears in the cycle will be  $\pm 1$ .

Conversely, given a nonzero 2-cycle in  $\ker(H_2(Q, \partial_v Q) \rightarrow H_2(T_f, \partial T_f))$  with coefficients  $\pm 1$ , we can first coorient the quads appropriately so that the coefficients are all 1. Then the quads will bound a component of  $\Delta \setminus Q$  for which they are cooriented out of.

The fact that we have  $\tilde{H}^0$  instead of  $H^0$  on the left hand side of [Proposition 3.7](#) means that if we add together the 2-cycles corresponding to each of the components of  $\Delta \setminus Q$ , the quads all cancel each other out and we get the zero sum.

### 3.3. Existence of single hook circuits.

**Proposition 3.8.** *There exists a choice of fiber surface  $S$  for which there is a Eulerian circuit that hooks around a sector of minimum weight, unless  $\Delta = \mathbf{cPcbbbdzxm}_{10}$ .*

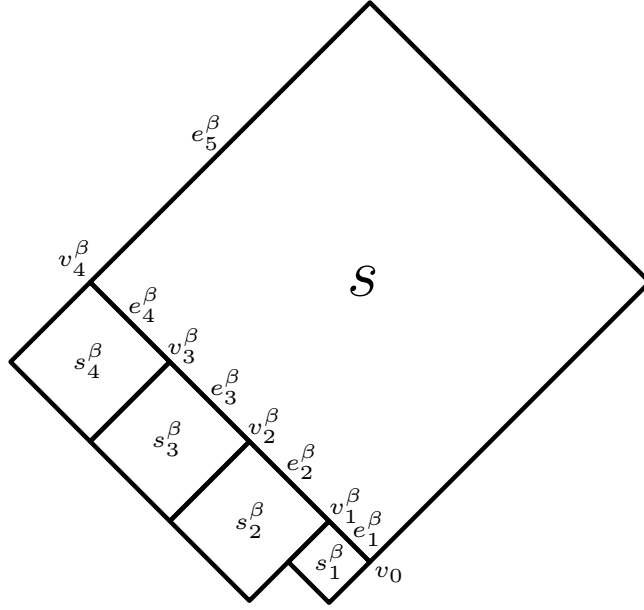


FIGURE 11. Setting up notation for the edges, sectors, and vertices adjacent to  $s$ . In this example,  $\delta_\beta = 4$ .

We remark that `cPcbbbdxm_10` is a triangulation of the figure eight knot complement, and is in fact the first member of the veering triangulation census [GSS].

The proof of [Proposition 3.8](#) is quite elaborate. It will first involve a multi-step analysis of the connectedness of resolutions of the dual graph determined by hooks, then go through an elimination process making use of a result on the flexibility of fiber surfaces. The proof will occupy the rest of this section.

We first set up some notation. Suppose  $s$  is a sector of  $B$  of minimum weight. Without loss of generality suppose that  $s$  is blue. Label the edges of  $\Gamma$  on the sides of  $s$  as in [Definition 3.2](#). Let  $s_k^\beta$  be the sector that has  $e_k^\beta$  as a top side. Let  $v_k^\beta$  be the top vertex of  $s_k^\beta$ . In other words,  $v_k^\beta$  is the vertex shared by  $e_k^\beta$  and  $e_{k+1}^\beta$ . By extension, we also let  $v_0^\beta$  be the bottom vertex of  $s$  and write  $v_0 = v_0^\beta$  for both sides  $\beta$ . See [Figure 11](#). For the figures in this section, we will take  $\beta$  to be the left hand side of  $s$ .

Notice that the vertices  $v_k^\beta$  are not necessarily distinct, but if we have  $v_{k_1}^\beta = v_{k_2}^\beta$  for distinct  $k_1, k_2 = 1, \dots, \delta_\beta$ , then the identification cannot be such that  $e_{k_1}^\beta = e_{k_2}^\beta$ , for otherwise the sector  $s$  will not be embedded in its interior. Also, we cannot have  $v_1^\beta = v_k^\beta$  for  $2 \leq k \leq \delta_\beta$ , since  $v_1^\beta$  is the top vertex of a toggle sector, whereas  $v_k^\beta$  are the top vertices of fan sectors for  $2 \leq k \leq \delta_\beta - 1$ , and  $v_{\delta_\beta}^\beta$  is of the opposite color as  $v_1^\beta$ , by [Proposition 2.11](#). For the same reason, we cannot have  $v_{\delta_\beta}^\beta = v_k^\beta$  for  $1 \leq k \leq \delta_\beta - 1$ .

Let  $h'_\beta$  be the edge path  $(e_2^\beta, \dots, e_{\delta_\beta}^\beta)$  and consider the resolution  $\Gamma(h'_\beta)$  of  $\Gamma$  determined by  $h'_\beta$ , for some chosen side  $\beta$ . Notice that all the resolutions in  $h'_\beta$  are B-resolutions of red vertices.

**Lemma 3.9.**  $\Gamma(h'_\beta)$  is always connected.

*Proof.* Notice that the lemma is vacuously true if  $\delta_\beta = 1$ , so we can assume that  $\delta_\beta \geq 2$ .

Suppose that  $\Gamma(h'_\beta)$  is not connected. Let  $C_0$  be the component that contains  $h'_\beta$  and let  $C_1$  be a component that is not  $C_0$ . Let  $J$  be the collection of indices  $k$  such that  $v_k^\beta$  meets the image of  $C_1$  under the map  $\Gamma(h'_\beta) \rightarrow \Gamma$ .  $J$  must be nonempty since the only resolutions we perform are at  $v_k^\beta$ .

Consider the union of sectors  $s_2^\beta \cup \dots \cup s_{\delta_\beta}^\beta$ , which is a rectangle. Since the only resolutions we perform are B-resolutions on red vertices, by following along the top sides of the rectangle, we see that the side vertex of  $s_{\delta_\beta}^\beta$  other than  $v_{\delta_\beta-1}^\beta$ , which we denote by  $v$ , meets  $C_0$ . If this vertex does not meet  $C_1$ , then again by the fact that the only resolutions we perform are B-resolutions of red vertices, by following along the bottom side of the rectangle that meets  $v$ , we see that none of the sides of the rectangle meet  $C_1$ . This implies that for any  $k \in J$ , the bottom vertex of  $s_{k+1}^\beta$  must be resolved and meets  $C_1$ , hence is equal to  $v_{k'}^\beta$  for some  $k' \in J$ .

The assignment  $k \mapsto k'$  thus defines a permutation  $\sigma : J \rightarrow J$ , under which  $C_1$  is the union of the top sides of  $s_k^\beta$  in the interior of the rectangle for  $k \in J$ , joined together according to  $\sigma$ . But then  $C_1$  will be a branch cycle containing only red vertices, contradicting [Proposition 2.12](#).

Hence  $v$  must be resolved and meets  $C_1$ , which implies that  $v = v_k^\beta$  for some  $k \in J$ . Moreover, as seen above, the top sides of the rectangle lie in  $C_0$ , hence the identification of vertices must be in the manner such that  $s_{\delta_\beta}^\beta = s_{k+1}^\beta$ .

However, since the top vertex of  $s_{\delta_\beta}^\beta$  is blue, we must have  $k = \delta_\beta - 1$ . But this cannot be since it implies that  $s_{\delta_\beta}^\beta$  is not embedded in its interior.  $\square$

[Lemma 3.9](#) forms the basis of our first application of [Proposition 3.7](#) in the following [Lemma 3.10](#).

Before that, we set up yet more notation. Let  $q_k^\beta$  be the B-quad in the tetrahedron dual to  $v_k^\beta$ , for  $k = 1, \dots, \delta_\beta - 1$ , and let  $q_{\delta_\beta}^\beta$  be the A-quad in the tetrahedron dual to  $v_{\delta_\beta}^\beta$ .

We illustrate these quads in [Figure 12](#) right, in the case when  $\beta$  is short at the top and in the case when  $\beta$  is long at the bottom. In the figure, we lay out the quads from left to right by the tetrahedra in which they lie from top to bottom in the stack. For each quad, the top left edge is the top edge of the tetrahedron it lies in, while the bottom right edge is the bottom edge of the tetrahedron it lies in. In particular, for each  $i$ , the two edges on the right of  $q_i^\beta$  are the same two edges on the left of  $q_{i-1}^\beta$ , so if we take the union  $\bigcup_{i=1}^{\delta_\beta} q_i^\beta$  of all the quads, they fit together to give a big diamond with two blue edges and two red edges in the boundary, see [Figure 13](#).

In the rest of this section, we will study the connectivity of  $\Delta \parallel \bigcup_{k \in J} q_k^\beta$  for various sets  $J \subset \{1, \dots, \delta_\beta\}$ . In this setting, each  $q_k^\beta$ ,  $k \in J$ , will meet one or two components of



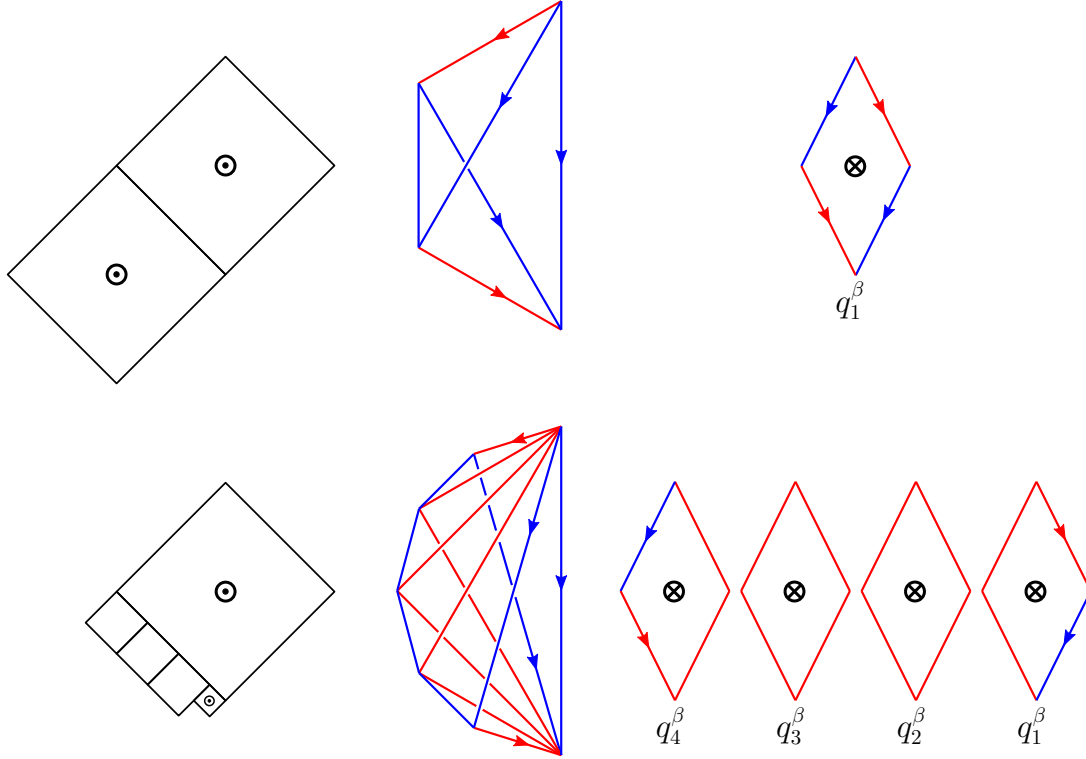


FIGURE 12. The quads that can appear in  $Q(h_\beta)$ . Top: When  $\beta$  is short. Bottom: When  $\beta$  is long. We lay out the quads from left to right by the tetrahedra in which they lie from top to bottom in the stack. For each quad, the top left edge is the top edge of the tetrahedron it lies in, while the bottom right edge is the bottom edge of the tetrahedron it lies in. Moreover, we have indicated a choice of orientation on some of the edges for ease of reference. We coorient the quads as indicated whenever consistent.

$\Delta \setminus \bigcup_{k \in J} q_k^\beta$ , and at least one of the components it meets will contain the hook  $h_\beta$ . If some  $q_k^\beta$  meets exactly two components, then we coorient it to point out of the component containing  $h_\beta$ . On the other hand, if  $q_k^\beta$  meets only one component, then there is no canonical way to coorient it. More succinctly, this means that we coorient the quads  $q_k^\beta$ ,  $k = 1, \dots, \delta_\beta$ , as indicated in Figure 12 (that is, into the page) whenever consistent.

**Lemma 3.10.** *If  $h_\beta$  is not deep, then  $\Gamma(h_\beta)$  is connected.*

*Proof.* Recall that the assumption means that  $h_\beta$  does not contain  $v_1^\beta$  in its interior.

Consider the 2-complex  $Q(h_\beta)$  as in Section 3.2. In our notation, we have  $Q(h_\beta) = \bigcup_{i=k_\beta}^{\delta_\beta} q_i^\beta$  for some  $k_\beta \geq 2$ . In particular, notice that since  $v_1^\beta$  is not resolved, there is at most one quad with a blue edge, namely the A-quad  $q_{\delta_\beta}^\beta$  which has exactly one blue edge (or no such quad exists if  $\beta$  is short).

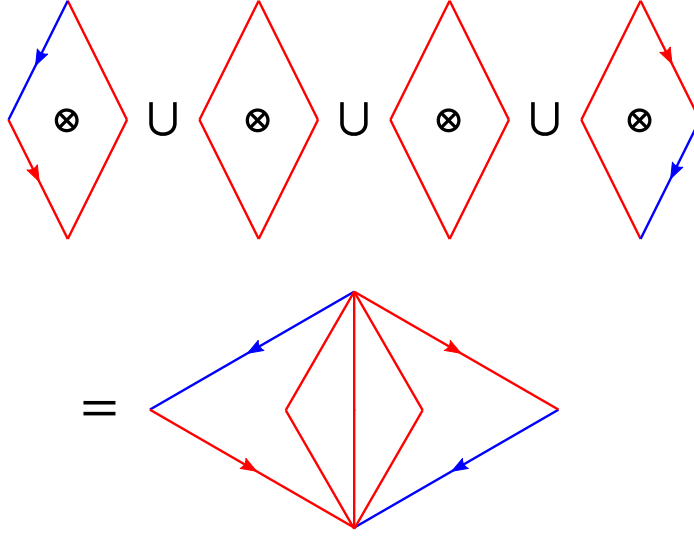


FIGURE 13. If we take the union  $\bigcup_{i=1}^{\delta_\beta} q_i^\beta$ , the quads fit together to give a big diamond with two blue edges and two red edges in the boundary. Here we illustrate the situation for Figure 12 bottom.

This implies that if we have a 2-cycle of  $Q(h_\beta)$  that is homologically trivial in  $T_f$  and where all the coefficients are  $\pm 1$ , then such a cycle cannot contain  $q_{\delta_\beta}$ , for otherwise the boundary of the cycle will contain a single blue edge with no other edge to cancel it out. But then the 2-cycle will in fact be a 2-cycle of  $Q(h'_\beta)$  that is homologically trivial in  $T_f$ , which contradicts Lemma 3.9 by Proposition 3.7.  $\square$

Thus if we have a minimum weight sector that has a non-deep hook, then we are already done. Such a scenario, however, is not always true, so we have to analyze how Lemma 3.10 fails when  $h_\beta$  is deep.

**Lemma 3.11.** *If  $h_\beta$  is deep, then  $\Gamma(h_\beta)$  is connected unless  $v_{\delta_\beta}^\beta$  is equal to the bottom vertex of  $s_1^\beta$ , in the manner such that the bottom side of  $s_1^\beta$  containing  $e_{\delta_\beta+1}^\beta$  meets  $v_0$  as well. See Figure 14 left.*

*In particular if  $s$  is fan, then  $v_{\delta_\beta}^\beta = v_0$ , in the manner such that  $(e_{\delta_\beta+1}^\beta, e_1^\beta)$  takes an anti-branching turn at  $v_0$ . See Figure 14 right.*

**Definition 3.12.** We say that a fan sector  $s$  satisfies condition (TBT) (abbreviating **T**op = **B**ottom by **T**ranslation) if it satisfies the condition in the second paragraph of Lemma 3.11.

*Proof of Lemma 3.11.* Since  $h_\beta$  is deep, the 2-complex  $Q(h_\beta) = \bigcup_{i=1}^{\delta_\beta} q_i^\beta$ .

Suppose  $\Gamma(h_\beta)$  is not connected. Consider the component containing  $h_\beta$ . This corresponds to some component  $C$  of  $\Delta \setminus Q(h_\beta)$ . Consider the 2-cycle  $x$  of  $Q(h_\beta)$  corresponding to  $C$ .

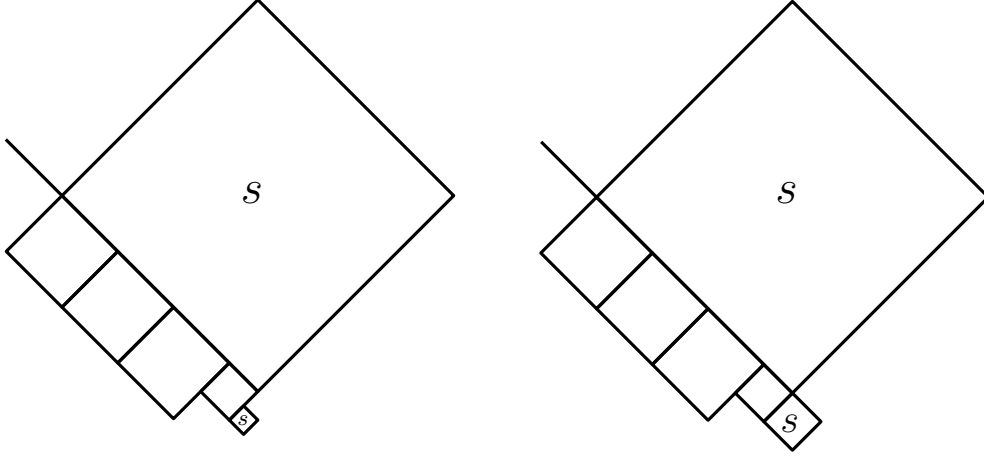


FIGURE 14.  $\Gamma(h_\beta)$  is connected unless the scenario depicted on the left occurs. If  $s$  is fan, then the left figure specializes to the right figure, and we say that  $s$  satisfies condition (TBT).

Since we have cooriented all the quads out of  $C$  whenever possible, we can assume that all the coefficients in  $x$  are 1.

As opposed to the situation in [Lemma 3.10](#), if  $\delta_\beta \geq 2$ , we now have 2 quads that have a blue edge, namely the B-quad  $q_1^\beta$  and the A-quad  $q_{\delta_\beta}^\beta$ , which each have exactly one blue edge, or if  $\delta_\beta = 1$ , the single A-quad has exactly two blue edges.

The 2-cycle  $x$  must contain both of the quads that have blue edges and the two blue edges must be the same edge in  $\Delta$ , for otherwise, as in [Lemma 3.10](#), there would be a contradiction to [Lemma 3.9](#). Moreover, the two blue edges have to be identified in such a way that they cancel each other out in the boundary of  $x$ .

Thus the first statement of the lemma follows from the fact that the 2 blue edges are dual to the sector with  $v_{\delta_\beta}^\beta$  as the bottom vertex and  $s_1^\beta$  respectively, and the manner of identification is as described in the lemma.

When  $s$  is fan,  $e_{\delta_\beta+1}^\beta$  will be a bottom side of  $s_1^\beta$  by [Proposition 2.11](#), hence the second statement follows.  $\square$

The intuition at this point is that  $\Gamma(h_\beta)$  should be connected for ‘generic’ sides  $\beta$ , since it is unlikely, for a ‘generic’ triangulation, to have many edge identifications as described in [Lemma 3.11](#). However, notice that we require  $\beta$  to be a side of a minimum weight sector in [Proposition 3.3](#), and at a first glance, minimum weight sectors might not seem ‘generic’. Fortunately, if we allow the fiber surface to vary, we have the following proposition that allows us to make an argument based on this intuition.

To simplify the language, let us call an arc on a sector *deep* if both of its endpoints lie on  $e_1^\beta$  for the two sides  $\beta$ , and let us call a sector *deep* if it contains a deep arc. In other words, both hooks of a sector  $s$  are deep if and only if  $s$  is deep.

**Proposition 3.13.** *For any sector  $s$ , there exists a fiber surface  $S$  such that  $s$  is the only deep sector.*

*Proof.* Fix some fiber surface  $S'$ . Consider the  $\mathbb{Z}$ -cover  $\widehat{T}_f$ . Recall that  $S'_r$  is the lift of  $S'$  at height  $r$ . Let  $\widehat{s}_0$  be the lift of  $s$  that is at height 0. Let  $R'$  be the union of sectors of  $\widehat{B}$  that can be reached from  $\widehat{s}_0$  via a path passing through  $\leq -3\chi(S)$  sectors.  $R'$  is a compact set, so there exists  $r_1 < r_2$  so that the region  $R$  bounded by  $S'_{r_1}$  and  $S'_{r_2}$  contains  $R'$ .

Now starting at  $\widehat{F}_0 = S'_{r_2}$ , inductively perform the following procedure: The image  $F_i$  of  $\widehat{F}_i$  in  $T_f$  is some fiber surface. If some sector  $t$  other than  $s$  has a deep arc  $a$ , push  $F_i$  downwards near  $a$  through a vertex of  $B$  to get another fiber surface  $F_{i+1}$ . In  $\widehat{T}_f$ , we have pushed  $\widehat{F}_i$  across a vertex of  $\widehat{B}$ . Since the intersection of  $\widehat{F}_i$  with  $\widehat{B}$  is a train track with  $-3\chi(S)$  branches, and since we never push across  $\widehat{s}_0$ ,  $\widehat{F}_i$  must stay within  $R$ . Since there are finitely many vertices in  $R$ , this procedure ends eventually and we have the desired fiber surface.  $\square$

The strategy to proving [Proposition 3.8](#) is now apparent: For each sector  $s$  of  $B$ , we take a fiber surface  $S$  as in [Proposition 3.13](#) and see if there is a minimum weight sector that is not deep. If so, [Lemma 3.10](#) and [Proposition 3.6](#) implies [Proposition 3.8](#). If not, that is, every minimum weight sector is deep, then  $s$  is the only minimum weight sector. Consider the two hooks  $h_\beta$  of  $s$ . If  $s$  is fan, then either some  $\Gamma(h_\beta)$  is connected, in which case [Proposition 3.6](#) implies [Proposition 3.8](#), or [Lemma 3.11](#) shows that  $s$  satisfies (TBT). By applying this argument to all fan sectors  $s$ , we see that either [Proposition 3.8](#) is true, or all fan sectors satisfy (TBT). The next ingredient we need in the proof is the following proposition which concerns the toggle sectors in the latter case.

**Lemma 3.14.** *Suppose condition (TBT) is satisfied for all fan sectors. Suppose  $s$  is a toggle sector and let  $h_\beta$  be a hook of  $s$ . Then  $\Gamma(h_\beta)$  is connected unless  $e_{\delta_\beta+1}^\beta = e_1^\beta$ . See [Figure 15](#) left.*

**Definition 3.15.** We say that a sector  $s$  satisfies condition (SBF) (abbreviating **Side = Bottom by Flip**) on the side  $\beta$  if it satisfies the condition in [Lemma 3.14](#).

We say that a sector  $s$  satisfies condition (BSBF) (abbreviating **Both Sides = Bottom by Flips**) if it satisfies (SBF) on both sides. See [Figure 15](#) right.

*Proof of [Lemma 3.14](#).* Suppose  $\Gamma(h_\beta)$  is not connected. Consider the component containing  $h_\beta$ . This corresponds to some component  $C$  of  $\Delta \setminus Q(h_\beta)$ , which in turn corresponds under [Proposition 3.7](#) to some 2-cycle  $x$  of  $Q(h_\beta)$ .

Recall the construction of  $x$ . We look at the union of quads in the boundary of  $C$  in  $\Delta$  and take their sum. Since  $C$  contains  $h_\beta$ , every quad  $q_k^\beta$  appears in the union. After taking the sum, the quad  $q_k^\beta$  does not appear in  $x$  if and only if it appears twice in the union, necessarily with opposite orientations. There is a dichotomy here. A quad  $q_k^\beta$  could

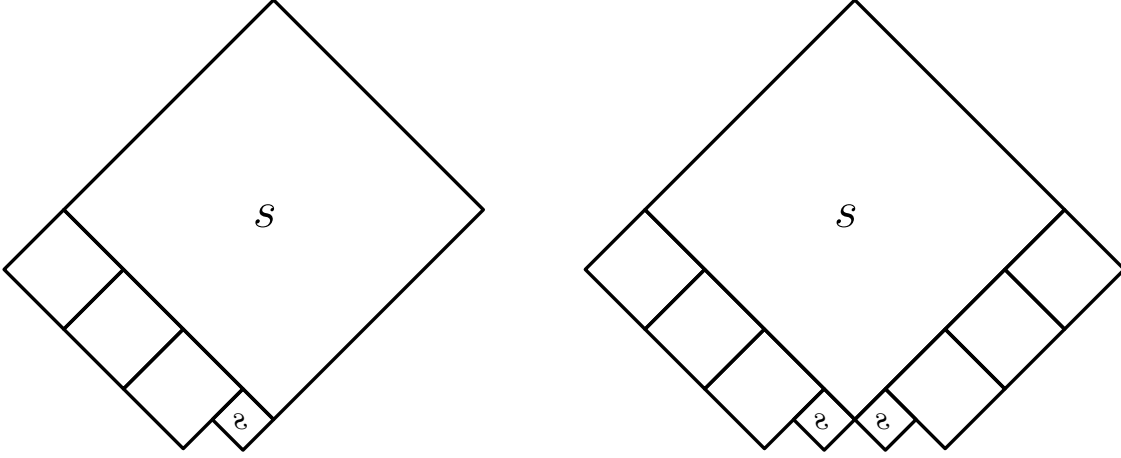


FIGURE 15. If condition (TBT) is satisfied for all fan sectors,  $\Gamma(h_\beta)$  is connected unless the scenario depicted on the left occurs, in which case we say that  $s$  satisfies (SBF) on the side  $\beta$ . If  $s$  satisfies (SBF) on both sides, then we have the right figure, and we say that  $s$  satisfies the condition (BSBF).

appear twice because  $q_k^\beta = q_{k'}^\beta$  for some  $k' \neq k$ , or it could appear twice even if it is distinct from all other  $q_{k'}^\beta$ . In the former case, we will say that  $q_k^\beta$  is *overlapped*, while in the latter case, we will say that  $q_k^\beta$  is *omitted*.

We claim that under the assumption of the lemma, no  $q_k^\beta$  is omitted.

First notice that as reasoned in the proof of [Lemma 3.11](#),  $q_1^\beta$  and  $q_{\delta_\beta}^\beta$  must appear in  $x$ , so they are not omitted. We show that  $q_k^\beta$ , for  $k = 2, \dots, \delta_\beta - 1$ , are not omitted by downwards induction.

Consider the sector  $s_{\delta_\beta-1}^\beta$ . It is fan, so by assumption it satisfies (TBT). Hence it is also the sector having  $v_{\delta_\beta-1}^\beta$  as its bottom vertex, and contains  $v_{\delta_\beta}^\beta$  on its bottom side that does not meet  $s_{\delta_\beta-2}^\beta$ . Now if  $q_{\delta_\beta-1}^\beta$  is omitted, the bottom vertex of  $s_{\delta_\beta}^\beta$  must be resolved, otherwise by following along the sides of  $s_{\delta_\beta-1}^\beta$ , we see that  $v_{\delta_\beta}^\beta$  does not meet any component of  $\Gamma(h_\beta)$  other than  $C$ , hence  $q_{\delta_\beta}^\beta$  must be omitted in  $x$ , contradicting what we established above. So we suppose that this bottom vertex is equal to  $v_j^\beta$  for some  $j$ . This identification cannot be so that  $v_{\delta_\beta-1}^\beta = v_{j+1}^\beta$ , for otherwise since  $v_{\delta_\beta-1}^\beta$  is red, we must have  $j \leq \delta_\beta - 2$ , and  $q_{\delta_\beta-1}^\beta$  would be overlapped (by  $q_{j+1}^\beta$ ), not omitted. But in the other manner of identification we also have that  $v_{\delta_\beta}^\beta$  does not meet any component of  $\Gamma(h_\beta)$  other than  $C$ , giving us a contradiction as above.

Inductively, suppose we have shown that  $q_k^\beta$  is not omitted for some  $3 \leq k \leq \delta_\beta - 1$ . Consider the sector  $s_k^\beta$ . Since it satisfies (TBT), both its top and bottom vertices are  $v_k^\beta$ . If  $v_{k-1}^\beta$  is omitted, then by following along the sides of  $s_k^\beta$  containing  $v_{k-1}^\beta$ , we see that  $v_k^\beta$  does not meet any component of  $\Gamma(h_\beta)$  other than  $C$ . So  $q_k^\beta$  must be overlapped, say  $q_k^\beta = q_j^\beta$ . But

then since  $v_{k-1}^\beta$  is red, we must have  $j \leq \delta_\beta - 2$ , and  $q_{k-1}^\beta$  would be overlapped (by  $q_{j+1}^\beta$ ), not omitted. By induction this proves our claim that no  $q_k^\beta$  is omitted.

We note that we could have alternatively performed upwards induction here, see [Remark 2.13](#).

The upshot here is that the edges in the boundary of the union  $\bigcup_{k=1}^{\delta_\beta} q_k^\beta$  must cancel themselves out. This is because the same is true for the 2-cycle  $x$ , and the edges in the boundary of quads not appearing in  $x$  cancel out in pairs of overlapped quads.

As pointed out before [Lemma 3.10](#), the boundary of  $\bigcup_{k=1}^{\delta_\beta} q_k^\beta$  consists of 4 edges, two of which are blue and two are red. The blue edges cancelling each other out is the content of [Lemma 3.11](#). Now we also know that the two red edges cancel each other out, which by [Proposition 2.11](#) and the fact that  $s$  is toggle, implies the statement of the current lemma.  $\square$

Returning to our proof of [Proposition 3.8](#), which was suspended before [Lemma 3.14](#), by now taking  $s$  to be each toggle sector, we see that either some  $\Gamma(h_\beta)$  is connected, in which case [Proposition 3.6](#) implies [Proposition 3.8](#), or all toggle sectors  $s$  satisfies (BSBF). Hence our proof of [Proposition 3.8](#) is finally concluded by the following proposition.

**Proposition 3.16.** *Let  $\Delta$  be a veering triangulation and  $B$  be its stable branched surface. If every fan sector of  $B$  satisfies (TBT) and every toggle sector of  $B$  satisfies (BSBF), then  $\Delta = \text{cPcbbb}d\text{zxm.10}$ .*

*Proof.* Let  $t$  be a toggle tetrahedron in  $\Delta$ . Suppose the top edge of  $t$  is blue. Then the vertex  $v$  of  $B$  dual to  $t$  is the bottom vertex of some blue sector  $s$ .  $s$  must be toggle, otherwise since every fan sector satisfies (TBT), the sector below  $s$  must be fan, hence blue, contradicting the fact that the bottom edge of  $t$  is red.

Hence  $s$  satisfies (BSBF), so the two blue side edges of  $t$  must be equal (and in fact equals the top edge of  $t$ ) and be identified in a parallel way.

Meanwhile, let  $s'$  be the sector that has  $v$  as the top vertex. Similarly as above, since  $s'$  satisfies (BSBF), the two red side edges of  $t$  must be equal (and in fact equals to the bottom edge of  $t$ ) and be identified in a parallel way.

Now consider a quadrilateral-with-4-ideal-vertices properly embedded in  $t$  with its 4 sides along the side edges of  $t$ . By our reasoning above, the sides match up in pairs to form an once-punctured torus  $T$  in  $T_f$ . The quadrilateral can be chosen so that the intersection of  $B$  with  $T$  is a train track  $\tau$  of the form illustrated in [Figure 16](#). In particular, using the language of [\[Lan23\]](#), no splitting of  $\tau$  can contain a *stable loop*. Thus by [\[Lan23, Proposition 4.4 and Proposition 4.6\]](#),  $T$  is a fiber surface.

Once-punctured torus bundles and their veering triangulations are well-studied. These triangulations are encoded by a periodic path in the Farey tessellation, with each edge corresponding to a turn in the path; blue edges for left turns and red edges for right turns. We refer to [\[Gué06\]](#) for details. In particular, it can be checked that no fan sector of these



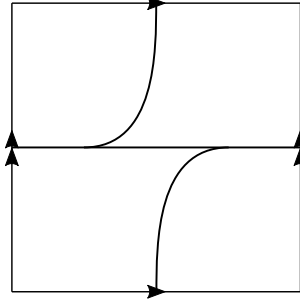


FIGURE 16. If every fan sector satisfies (TBT) and every toggle sector satisfies (BSBF), then we can find an equatorial quadrilateral that meets  $B$  in the depicted train track.

can satisfy (TBT). Moreover, (BSBF) for a single toggle sector implies that the path in the Farey tessellation has period 2, and that the triangulation is `cPcbbbdxm_10`.  $\square$

**Remark 3.17.** [Proposition 3.8](#) is sharp in the sense that when  $\Delta = \text{cPcbbbdxm\_10}$ ,  $\Gamma(h_\beta)$  is disconnected for every deep hook  $h_\beta$ .

[Proposition 3.3](#) and [Proposition 3.8](#) give the first main theorem of this paper.

**Theorem 3.18.** *Let  $f : S \rightarrow S$  be a fully-punctured pseudo-Anosov map with normalized dilatation  $\lambda^{-\chi}$ . Then the mapping torus of  $f$  admits a veering triangulation with less than or equal to  $\frac{1}{2}\lambda^{-2\chi}$  tetrahedra.*

*Proof.* If  $\Delta \neq \text{cPcbbbdxm\_10}$ , then by [Proposition 3.8](#), there exists an Eulerian circuit that hooks around a sector of minimum weight, thus the theorem follows from [Proposition 3.3](#).

If  $\Delta = \text{cPcbbbdxm\_10}$ , then  $T_f$  fibers in a unique way as an once-punctured torus bundle. In this case, it is straightforward to calculate that  $\lambda = \mu^2$  and  $\chi = -1$ , so we can check that the number of tetrahedra, which is 2, is less than  $\frac{1}{2}\lambda^{-2\chi} = \frac{1}{2}\mu^4 \approx 3.43$ .  $\square$

[Theorem 1.4](#) follows immediately from [Theorem 3.18](#).

For non-fully-punctured pseudo-Anosov maps, we have the following corollary.

**Corollary 3.19.** *Let  $f : S_{g,s} \rightarrow S_{g,s}$  be a pseudo-Anosov map on the surface  $S_{g,s}$  with genus  $g$  and  $s$  punctures with dilatation  $\lambda$ . Suppose  $\lambda^{2g-2+\frac{2}{3}s} \leq P$ , then the fully-punctured mapping torus of  $f$  admits a veering triangulation with less than or equal to  $\frac{1}{2}P^6$  tetrahedra.*

*Proof.* We can fully puncture  $f$  at its singularities to get  $f^\circ : S^\circ \rightarrow S^\circ$ . Since each singularity is at least 3-pronged, and each puncture on  $S_{g,n}$  is at least 1-pronged, we at most puncture at  $2(-\chi(S_{g,n}) - \frac{n}{2}) = 4g - 4 + n$  points. Hence  $\chi(S^\circ) \leq -\chi(S_{g,n}) + (4g - 4 + n) = 3(2g - 2 + \frac{2}{3}n)$  and the corollary follows from [Theorem 1.4](#).  $\square$

## 4. DOUBLE HOOK CIRCUITS

As explained in the introduction, we must further improve the bound of [Theorem 1.4](#) in order to prove [Theorem 1.6](#) (at least in the one boundary component case). In this section we present one possible approach for obtaining an improvement. The idea is to use two hook circuits or a circuit that hooks twice. In contrast with using single hook circuits in [Section 3](#), we refer to this approach as using double hook circuits. The resulting improved bound is recorded as [Proposition 4.3](#), which we will explain in [Section 4.1](#).

Unfortunately, we are unable to show that such double hook circuits always exist. In [Section 4.2](#), we describe the obstructions to their existence. This understanding of obstructions will be used in [Section 5](#) to show that when  $T_f$  has only one boundary component, we can sometimes bypass the obstructions and use the sharper bound in [Proposition 4.3](#).

**4.1. Bounding the number of vertices using double hook circuits.** We continue the notation from [Section 3](#). In addition, we introduce two more pieces of terminology.

**Definition 4.1.** Let  $\{c_1, \dots, c_n\}$  be a collection of circuits in a directed graph. The collection is said to be *Eulerian* if every edge is tranversed exactly once by some  $c_i$ .

**Definition 4.2.** Let  $s$  be a sector of  $B$ . A circuit of  $\Gamma$  is said to *hook around  $s$  twice* if it contains both hooks of  $s$ . If the sector  $s$  is understood, we say that a vertex of  $c$  is a hook vertex if it lies in the interior of  $h_1$  or  $h_2$ .

**Proposition 4.3.** *Let  $s$  be a sector of  $B$  of minimum weight. Suppose one of the following two scenarios is true:*

- (i) *There exists an Eulerian collection of two circuits  $\{c_1, c_2\}$  in  $\Gamma$  where both  $c_1$  and  $c_2$  hook around  $s$*
- (ii) *There exists an Eulerian circuit  $c$  in  $\Gamma$  that hooks around  $s$  twice*

*Then the number of tetrahedra in the veering triangulation is  $\leq \frac{1}{4}\lambda^{-2x} + 1$ .*

*Proof.* We first show the bound in case (i). The argument reuses a lot of the ideas from [Proposition 3.3](#).

Suppose  $c_i$  contains the hook  $h_i$  of  $s$ , for  $i = 1, 2$ . Let  $\widehat{s}_0$  be the lift of  $s$  in  $\widehat{B}$  that is of height 0. For each  $i$ , take the basepoint of  $c_i$  to be the top vertex of  $s$ . Lift  $c_i$  to a path  $\widehat{c}_i$  ending at the top vertex of  $\widehat{s}_0$ , reverse its orientation, then push it downwards to get a descending path  $\alpha_i$ .

Let the length of  $c_i$  be  $n_i$ , and suppose it intersects the fiber surface  $S$  for  $p_i$  times. Then since  $\{c_1, c_2\}$  is Eulerian,  $n_1 + n_2$  is equal to two times the number of tetrahedra  $N$  in the triangulation, while  $p_1 + p_2$  is equal to  $-2\chi(S)$ .

As in the proof of [Proposition 3.3](#), we get two equations

$$(4.1) \quad \lambda^{p_i} w = w + \sum_{j=1}^{n_i} w_{i,j}$$

where  $w_{i,j}$  is the weight of the  $j^{\text{th}}$  sector merging into  $\alpha_i$ .

Also as in [Proposition 3.3](#), we say that a vertex  $v$  in  $\Gamma$  is *A-resolved* if the  $c_i$  take an anti-branching turn the two times they visit  $v$ , and say that  $v$  is *B-resolved* otherwise.

For a term in  $W = \sum_{j=1}^{n_1} w_{1,j} + \sum_{j=1}^{n_2} w_{2,j}$  corresponding to a vertex  $v$  of  $c$  not covering a hook vertex of  $c_1$  or  $c_2$ , we can use the lower bound  $\lambda^{-r_v} w \geq w$  where  $r_v$  is the height of  $v$ .

As in [Proposition 3.3](#), for each B-resolved hook vertex  $u$ , we group together the two terms in  $W$  that correspond to the two vertices of  $\hat{c}$  covering the vertex of  $\Gamma$  that  $u$  lies at. The same argument shows that the sum of the pair of terms is bounded below by  $\lambda^{-r_1+d_u} w + \lambda^{-r_2-d_u} w \geq 2w$ .

In this setting, there are two A-resolved hook vertices, so the argument implies that  $W \geq (2N - 2)w$ . Meanwhile, we can multiply [Equation \(4.1\)](#) for  $i = 1, 2$  to get

$$\lambda^{-2x} = \left(1 + \frac{1}{w} \sum_{j=1}^{n_1} w_{1,j}\right) \left(1 + \frac{1}{w} \sum_{j=1}^{n_2} w_{2,j}\right)$$

where  $\left(1 + \frac{1}{w} \sum_{j=1}^{n_1} w_{1,j}\right) + \left(1 + \frac{1}{w} \sum_{j=1}^{n_2} w_{2,j}\right) = 2 + \frac{1}{w} W \geq 2N$ .

Here is where we bring in a new ingredient: We claim that  $\frac{1}{w} \sum_{j=1}^{n_i} w_{i,j} \geq 1$  for each  $i$ . If the hook  $h_i$  is simple, that is, the degenerate case in [Definition 3.2](#) does not occur, then this is because the term corresponding to the first non-hook vertex is the weight of a sector at non-positive height, hence is  $\geq w$ . If  $h_i$  is not simple, then observe that the starting point and ending point of  $\alpha_i$  belong to adjacent sectors. We can take a descending path from the former to the latter that intersects the branch locus of  $\hat{B}$  exactly once, and the weight added along that intersection is the weight of a sector at non-positive height, hence is  $\geq w$ . See [Figure 17](#) where we highlight this descending path in orange. Hence  $\sum_{j=1}^{n_i} w_{i,j} = \lambda^{p_i} w - w \geq w$ .

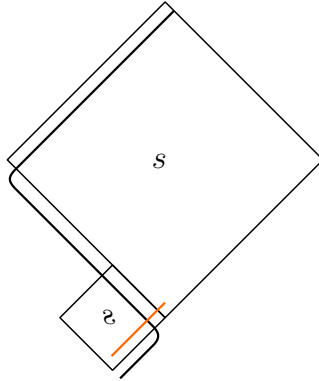


FIGURE 17. If  $h_i$  is not simple, we can use a descending path (in orange) to show that  $\frac{1}{w} \sum_{j=1}^{n_i} w_{i,j} \geq 1$ .

The claim implies that

$$\lambda^{-2x} = \left(1 + \frac{1}{w} \sum_{j=1}^{n_1} w_{1,j}\right) \left(1 + \frac{1}{w} \sum_{j=1}^{n_2} w_{2,j}\right) \geq 2(2N - 2)$$

which implies the bound in the proposition.

Now for case (ii), if the top vertex of  $s$  is not a hook vertex of  $c$ , then we can cut and paste  $c$  at that point to get an Eulerian collection of circuits  $\{c_1, c_2\}$ , where each  $c_i$  hooks around  $s$ , so we reduce to case (i).

If the top vertex of  $s$  is a hook vertex, say it lies in the interior of  $h_1$ , then we can do the cut and paste operation anyway to get an Eulerian collection of circuits  $\{c_1, c_2\}$ . See [Figure 18](#). The difference here is that the component containing the vertices in the interior of  $h_1$ , say  $c_1$ , may no longer contain the entirety of  $h_1$  hence not hook around  $s$  by definition. However the above argument still works since the only place we use the fact that  $c_1$  contains the entirety of  $h_1$  is to say that the terms  $w_{1,j}$  corresponding to vertices of  $\widehat{c}_1$  not covering hook vertices are weights of sectors of non-positive height (hence are  $\geq w$ ). In this case there are simply no such vertices and so we do not have to worry about establishing the lower bounds for them. Thus the argument in case (i) carries through to show the same bound.  $\square$

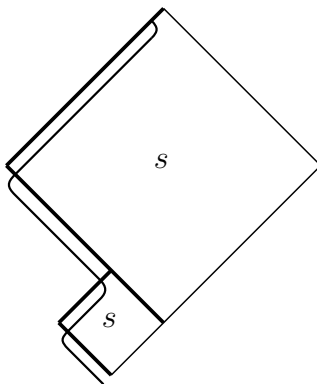


FIGURE 18. In case (ii), if  $e_{\delta_2+1}^2 = e_1^1$ , then we can cut and paste  $c$  to get an Eulerian collection of circuits  $\{c_1, c_2\}$ .  $c_1$  will not contain the hook  $h_1$  (thickened) but the argument goes through.

**4.2. Obstructions to double hook circuits.** We have the following analogue of [Proposition 3.6](#) for applying [Proposition 4.3](#).

**Proposition 4.4.** *Let  $s$  be a sector of  $B$ . Suppose one of the following two statements about the resolved dual graph  $\Gamma(h_1 \cup h_2)$  is true:*

- (I)  $\Gamma(h_1 \cup h_2)$  is connected
- (II)  $\Gamma(h_1 \cup h_2)$  has two components, with one component containing  $h_1$  and the other containing  $h_2$

Then the hypothesis of [Proposition 4.3](#) is true. That is, one of the following two scenarios is true:

- (i) There exists an Eulerian collection of two circuits  $\{c_1, c_2\}$  in  $\Gamma$  where both  $c_1$  and  $c_2$  hook around  $s$
- (ii) There exists an Eulerian circuit  $c$  in  $\Gamma$  that hooks around  $s$  twice

*Proof.* In case (I), we can find an Eulerian circuit in  $\Gamma(h_1 \cup h_2)$  whose image in  $\Gamma$  is an Eulerian circuit that hooks around  $s$  twice, so (ii) is true.

In case (II), we can find an Eulerian circuit in each component of  $\Gamma(h_1 \cup h_2)$  whose images in  $\Gamma$  form an Eulerian collection of circuits that each hook around  $s$ , so (i) is true.  $\square$

For the rest of this section, we will state and prove some conditions on  $s$  under which we can show that (I) or (II) in [Proposition 4.4](#) is true. Some of these will be analogues of statements in [Section 3.3](#), and our approach in fact will closely mirror that in [Section 3.3](#).

We fix a sector  $s$  of  $B$ . Suppose without loss of generality that  $s$  is blue. We will use the same notation as in [Section 3.3](#) for the edges, sectors, and vertices adjacent to  $s$ .

Recall that  $h'_\beta = (e_2^\beta, \dots, e_{\delta_\beta}^\beta)$ . Consider the resolution  $\Gamma(h'_1 \cup h'_2)$  determined by the two paths  $h'_1$  and  $h'_2$ . As in [Lemma 3.9](#), all the resolutions are B-resolutions of red vertices.

**Lemma 4.5.**  $\Gamma(h'_1 \cup h'_2)$  is either connected or has two components. In the latter case,  $v_{\delta_1}^1 = v_{\delta_2}^2$  and the component not containing  $h'_1 \cup h'_2$  contains at least one branch cycle.

**Definition 4.6.** We say that a sector  $s$  satisfies condition (FRC) (abbreviating **F**an **R**esolution **C**onected) if the resolution  $\Gamma(h'_1 \cup h'_2)$  is connected for  $s$ .

*Proof of Lemma 4.5.* Notice that if some  $\delta_\beta = 1$ , then this reduces to [Lemma 3.10](#), so we can assume that  $\delta_1, \delta_2 \geq 2$ .

Suppose that  $\Gamma(h'_1 \cup h'_2)$  is not connected. By following the bottom sides of  $s$ , we see that  $h'_1$  and  $h'_2$  lie in the same component  $C_0$ . Let  $C_1$  be a component that is not  $C_0$ . Similarly as in [Lemma 3.9](#), let  $J$  be the collection of  $(\beta, k)$  such that  $v_k^\beta$  meets  $C_1$ .

Let  $v^\beta$  be the side vertex of  $s_{\delta_\beta}^\beta$  other than  $v_{\delta_\beta-1}^\beta$ . The same argument as in [Lemma 3.9](#) shows that at least one of  $v^\beta$ , say,  $v^1$ , must be resolved and meets  $C_1$ , otherwise a permutation on  $J$  would give rise to a branch cycle only meeting red vertices, contradicting [Proposition 2.12](#).

Suppose  $v^1 = v_k^\sigma$ . The same argument as in [Lemma 3.9](#) shows that, since  $v_{\delta_1}^1$  is blue,  $k$  must be  $\delta_\sigma - 1$ . Thus  $\sigma \neq 1$  otherwise  $s_{\delta_1}^1$  is not embedded in its interior. This shows that  $s_{\delta_1}^1 = s_{\delta_2}^2$  and  $v_{\delta_1}^1 = v_{\delta_2}^2$ . See [Figure 19](#).

If  $v^2$  only meets  $C_0$  and no other component of  $\Gamma(h'_1 \cup h'_2)$ , then  $C_1$  is uniquely determined to be the component which  $v^1$  meets other than  $C_0$ . Since we picked  $C_1$  arbitrarily at the start, this shows that  $\Gamma(h'_1 \cup h'_2)$  has exactly two components in this case.

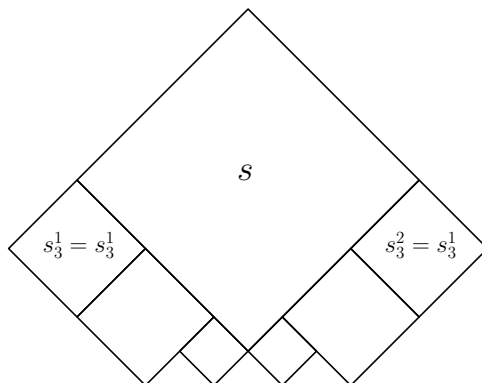


FIGURE 19. When  $\Gamma(h'_1 \cup h'_2)$  is not connected, the component not containing  $h'_1 \cup h'_2$  contains at least one branch cycle (in orange).

If  $v^2$  meets some component  $C_2 \neq C_0$ , then the bottom vertex of  $s_{\delta_1}^1 = s_{\delta_2}^2$  does not meet  $C_0$ , hence is not resolved. Thus  $C_1 = C_2$ , and  $C_1$  is again uniquely determined to be the component which  $v^1$  meets other than  $C_0$ , showing that  $\Gamma(h'_1 \cup h'_2)$  has exactly two components.

Since the only resolutions we perform are B-resolutions, any branch cycle either lies completely in  $C_0$  or completely in  $C_1$ , so  $C_1$  contains at least one branch cycle.  $\square$

In the one boundary component case, we will often be able to bypass the obstruction described in [Lemma 4.5](#) and have (FRC). With this in mind, for the rest of this section, we prove some lemmas providing some sets of conditions, which when taken together with (FRC), guarantee that the assumptions of [Proposition 4.4](#) are satisfied.

To prove these lemmas, we use the A/B-quads as described in [Section 3.2](#) and [Section 3.3](#). We continue the notation from there. Since we consider both sides of  $s$  now, we have two groups of quads, one group for each side of  $s$  as laid out in [Figure 12](#).

We have the following analogue of [Lemma 3.11](#).

**Lemma 4.7.** *Suppose  $s$  satisfies (FRC), then  $\Gamma(h_1 \cup h_2)$  is connected unless some  $h_\beta$  is deep and  $v_{\delta_{\beta'}}^{\beta'}$  is equal to the bottom vertex of  $s_1^\beta$  for some  $\beta'$ , in the manner such that the bottom side of  $s_1^\beta$  containing  $e_{\delta_{\beta'}+1}^{\beta'}$  meets  $v_0$  as well. See [Figure 20](#).*

*In particular if  $s$  is fan, then the top vertex of  $s$  is equal to the bottom vertex of  $s$ .*

*Proof.* The 2-complex  $Q(h_1 \cup h_2)$  corresponding to the resolution is  $\bigcup_{i=k_1}^{\delta_1} q_i^1 \cup \bigcup_{i=k_2}^{\delta_2} q_i^2$ . There are at most four blue sides in  $Q(h_1 \cup h_2)$ , belonging to at most four quads, namely,  $q_1^1$ ,  $q_{\delta_1}^1$ ,  $q_1^2$ , and  $q_{\delta_2}^2$ . For simplicity of the language let us assume that  $\delta_1, \delta_2 \geq 2$ , so that these four quads are distinct. The same argument will work for  $\delta_1$  or  $\delta_2 = 1$  with some more careful wording. We let the reader fill this out themselves.

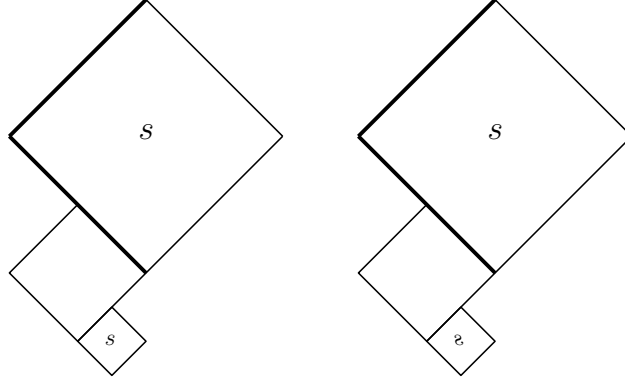


FIGURE 20. If  $s$  satisfies (FRC) but  $\Gamma(h_1 \cup h_2)$  is not connected, then some  $h_\beta$  (thickened) is deep and  $v_{\delta_{\beta'}}^{\beta'}$  is equal to the bottom vertex of  $s_1^\beta$  for some  $\beta'$ , in a manner such that the bottom side of  $s_1^\beta$  containing  $e_{\delta_{\beta'}+1}^{\beta'}$  meets  $v_0$  as well. In these examples  $\beta$  is the left side, and  $\beta'$  is the left/right side in the left/right figure respectively.

Since we assumed that  $s$  satisfies (FRC), if  $\Gamma(h_1 \cup h_2)$  is not connected, then the 2-cycle  $x$  of  $Q(h_1 \cup h_2)$  corresponding to a component must involve at least two of these four quads and identify two of their blue edges.

If the blue edge of  $q_{\delta_1}^1$  is identified with that of  $q_{\delta_2}^2$ , then  $q_{\delta_1}^1$  and  $q_{\delta_2}^2$  must be the same quad. Hence the 2-cycle  $x$  needs to contain at least one of  $q_1^1$  and  $q_1^2$  and identify one of their blue edges to the blue edge of  $q_{\delta_1}^1 = q_{\delta_2}^2$  in order to cancel it out.

Similarly (symmetrically, even, see [Remark 2.13](#)), if the blue edge of  $q_1^1$  is identified with that of  $q_1^2$ , then  $q_1^1$  and  $q_1^2$  must be the same quad. Hence the 2-cycle  $x$  needs to contain at least one of  $q_{\delta_1}^1$  and  $q_{\delta_2}^2$  and identify one of their blue edges to the blue edge of  $q_1^1 = q_1^2$ .

Hence we conclude that the blue edge of some  $q_1^\beta$  must be identified with the blue edge of some  $q_{\delta_{\beta'}}^{\beta'}$ . This in particular implies that  $q_1^\beta$  is contained in  $Q(h_1 \cup h_2)$ , hence  $h_\beta$  is deep.

The edge identification implies that  $v_{\delta_{\beta'}}^{\beta'}$  is equal to the bottom vertex of  $s_1^\beta$ . There are two manners of identification here. One is such that  $e_{\delta_{\beta'}+1}^{\beta'}$  and  $v_0$  lie on the same side of  $s_1^\beta$ , which is the statement of the lemma, while the other is such that they lie on different sides of  $s_1^\beta$ , which we tackle for the rest of the proof.

If  $h_\beta$  and  $h_{\beta'}$  lie in the same component  $C_0$  of  $\Gamma(h_1 \cup h_2)$ , then by following along the sides of  $s_1^\beta$ , we see that  $v_{\delta_{\beta'}}^{\beta'}$  only meets  $C_0$  and no other component, contradicting the fact that  $q_{\delta_{\beta'}}^{\beta'}$  is included in the 2-cycle.

The only case where  $h_\beta$  and  $h_{\beta'}$  do not lie in the same component is if  $\beta \neq \beta'$ , and the bottom vertex of  $s$  is resolved, which implies that it is equal to  $v_{\delta_\beta}^\beta$  or  $v_{\delta_{\beta'}}^{\beta'}$ , since these are the only two blue vertices we resolve.



In the former case, the identification must be so that  $s = s_1^\beta$ , otherwise  $h_\beta$  and  $h_{\beta'}$  lie in the same component, but then the statement of the lemma is still true. See [Figure 21](#) left (where we take  $\beta$  to be the left side). Similarly, in the latter case, the identification must be so that  $s = s_1^{\beta'}$ . But since we are assuming that  $e_{\delta_{\beta'}+1}^{\beta'}$  lies on a bottom side of  $s_1^\beta$ , we must have  $s_1^\beta = s$  so we are in fact the former case again. See [Figure 21](#) right.

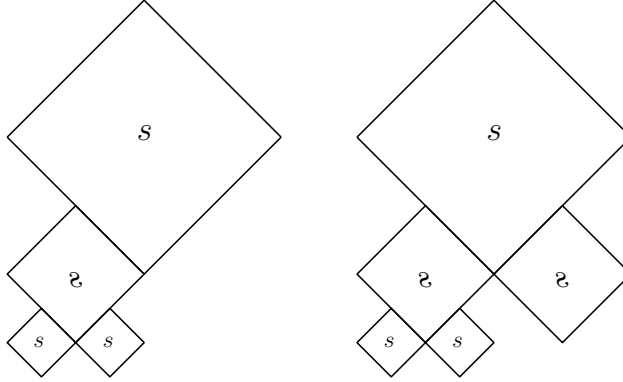


FIGURE 21. Reasoning that [Lemma 4.7](#) still holds when  $h_\beta$  and  $h_{\beta'}$  do not lie in the same component.

Finally, the second statement follows from [Proposition 2.11](#) as in [Lemma 3.9](#).  $\square$

Here are two more situations where we can show that  $\Gamma(h_1 \cup h_2)$  is connected.

**Lemma 4.8.** *Suppose that:*

- $s$  satisfies (FRC)
- $v_{\delta_1}^1 = v_{\delta_2}^2$
- $e_{\delta_1+1}^1 \neq e_1^1$  and  $e_{\delta_2+1}^2 \neq e_1^2$

Then  $\Gamma(h_1 \cup h_2)$  is connected, i.e. (I) of [Proposition 4.4](#) is true.

*Proof.* Let  $C_i$  be the component of  $\Gamma(h_1 \cup h_2)$  containing  $h_i$ , for  $i = 1, 2$ . We first claim that  $C_1 = C_2$ .

If the bottom vertex of  $s$  is not resolved, then this is clear. Otherwise this bottom vertex must be  $v_{\delta_1}^1 = v_{\delta_2}^2$ . The third condition in the assumption implies that the identification must be such that  $e_{\delta_2+1}^2 = e_1^1$ , so by following along the sides of  $s$ , we see that  $C_1 = C_2$  in this case as well.

Now suppose  $\Gamma(h_1 \cup h_2)$  is not connected. Consider the 2-cycle of  $Q(h_1 \cup h_2)$  corresponding to  $C_1$ . Since  $v_{\delta_1}^1 = v_{\delta_2}^2$ ,  $C_1$  is the only component of  $\Gamma(h_1 \cup h_2)$  that meets this vertex, so the quad  $q_{\delta_1}^1 = q_{\delta_2}^2$  will not be included in the 2-cycle. Since  $s$  satisfies (FRC), the 2-cycle must then contain the quads  $q_1^1$  and  $q_1^2$  and identify their blue edges. But this implies that  $v_1^1 = v_1^2$ , and that this common vertex only meets  $C_1$ . So these quads are not in the 2-cycle as well, giving us a contradiction.  $\square$

**Lemma 4.9.** *Suppose that:*

- $s$  satisfies (FRC)
- $v_1^1 = v_1^2$
- $e_{\delta_1+1}^1 \neq e_1^1$  and  $e_{\delta_2+1}^2 \neq e_1^2$

Then  $\Gamma(h_1 \cup h_2)$  is connected, i.e. (I) of [Proposition 4.4](#) is true.

*Proof.* This lemma is similar (symmetric, even, see [Remark 2.13](#)) to [Lemma 4.8](#).

The same argument as in [Lemma 4.8](#) shows that  $h_1$  and  $h_2$  lie in a common component  $C$ .

If  $\Gamma(h_1 \cup h_2)$  is not connected, consider the 2-cycle of  $Q(h_1 \cup h_2)$  corresponding to  $C$ . Since  $v_1^1 = v_1^2$ ,  $C$  is the only component of  $\Gamma(h_1 \cup h_2)$  that meets this vertex, so the quad  $q_1^1 = q_1^2$  will not be included in the 2-cycle. Since  $s$  satisfies (FRC), the 2-cycle must then contain the quads  $q_{\delta_1}^1$  and  $q_{\delta_2}^2$  and identify their blue edges. But this implies that  $v_{\delta_1}^1 = v_{\delta_2}^2$ , and that this common vertex only meets  $C$ . So these quads are not in the 2-cycle as well, giving us a contradiction.  $\square$

Now we state two sets of conditions under which we can show the other scenario in [Proposition 4.4](#) is true.

**Lemma 4.10.** *Suppose that:*

- $\Gamma(h_1 \cup h'_2)$  is connected (in particular  $s$  satisfies (FRC))
- $e_{\delta_2+1}^2 = e_1^2$

Then (II) in [Proposition 4.4](#) is true.

*Proof.* We can assume that  $h_2$  is deep here, since resolving less vertices cannot create more components for the resolved dual graph.

Since  $\Gamma(h_1 \cup h'_2)$  is connected, by resolving two more points  $v_{\delta_2}^2$  and  $v_1^2$ , we get at most 3 components in  $\Gamma(h_1 \cup h_2)$ . Here  $(e_i^2)_{i \in \mathbb{Z}/\delta_2}$  is clearly a component on its own, so it remains to show that  $\Gamma(h_1 \cup h_2)$  does not have 3 components.

Suppose otherwise. Let  $C_0$  be the component that is  $(e_i^2)_{i \in \mathbb{Z}/\delta_2}$ . In this case,  $v_{\delta_2}^2$  must meet components  $C_0$  and  $C_1$ , while  $v_1^2$  must meet components  $C_0$  and  $C_2$ , where  $C_1 \neq C_2$ .

In particular  $e_1^1$  lies in  $C_1$  and  $e_{\delta_1+1}^1$  lies in  $C_2$ . But then following along the sides of  $s$ , we see that  $C_1 = C_2$ , giving us a contradiction.  $\square$

**Lemma 4.11.** *Suppose that:*

- $s$  satisfies (FRC)
- $h_1$  is not deep
- $e_{\delta_2+1}^2 = e_1^2$

Then (II) in [Proposition 4.4](#) is true.

*Proof.* By assumption,  $\Gamma(h'_1 \cup h'_2)$  is connected. So if we resolve one more point  $v_{\delta_1}^1$ ,  $\Gamma(h_1 \cup h'_2)$  has at most 2 components. However,  $Q(h_1 \cup h'_2)$  only has one blue edge, namely that of  $q_{\delta_1}^1$ , so there cannot be any 2-cycle containing  $q_{\delta_1}^1$ . Hence  $\Gamma(h_1 \cup h'_2)$  is connected. Now the lemma follows from [Lemma 4.10](#).  $\square$

## 5. ONE BOUNDARY COMPONENT CASE

As pointed out at the start of [Section 4](#), we are unable to show that double hook circuits exist in the general case. What we are able to do, however, is when  $T_f$  has only one boundary component, we can show that double hook circuits exist in certain cases, and in the complement of those cases, we can upgrade the argument of [Proposition 3.3](#) using a variety of ideas.

The description of what these cases are is quite complicated. We divide their descriptions and the corresponding arguments into four rough parts, contained in [Section 5.1](#) to [Section 5.4](#). In [Section 5.5](#), we will put these arguments together, using a strategy of elimination, similar to that in [Section 3.3](#) but even more elaborate. For the reader's convenience, we have provided a flow chart in [Figure 31](#) as a summary of this strategy, intended to be consulted after a first reading of this section.

We briefly remark on the type of upgrades we will apply on [Proposition 3.3](#). We can summarize the argument of [Proposition 3.3](#) by [Table 3](#). Here we think of each vertex of  $-c$  as contributing a term in the sum on the right hand side of [Equation \(3.1\)](#), and we table up the quantity and contributions of each type of vertex. What we will do is, with certain knowledge of the stable branched surface, show that the contribution from certain vertices can be improved. When we do so, we will summarize the proof in tables like [Table 3](#) but with more rows.

TABLE 3. The argument in [Proposition 3.3](#).

Vertices of $-c$	Quantity	Contribution
Pairs of vertices that meet a B-resolved hook vertex	$\#$ hook vertices $- 1$	$2w$
Remaining non-hook vertices	$2N - 2(\# \text{ hook vertices}) + 1$	$w$

For the rest of this section, we fix the following setting. Let  $T_f$  be the mapping torus of a fully-punctured pseudo-Anosov map  $f$ , where  $T_f$  has only one boundary component. Let  $\Delta$  be the veering triangulation on  $T_f$  that carries  $\Lambda^s$ , let  $B$  be the stable branched surface of  $\Delta$ , and let  $\Gamma$  be the dual graph of  $\Delta$ . Finally, let  $S$  be a fiber surface. We use the notation as in [Section 2.3](#).

**5.1. When the number of branch cycles is large.** The crucial fact about  $T_f$  having only one boundary component is if there are  $l$  branch cycles in the stable branched surface, then each branch cycle intersects the fiber surface  $-\frac{2}{l}\chi(S)$  times. This is because all the

branch cycles are homotopic to the same slope on the boundary of  $T_f$  (sometimes known as the *degeneracy slope* in the literature), hence are homotopic to each other.

Now consider a sector  $s$  of  $B$  of minimum weight. Let  $c$  be a branch cycle that meets a bottom side of  $s$ . Take the bottom vertex of  $s$  to be the basepoint of  $c$ . Let  $\widehat{s}_0$  be the lift of  $s$  in  $\widehat{B}$  that is of height 0. Lift  $c$  to a path  $\widehat{c}$  ending at the bottom vertex of  $\widehat{s}_0$ , then push  $\widehat{c}$  *upwards* on the side of  $\widehat{s}_0$  and reverse its orientation to get a descending path  $\alpha$ . The starting point of  $\alpha$  lies on  $\widehat{s}_0$  which is of weight  $w$ , while the ending point of  $\alpha$  lies on  $g^{\frac{2}{l}\chi}\widehat{s}$  which is of weight  $\lambda^{-\frac{2}{l}\chi}w$ , since  $c$  intersects the fiber surface  $-\frac{2}{l}\chi$  times. Moreover, at each intersection point of  $\alpha$  with the branch locus of  $\widehat{B}$ , the sector that merges in is of non-positive height, hence has weight  $\geq w$ .

Therefore if  $\lambda^{-\frac{2}{l}\chi} < n + 2$  for integer  $n$ , then  $\alpha$  must intersect the branch locus of  $\widehat{B}$  at most  $n$  times. This implies that the branch cycle  $c$  meets at most  $n$  vertices of the same color as  $s$ .

Notice that this immediately implies that  $\lambda^{-\frac{2}{l}\chi} < 2$  is impossible. We will not need to use this fact in full but we record it as a proposition anyway.

**Proposition 5.1.** *Let  $f$  be a fully-punctured pseudo-Anosov map with normalized dilatation  $\lambda^{-x}$ . Suppose the mapping torus  $T_f$  of  $f$  only has one boundary component, then the stable branched surface  $B$  has less than or equal to  $\frac{2\log\lambda^{-x}}{\log 2}$  branch cycles.*

We will focus on the case when  $\lambda^{-\frac{2}{l}\chi} < 4$  in this subsection. This occurs when  $l$  is large enough (relative to  $\lambda^{-x}$ ), hence the name of the subsection.

Let  $s$  be a sector of  $B$  of minimum weight and let  $c$  be an Eulerian circuit that hooks around  $s$ , say  $c$  contains the hook  $h_1$ . Such a pair  $(s, c)$  exists unless  $\Delta = \text{cPcbbbdxm.10}$  by [Proposition 3.8](#). But for  $\Delta = \text{cPcbbbdxm.10}$ ,  $l = 1$  and  $\lambda^{-x} = \mu^2$  so  $\lambda^{-\frac{2}{l}\chi} < 4$  does not hold anyway, thus we can ignore this exceptional case in this subsection. We use the same notation on the edges, vertices, and sectors adjacent to  $s$  as in the previous sections.

If  $\lambda^{-\frac{2}{l}\chi} < 4$ , each branch cycle meeting a bottom side of  $s$  meets at most 2 vertices of the same color as  $s$ . This implies that  $v_{\delta_1}^1$  is equal to the bottom vertex of  $s_1^2$  in a way such that  $e_{\delta_1+1}^1$  and  $v_0$  lie on different sides of  $s_1^2$ , and similarly,  $v_{\delta_1}^2$  is equal to the bottom vertex of  $s_1^1$  in a way such that  $e_{\delta_1+1}^2$  and  $v_0$  lie on different sides of  $s_1^1$ . See [Figure 22](#).

If  $s$  fails (FRC), then by [Lemma 4.5](#),  $v_{\delta_1}^1 = v_{\delta_2}^2$ . If  $s$  satisfies (FRC) but  $\Gamma(h_1 \cup h_2)$  is not connected, then  $v_{\delta_{\beta'}}^{\beta'}$  is equal to the bottom vertex of  $s_1^\beta$  for some  $\beta, \beta'$  in a way such that  $e_{\delta_{\beta'}+1}^{\beta'}$  and  $v_0$  lie on the same side of  $s_1^\beta$ , by [Lemma 4.7](#). But in the current setting, this implies that  $v_{\delta_1}^1 = v_{\delta_2}^2$ . So we see that unless  $\Gamma(h_1 \cup h_2)$  is connected, we must have  $v_{\delta_1}^1 = v_{\delta_2}^2$ .

**Proposition 5.2.** *Suppose that  $l > \frac{\log\lambda^{-x}}{\log 2}$ . Then the number of tetrahedra in  $\Delta$  is  $\leq \max\{\frac{1}{4}\lambda^{-2x} + 1, \frac{1}{2}(\lambda^{-2x} - \frac{\lambda^{-2x} - \lambda^{-\frac{2}{l}\chi}}{\lambda^{-\frac{2}{l}\chi} - 1} + l)\}$*

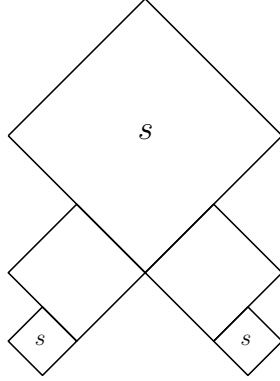


FIGURE 22. If  $\lambda^{-\frac{2}{l}\chi} < 4$ , each branch cycle meeting a bottom side of  $s$  meets at most 2 vertices of the same color as  $s$ .

*Proof.* If  $\Gamma(h_1 \cup h_2)$  is connected, then the proposition follows from [Proposition 4.4](#) and [Proposition 4.3](#).

If  $\Gamma(h_1 \cup h_2)$  is not connected, then by the reasoning before the proposition, we have  $v_{\delta_1}^1 = v_{\delta_2}^2$ . The way we will prove the proposition is to improve the estimates made in [Proposition 3.3](#) when that argument is applied to the Eulerian hook circuit  $c$ .

First notice that  $v_{\delta_1}^1 = v_{\delta_2}^2$  implies that the sides of  $s$  lie along two branch cycles, say  $c_1$  and  $c_2$  among the  $l$  branch cycles  $c_1, \dots, c_l$ . Let  $u_i, i = 3, \dots, l$  be the last vertex of  $-c$  that lies on  $c_i$ . By definition,  $c$  takes an anti-branching turn at each  $u_i$ , and each  $u_i$  does not lie on the sides of  $s$ . Without loss of generality, suppose that  $-c$  meets  $u_i$  in the order of increasing  $i$ .

In the argument of [Proposition 3.3](#), the contribution of the terms corresponding to each  $u_i$  is  $w$ , since each  $u_i$  lies on  $c_i$  hence does not meet a hook vertex. But between the last vertex on the hook and  $u_i$ ,  $-c$  will have passed through  $c_3, \dots, c_i$  in their entirety, hence will have intersected the fiber surface at least  $-\frac{2(i-2)}{l}\chi$  times. So the sector in the term corresponding to  $u_i$  is in fact at height  $\leq \frac{2(i-2)}{l}\chi$ , hence of weight  $\geq \lambda^{-\frac{2(i-2)}{l}\chi}w$ . This implies that we can obtain a sharper bound if we replace the  $w$  contributed by  $u_i$  to  $\lambda^{-\frac{2(i-2)}{l}\chi}w$ .

We can make one more improvement, the source of the improvement differing in two cases which we can divide into.

Case 1 is if  $v_{\delta_1}^1 = v_{\delta_2}^2$  is not the bottom vertex of  $s$ . In this case, the edges of  $\Gamma$  that lie on the sides of  $s$  are all distinct. Let  $p_k^\beta$  be the number of intersection points between  $e_k^\beta$  and the fiber surface. Then  $\sum_{k=1}^{\delta_1+1} p_k^1 + \sum_{k=1}^{\delta_2+1} p_k^2$  is at most the number of intersection points of  $c_1$  and  $c_2$  with the fiber surface, which is  $\frac{2}{l} \cdot (-2\chi)$ . But  $\sum_{k=1}^{\delta_1+1} p_k^1 = \sum_{k=1}^{\delta_2+1} p_k^2$  since every arc has endpoints on different sides of  $s$ , so  $\sum_{k=1}^{\delta_1+1} p_k^1 = \sum_{k=1}^{\delta_2+1} p_k^2 \leq -\frac{2}{l}\chi$ .

Now consider the last vertex of  $-c$ , which we denote by  $u$ .  $u$  sits at the top vertex of  $s$ . Between the last vertex on the hook and  $u$ ,  $c$  will have intersected the fiber surface for  $-2\chi - \sum_{k=1}^{\delta_1+1} p_k^1 \geq -\frac{2(l-1)}{l}\chi$  times. Since  $v_{\delta_1}^1 = v_{\delta_2}^2$  is not the bottom vertex of  $s$ ,  $u$  is not a

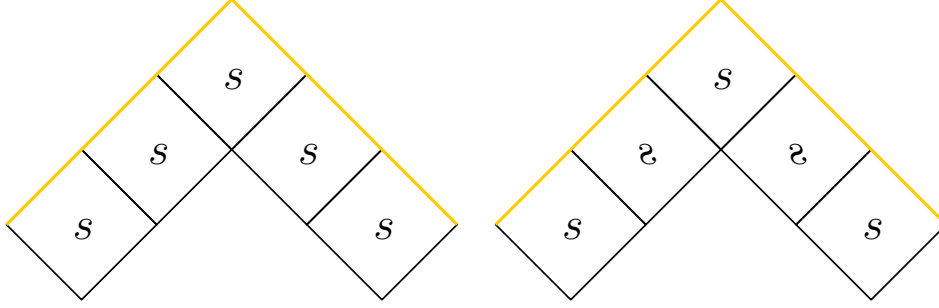


FIGURE 23. If  $v_{\delta_1}^1 = v_{\delta_2}^2$ , then  $s$  has to be toggle, otherwise the top sides of  $s$  form one or two branch cycles (in yellow) meeting vertices of only one color.

hook vertex. As a result, in the argument of [Proposition 3.3](#), the contribution of  $u$  is  $w$ , and we can replace this contribution by  $\lambda^{-\frac{2(l-1)}{l}\chi}w$  to get a better bound.

Case 2 is if  $v_{\delta_1}^1 = v_{\delta_2}^2$  is the bottom vertex of  $s$ . Notice that in this case  $s$  must be toggle, otherwise the top sides of  $s$  form one or two branch cycles meeting vertices of only one color, contradicting [Proposition 2.12](#). See [Figure 23](#).

In this case, we consider the last vertex  $u$  of  $-c$  as well. The term corresponding to  $u$  is the weight of a sector of  $\widehat{B}$  covering  $s$ . If we let  $p_k^\beta$  be the number of intersection points between  $e_k^\beta$  and the fiber surface as above, then the height of this sector will be  $2\chi + \sum_{k=1}^{\delta_\beta} p_k^\beta$  for  $\beta = 1$  or  $2$  depending on the manner of identification of  $v_{\delta_1}^1 = v_{\delta_2}^2$  with the bottom vertex of  $s$ , and whether  $c$  takes an antibranching or branching turn at  $u$ . In either case,  $\sum_{k=1}^{\delta_\beta} p_k^\beta$  is at most the number of intersection points of one branch cycle with the fiber surface, which is  $-\frac{2}{l}\chi$ .

We can now replace the contribution of  $u$  by  $\lambda^{-\frac{2(l-1)}{l}\chi}w$ . However, there is a difference with the previous case here. The original contribution of  $u$  is not necessarily  $w$ . If  $u$  is paired up with a B-resolved hook vertex, then the contribution of the pair is  $2w$ , while the contribution of  $u$  itself is greater than  $w$ . So what we do here is remove the contributions of both terms in the pair, and replace them by  $\lambda^{-\frac{2(l-1)}{l}\chi}w$ .

With these optimizations, [Equation \(3.1\)](#) becomes

$$\begin{aligned} \lambda^{-2\chi}w &\geq 2Nw + (\lambda^{-\frac{2}{l}\chi}w - w) + \dots + (\lambda^{-\frac{2(l-2)}{l}\chi}w - w) + (\lambda^{-\frac{2(l-1)}{l}\chi}w - w) \\ &= 2Nw + \frac{\lambda^{-2\chi} - \lambda^{-\frac{2}{l}\chi}}{\lambda^{-\frac{2}{l}\chi} - 1}w - (l-1)w \end{aligned}$$

in case 1 and

$$\begin{aligned} \lambda^{-2\chi}w &\geq 2Nw + (\lambda^{-\frac{2}{l}\chi}w - w) + \dots + (\lambda^{-\frac{2(l-2)}{l}\chi}w - w) + (\lambda^{-\frac{2(l-1)}{l}\chi}w - 2w) \\ &= 2Nw + \frac{\lambda^{-2\chi} - \lambda^{-\frac{2}{l}\chi}}{\lambda^{-\frac{2}{l}\chi} - 1}w - lw \end{aligned}$$

in case 2.

So in both cases, we have

$$\lambda^{-2x} \geq 2N + \frac{\lambda^{-2x} - \lambda^{-\frac{2}{l}x}}{\lambda^{-\frac{2}{l}x} - 1} - l$$

$$N \leq \frac{1}{2} \left( \lambda^{-2x} - \frac{\lambda^{-2x} - \lambda^{-\frac{2}{l}x}}{\lambda^{-\frac{2}{l}x} - 1} + l \right)$$

□

As promised, we summarize the part of the proof of [Proposition 5.2](#) where we improve [Proposition 3.3](#) in [Table 4](#).

TABLE 4. The argument in [Proposition 5.2](#).

Vertices of $-c$	Quantity	Contribution
Last vertex on $c_i$ , $i = 3, \dots, l$	$l - 2$	$\lambda^{-\frac{2(i-2)}{l}x}w$
Last vertex	1	$\lambda^{-\frac{2(l-1)}{l}x}w$
Remaining pairs of vertices that meet a B-resolved hook vertex	Case 1: # hook vertices $- 1$ Case 2: # hook vertices $- 2$	$2w$
Remaining non-hook vertices	Case 1: $2N - 2(\# \text{ hook vertices}) - l + 2$ Case 2: $2N - 2(\# \text{ hook vertices}) - l + 3$	$w$

We note that when  $\lambda^{-x} = \mu^4$ ,  $l > \frac{\log \lambda^{-x}}{\log 2}$  reads  $l > 2.78$ , that is,  $l \geq 3$ . So for our applications in the fully-punctured normalized dilatation problem, as explained in the introduction, we must now turn our attention to the case when  $l = 1$  or  $2$ .

**5.2. When the number of branch cycles is small.** As in the last subsection, let  $s$  be a sector of minimum weight. Without loss of generality assume that  $s$  is blue. Let  $c$  be an Eulerian circuit that hooks around  $s$ , say  $c$  contains the hook  $h_1$ . We use the same notation on the edges, vertices, and sectors adjacent to  $s$  as always. Suppose  $B$  has  $l$  branch cycles, where  $l = 1$  or  $2$ .

The key property that  $l = 1$  or  $2$  buys us is [Proposition 5.4](#), which says that we can assume that  $s$  satisfies (FRC) hence apply the lemmas in [Section 4.2](#), for otherwise we have an improved bound by other means. Before proving [Proposition 5.4](#), it will be in our advantage to prove [Proposition 5.3](#) first.

**Proposition 5.3.** *When  $l = 1$  or  $2$ , either  $e_{\delta_1+1}^1 \neq e_1^2$  and  $e_{\delta_2+1}^2 \neq e_1^1$ , or the number of tetrahedra in  $\Delta$  is  $\leq \frac{1}{4}\lambda^{-2x} + 1$ .*

*Proof.* If  $l = 1$  and, say,  $e_{\delta_1+1}^1 = e_1^2$ , then  $(e_i^1)_{i \in \mathbb{Z}/\delta_1}$  is the sole branch cycle of  $B$ . But this branch cycle only meets one blue vertex, contradicting the fact that any Eulerian circuit must meet each vertex twice.



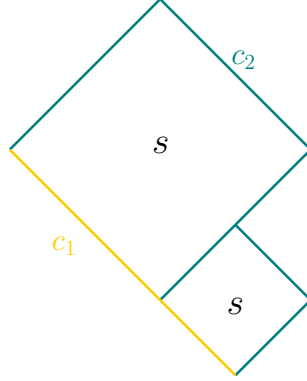


FIGURE 24. If  $e_{\delta_1+1}^1 = e_1^2$  and  $e_{\delta_2+1}^2 \neq e_1^1$ , then one bottom side of  $s$  lies along the branch cycle  $c_1 = (e_i^1)_{i \in \mathbb{Z}/\delta_1}$  (in yellow) while all other sides of  $s$  lie on  $c_2$  (in teal).

If  $l = 2$  and, say,  $e_{\delta_1+1}^1 = e_1^2$ , then as above,  $(e_i^1)_{i \in \mathbb{Z}/\delta_1}$  is a branch cycle of  $B$ . We denote this branch cycle by  $c_1$ , and denote the other branch cycle of  $B$  by  $c_2$ .

If  $e_{\delta_2+1}^2 = e_1^1$ , then  $c_2 = (e_i^2)_{i \in \mathbb{Z}/\delta_2}$ . In this case,  $(e_1^1, \dots, e_{\delta_1}^1, e_1^2, \dots, e_{\delta_2}^2)$  is an Eulerian circuit that hooks around  $s$  twice, implying that the number of tetrahedra in  $\Delta$  is  $\leq \frac{1}{4}\lambda^{-2\chi} + 1$  by [Proposition 4.3](#).

On the other hand, if  $e_{\delta_2+1}^2 \neq e_1^1$ , then all sides of  $s$  other than  $(e_1^1, \dots, e_{\delta_1}^1)$  lie on  $c_2$ . See [Figure 24](#). Here we use the fact that if  $e_{\delta_1+1}^1 = e_1^1$ , then  $s$  will not be embedded in its interior near  $v_0$ , which is a contradiction. Moreover, the edges  $e_k^2$ ,  $k = 1, \dots, \delta_2 + 1$  are distinct. Here we use the fact that if  $e_{\delta_2+1}^2 = e_1^2$ , then again  $s$  will not be embedded in its interior near  $v_0$ .

Let  $p_k^\beta$  be the number of intersections of  $e_k^\beta$  with the fiber surface. We have the following equations:

- $\sum_{k=1}^{\delta_1+1} p_k^1 = \sum_{k=1}^{\delta_2+1} p_k^2$
- $\sum_{k=1}^{\delta_1} p_k^1 = -\chi$
- $p_{\delta_1+1}^1 = p_1^2$
- $\sum_{k=1}^{\delta_2+1} p_k^2 \leq -\chi$

which imply that  $p_{\delta_1+1}^1 = p_1^2 = 0$  and  $\sum_{k=2}^{\delta_2+1} p_k^2 = -\chi$ . That is, the intersection points of  $c_2$  with the fiber surface are all lie on  $e_k^2$ ,  $k = 2, \dots, \delta_2 + 1$ .

Consider cutting and pasting the branch cycle  $c_2$  at  $v_{\delta_2}^2$ . This gives two cycles of  $\Gamma$ , one containing  $e_k^2$ ,  $k = 2, \dots, \delta_2 + 1$ , and the other not containing any of these edges, thus does not intersect the fiber surface. But this latter cycle would then contradict [Proposition 2.20](#).  $\square$

**Proposition 5.4.** *Suppose  $l = 1$  or  $2$  and suppose there is an Eulerian circuit  $c$  that hooks around  $s$ . Then either the minimum weight sector  $s$  satisfies (FRC) or the number of tetrahedra in  $\Delta$  is  $\leq \max\{\frac{1}{4}\lambda^{-2\chi} + 1, \frac{1}{2}(\lambda^{-2\chi} - \lambda^{-\frac{4}{3}\chi} - \lambda^{-\chi}) + 1\}$ .*

*Proof.* By [Lemma 4.5](#), if  $s$  does not satisfy (FRC), then  $v_{\delta_1}^1 = v_{\delta_2}^2$  and the component of  $\Gamma(h'_1 \cup h'_2)$  not containing  $h'_1 \cup h'_2$  contains at least one branch cycle. This immediately implies that if  $l = 1$ , then  $s$  must satisfy (FRC), so we assume that  $l = 2$  and  $s$  does not satisfy (FRC) in the rest of the proof.

In this case, the component not containing  $h'_1 \cup h'_2$  contains exactly one branch cycle, which we denote by  $c_2$ . All the sides of  $s$  are contained in the other component of  $\Gamma(h'_1 \cup h'_2)$ , hence contained in the branch cycle other than  $c_2$ , which we denote by  $c_1$ .

If  $v_{\delta_1}^1 = v_{\delta_2}^2$  is equal to the bottom vertex of  $s$  and  $e_{\delta_1+1}^1 = e_1^2$  (equivalently,  $e_{\delta_2+1}^2 = e_1^1$ ), then the number of tetrahedra in  $\Delta$  is  $\leq \frac{1}{4}\lambda^{-2\chi} + 1$  by [Proposition 5.3](#).

If  $v_{\delta_1}^1 = v_{\delta_2}^2$  is equal to the bottom vertex of  $s$  and  $e_{\delta_1+1}^1 = e_1^1$  (equivalently,  $e_{\delta_2+1}^2 = e_1^2$ ), first notice that the hook  $h_1$  is not deep, otherwise  $\Gamma(h_1)$  is not connected, for  $(e_i^1)_{i \in \mathbb{Z}/\delta_1}$  would be its own component, contradicting the hypothesis that there is a hook circuit  $c$  containing  $h_1$ . Let  $p_k^\beta$  be the number of intersections of  $e_k^\beta$  with the fiber surface. Then we have the equations:

- $\sum_{k=1}^{\delta_1+1} p_k^1 = \sum_{k=1}^{\delta_2+1} p_k^2$
- $p_{\delta_1+1}^1 = p_1^1 = 0$
- $p_{\delta_2+1}^2 = p_1^2$
- $\sum_{k=1}^{\delta_1} p_k^1 + \sum_{k=1}^{\delta_2} p_k^2 \leq -\chi$

which imply that the number of times the hook  $h_1$  intersects the fiber surface, which is  $\sum_{k=2}^{\delta_1+1} p_k^1$ , is at most  $-\frac{2}{3}\chi$ .

What we can do now is to replace the contribution of the last vertex of  $-c$  on  $c_2$ , which we denote by  $u_2$ , from  $w$  to  $\lambda^{-\chi}w$ . As in [Proposition 5.2](#), the new estimate arises from the fact that  $-c$  would have traversed  $c_2$  all the way by the time it reached  $u_2$ , hence intersected the fiber surface at least  $-\chi$  times, while the old estimate is  $w$  because  $u_2$  lies on  $c_2$  (and  $c$  takes an anti-branching turn at  $u_2$ ) hence cannot meet a hook vertex.

We also replace the contribution of the last vertex of  $-c$ , which we denote by  $u$ , from  $w$  to  $\lambda^{-\frac{4}{3}\chi}w$ . The original contribution is  $w$  because  $h_1$  is not deep, so  $u$  does not meet a hook vertex. The new contribution arises from the fact that between the last vertex on the hook and  $u$ ,  $-c$  meets the fiber surface for  $\geq -2\chi + \frac{2}{3}\chi = -\frac{4}{3}\chi$  times.

With these improvements, [Equation \(3.1\)](#) becomes

$$\begin{aligned} \lambda^{-2\chi}w &\geq w + (2N - 1)w + (\lambda^{-\chi}w - w) + (\lambda^{-\frac{4}{3}\chi}w - w) \\ N &\leq \frac{1}{2}(\lambda^{-2\chi} - \lambda^{-\frac{4}{3}\chi} - \lambda^{-\chi}) + 1 \end{aligned}$$

If  $v_{\delta_1}^1 = v_{\delta_2}^2$  does not equal to the bottom vertex of  $s$ , then we can improve the estimates for the same two vertices. Namely, we first replace the contribution of  $u_2$ , from  $w$  to  $\lambda^{-\chi}w$ , with the same justification as in the last case. For  $u$ , we can actually replace  $w$  by  $\lambda^{-\frac{3}{2}\chi}w$ . This is because our equations regarding the  $p_k^\beta$  now becomes

- $\sum_{k=1}^{\delta_1+1} p_k^1 = \sum_{k=1}^{\delta_2+1} p_k^2$
- $\sum_{k=1}^{\delta_1+1} p_k^1 + \sum_{k=1}^{\delta_2+1} p_k^2 \leq -\chi$

so the number of times the hook  $h_1$  intersects the fiber surface is  $\leq \sum_{k=1}^{\delta_1+1} p_k^1 \leq -\frac{1}{2}\chi$ .

With these improvements, [Equation \(3.1\)](#) becomes

$$\begin{aligned} \lambda^{-2x}w &\geq w + (2N - 1)w + (\lambda^{-x}w - w) + (\lambda^{-\frac{3}{2}x}w - w) \\ N &\leq \frac{1}{2}(\lambda^{-2x} - \lambda^{-\frac{3}{2}x} - \lambda^{-x}) + 1 \leq \frac{1}{2}(\lambda^{-2x} - \lambda^{-\frac{4}{3}x} - \lambda^{-x}) + 1 \end{aligned}$$

□

As before, we summarize the argument in [Proposition 5.4](#) using [Table 5](#).

TABLE 5. The argument in [Proposition 5.4](#)

Vertices of $-c$	Quantity	Contribution
Last vertex on $c_2$	1	$\lambda^{-x}w$
Last vertex	1	$\lambda^{-\frac{4}{3}x}w$
Pairs of vertices that meet a B-resolved hook vertex	# hook vertices $- 1$	$2w$
Remaining non-hook vertices	$2N - 2(\# \text{ hook vertices}) - 1$	$w$

**5.3. When the sector is fan.** In this subsection, we explain some arguments that work when  $s$  is fan.

As in the last subsection, let  $s$  be a sector of minimum weight. Suppose  $s$  is fan. Let  $c$  be an Eulerian circuit that hooks around  $s$ , say  $c$  contains the hook  $h_1$ . We use the same notation on the edges, vertices, and sectors adjacent to  $s$  as always.

Suppose that  $s = s_1^1$ , then by [Proposition 2.12](#),  $e_1^1 = e_2^1$ . If  $e_1^1 = e_2^1$  does not intersect the fiber surface, then  $(e_1^1)$  is a cycle of  $\Gamma$  that does not intersect the fiber surface, contradicting [Proposition 2.20](#). So  $e_1^1 = e_2^1$  intersects the fiber surface, and the hook  $h_1$  is deep. But then  $\Gamma(h_1)$  will not be connected, since  $(e_1^1)$  is its own component, contradicting our assumption that the hook circuit  $c$  exists.

Now suppose that  $s = s_1^2$ , then by [Proposition 2.12](#),  $e_1^2 = e_2^2$ . Notice that in this case,  $h_2'$  is empty, so by [Lemma 4.10](#), [Proposition 4.4](#), and [Proposition 4.3](#), we know that the number of tetrahedra in  $\Delta$  is  $\leq \frac{1}{4}\lambda^{-2x} + 1$ .

We record this reasoning as a proposition.

**Proposition 5.5.** *Let  $s$  be a minimum weight sector. Suppose  $s$  is fan and suppose there is an Eulerian circuit  $c$  that hooks around  $s$ . If  $s = s_1^1$  or  $s_1^2$ , then the number of tetrahedra in  $\Delta$  is  $\leq \frac{1}{4}\lambda^{-2x} + 1$ .*

We then have the following argument.

**Proposition 5.6.** *Let  $s$  be a sector of minimum weight. Suppose that:*

- $s$  is fan
- $s \neq s_1^1$  or  $s_1^2$
- $s$  satisfies (FRC) but does not satisfy (TBT)

*Then the number of tetrahedra in  $\Delta$  is  $\leq \max\{\frac{1}{4}\lambda^{-2\chi} + 1, \frac{1}{3}\lambda^{-2\chi} + \frac{1}{2}\}$ .*

*Proof.* By Lemma 4.7,  $\Gamma(h_1 \cup h_2)$  is connected unless the bottom vertex of  $s$  is equal to the top vertex of  $s$ . When  $\Gamma(h_1 \cup h_2)$  is connected, Proposition 4.4 and Proposition 4.3 imply that the number of tetrahedra in  $\Delta$  is  $\leq \frac{1}{4}\lambda^{-2\chi} + 1$ , so we assume in the rest of the proof that the bottom vertex of  $s$  is equal to the top vertex of  $s$ . Since  $s$  does not satisfy (TBT), the identification must be such that  $(e_{\delta_1}^1, e_1^1)$  takes a branching turn at  $v_0$ .

Let  $\widehat{s}_0$  be the lift of  $s$  in  $\widehat{B}$  that is at height 0. Let  $b$  be the number of arcs on  $s$ . Then the sector having the bottom vertex of  $\widehat{s}_0$ , which we denote by  $\widehat{v}_0$ , as its top vertex is  $g^{-b}\widehat{s}_0$ . Suppose the weight of the two fins at  $\widehat{v}_0$  are  $aw$  and  $a'w$ , with  $a \geq a'$ . Then we have  $\lambda^b w = w + aw + a'w \leq w + 2aw$ , which implies that  $a \geq \frac{\lambda^b - 1}{2}$ . Meanwhile, the fins at  $\widehat{v}_0$  are at height  $\leq 0$ , thus  $a, a' \geq 1$ , and  $\lambda^b w = w + aw + a'w \geq 3w$ , which implies that  $\lambda^b \geq 3$ .

Now notice that both  $\Gamma(h_1)$  and  $\Gamma(h_2)$  are connected, since otherwise  $s$  satisfies (TBT) by Lemma 3.11. We claim that both  $\Gamma(h_1 \cup \{(v_0, \text{A-resolution})\})$  and  $\Gamma(h_2 \cup \{(v_0, \text{A-resolution})\})$  are connected as well. This is because by following along the sides of  $s$ , we see that the  $v_0$  only meets one component of  $\Gamma(h_\beta \cup \{(v_0, \text{A-resolution})\})$ , so the additional A-resolution at  $v_0$  cannot disconnect  $\Gamma(h_\beta)$ .

Let  $c_\beta$  be an Eulerian circuit of  $\Gamma$  which is the image of an Eulerian circuit of  $\Gamma(h_\beta \cup \{(v_0, \text{A-resolution})\})$ . For one of the  $c_\beta$ , without loss of generality say  $c_1$ , when we apply the argument of Proposition 3.3, the last term in Equation (3.1) is the weight of a sector which is a translate of the one with weight  $aw$  (as opposed to the one with weight  $a'w$ ). See Figure 25.

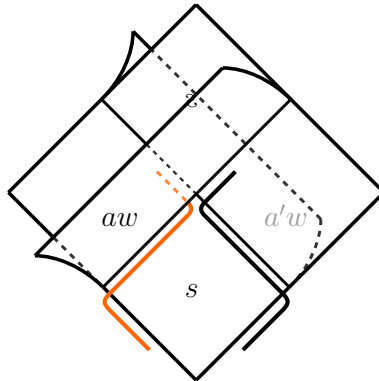


FIGURE 25. The last term in one of the  $c_\beta$  (the orange one in the figure) will be the weight of a sector which is a translate of the one with weight  $aw$  (as opposed to the one with weight  $a'w$ ).

More precisely, we can replace the contribution of the last vertex of  $c_1$  from  $w$  to  $\lambda^{-2x-b}aw$ . Here we use the second item in the hypothesis to ensure that this vertex is not a hook vertex. Equation (3.1) then becomes

$$\begin{aligned} \lambda^{-2x}w &= w + (2N - 1)w + (\lambda^{-2x-b}aw - w) \\ &\geq (2N - 1)w + \lambda^{-2x}\frac{w - \lambda^{-b}w}{2} \\ &\geq (2N - 1)w + \lambda^{-2x}\frac{w - \frac{1}{3}w}{2} \\ &= (2N - 1)w + \frac{1}{3}\lambda^{-2x}w \\ N &\leq \frac{1}{3}\lambda^{-2x} + \frac{1}{2} \end{aligned}$$

□

As usual, we summarize the main part of the proof of Proposition 5.6 in Table 6.

TABLE 6. The argument in Proposition 5.6.

Vertices of $-c$	Quantity	Contribution
Last vertex	1	$\frac{1}{3}\lambda^{-2x}w$
Pairs of vertices that meet a B-resolved hook vertex	# hook vertices $- 1$	$2w$
Remaining non-hook vertices	$2N - 2(\# \text{ hook vertices})$	$w$

Thus we can add to our assumptions that  $s$  satisfies (TBT). For the rest of this subsection, we will also assume that  $h_1$  is not deep. This assumption will fit into the scheme of the proof in quite an intricate way. In this case the side of the dual edge to  $s$  containing  $h_1$  must be long. Depending on whether the other side is long, Proposition 5.7 and Proposition 5.9 will conclude our arguments in this subsection.

**Proposition 5.7.** *Let  $s$  be a sector of minimum weight. Suppose that there is an Eulerian circuit  $c$  containing the hook  $h_1$  of  $s$ , and suppose that:*

- $s$  is fan
- $s \neq s_1^1$  or  $s_1^2$
- $s$  satisfies (FRC) and (TBT)
- $h_1$  is not deep
- Both sides of the dual edge  $e$  of  $s$  are long

Then the number of tetrahedra in  $\Delta$  is  $\leq \min\{\frac{1}{4}\lambda^{-2x} + 1, \frac{1}{2}\lambda^{-2x} - \lambda^{-x}\}$ , provided that  $\lambda^{-x} \geq 2$

Here the assumption  $\lambda^{-x} \geq 2$  is only used to simplify the statement of [Claim 5.8](#), and does not play a role in the main argument. Also, as we shall prove in [Theorem 1.6](#), this hypothesis is actually always true, but here we need to include it to avoid circular reasoning.

*Proof of [Proposition 5.7](#).* Without loss of generality suppose that  $s$  is blue. If  $v_{\delta_1}^1 = v_{\delta_2}^2$  then by [Lemma 4.8](#),  $\Gamma(h_1 \cup h_2)$  is connected, and by [Proposition 4.4](#) and [Proposition 4.3](#),  $N \leq \frac{1}{4}\lambda^{-2x} + 1$ . Similarly, if  $v_1^1 = v_1^2$  then by [Lemma 4.9](#), [Proposition 4.4](#), and [Proposition 4.3](#),  $N \leq \frac{1}{4}\lambda^{-2x} + 1$ . Hence we can assume that  $v_{\delta_1}^1 \neq v_{\delta_2}^2$  and  $v_1^1 \neq v_1^2$  in the rest of this proof.

We claim that  $\Gamma(h_1 \cup \{(v_0, \text{B-resolution}), (v_1^2, \text{A-resolution})\})$  is connected. First notice that by following along the sides of  $s$  containing  $h_1$ , we see that  $v_0$  only meets one component of  $\Gamma(h_1 \cup \{(v_0, \text{B-resolution}), (v_1^2, \text{A-resolution})\})$ . Here we use the fact that  $s$  satisfies (TBT) and  $v_1^1 \neq v_1^2$ . Hence it suffices to show that  $\Gamma(h_1 \cup \{(v_1^2, \text{A-resolution})\})$  is connected.

Notice that the bottom vertex of  $s_1^2$  is  $v_{\delta_2}^2$  since  $s$  satisfies (TBT), and this is not equal to  $v_{\delta_1}^1$  by our assumption in the first paragraph. Hence if  $v_1^2$  does not meet the bottom sides of  $s_1^2$  then by following along the sides of  $s_1^2$  we see that  $v_1^2$  only meets one component of  $\Gamma(h_1 \cup \{(v_1^2, \text{A-resolution})\})$ .

If  $v_1^2$  does meet the bottom sides of  $s_1^2$  then it must do so on the bottom side other than  $s_1^2$ . But if the identification is such that  $e_1^2$  lies on the bottom side of  $s_1^2$ , then we will have  $s = s_1^2$ , contradicting the second item in the hypothesis. See [Figure 26](#) left. In the other manner of identification, we see that  $v_1^2$  only meets one component of  $\Gamma(h_1 \cup \{(v_1^2, \text{A-resolution})\})$ . See [Figure 26](#) right.

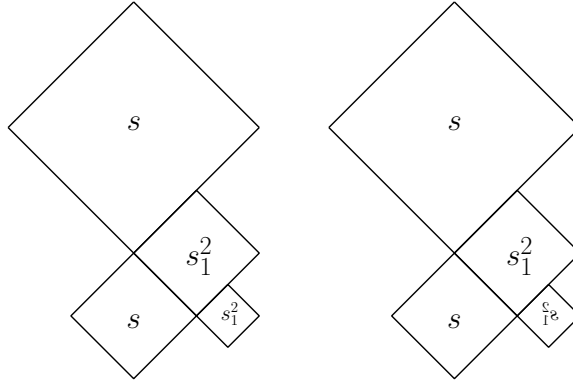


FIGURE 26. Reasoning that  $\Gamma(h_1 \cup \{(v_1^2, \text{A-resolution})\})$  is connected even if  $v_1^2$  meets the bottom sides of  $s_1^2$ .

The point of the claim is that by taking the hook circuit  $c$  to be the image of an Eulerian circuit in  $\Gamma(h_1 \cup \{(v_0, \text{B-resolution}), (v_1^2, \text{A-resolution})\})$ , we can assume that  $c$  takes a branching turn at  $v_0$  and an anti-branching turn at  $v_1^2$ . This forces what the last two vertices of  $-c$  can be.

We now let  $t_i$  be the sector that has the top side of  $s_1^i$  other than  $e_1^i$  along its bottom side, for  $i = 1, 2$ . See [Figure 27](#). By the assumption that  $v_1^1 \neq v_1^2$ , we know that  $t_1$  and  $t_2$  are distinct from  $s$ . (But  $t_1$  and  $t_2$  could be equal.) Let the weight of  $t_i$  be  $a_i w$ , and let the

number of times the bottom side of  $t_i$  meeting  $s_1^i$  intersects the fiber surface be  $p_i$ . We highlighted these bottom sides in orange in [Figure 27](#).

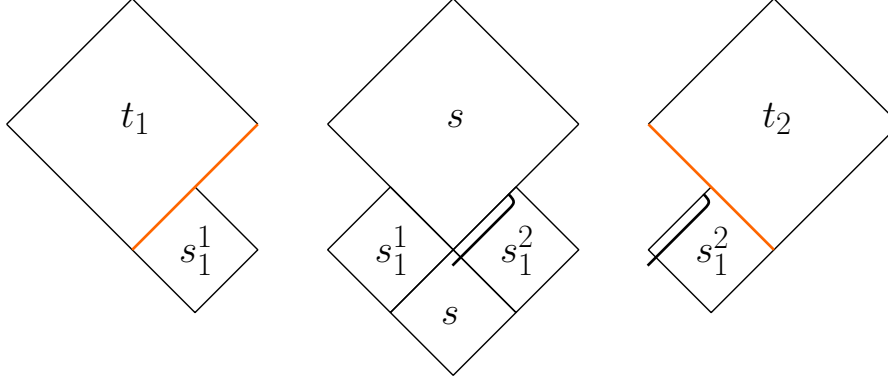


FIGURE 27. The set up to the main argument of [Proposition 5.7](#). We first argue that we can assume the ending portion of  $-c$  is as indicated. Then we consider the weights of  $t_i$  and the highlighted bottom sides of  $t_i$  to improve the estimates in [Equation \(3.1\)](#).

We first claim that  $\lambda^{p_i} \geq \frac{2}{a_i}$ . This can be shown by taking the height 0 lift of  $t_i$ , pushing the bottom side we highlighted upwards on the side of  $t_i$  and reversing its orientation to get a descending path. The starting point of the path is on a sector of height  $p_i$  hence of weight  $\geq \lambda^{-p_i}w$  while its ending point is on the height 0 lift of  $t_i$  which is of weight  $a_iw$ , and the path intersects the branch locus once, where a sector of height  $\leq p_i$  hence of weight  $\geq \lambda^{-p_i}w$  merges in. This gives the equation  $a_iw \geq 2\lambda^{-p_i}w$  which implies the claim.

Let  $b$  be the number of arcs on  $s$ . We claim that  $2b + p_1 + p_2 \leq -2\chi$ . This is because the bottom sides of the  $t_i$  meeting  $s_1^i$  are disjoint from the sides of  $s$ , and the dual graph  $\Gamma$  intersects the fiber surface for a total of  $-2\chi$  times. Together with the previous claim, this implies that  $\lambda^b \leq \lambda^{-\chi} \frac{\sqrt{a_1 a_2}}{2}$ . When  $a_1, a_2 > 2$ , this bound is actually not ideal, since we can just use the fact that  $2b \leq 2b + p_1 + p_2 \leq -2\chi$  to write  $\lambda^b \leq \lambda^{-\chi}$ . So we combine the two inequalities to get  $\lambda^b \leq \min\{\lambda^{-\chi} \frac{\sqrt{a_1 a_2}}{2}, \lambda^{-\chi}\}$ .

Now let  $u_i$  be the vertex of the Eulerian hook circuit  $c$  sitting at  $s_1^i$  for which  $t_i$  merges in at the corresponding intersection point with the branch locus. The  $u_i$  cannot meet hook vertices since they are the top vertices of blue toggle sectors and  $h_1$  is not deep, thus we can improve the contribution of  $u_i$  in [Equation \(3.1\)](#) from  $w$  to  $a_iw$ .

Meanwhile let  $u$  and  $u'$  be the last and second-to-last vertex of  $-c$  respectively.  $u$  is blue hence different from  $u_1, u_2, u'$ , while  $u'$  is distinct from  $u_1, u_2$  since we assumed that  $v_1^1 \neq v_1^2$  and  $c$  takes an anti-branching turn at  $v_1^2$ .  $u$  does not meet a hook vertex by the second item in the hypothesis and  $u'$  does not meet a hook vertex since  $h_1$  is not deep. Hence their original contributions to [Equation \(3.1\)](#) are  $w$ .

We replace the contribution of  $u$  by  $\lambda^{-2\chi-b}w$  since the corresponding intersection point has height  $-2\chi - b$ , and also replace the contribution of  $u'$  by  $\lambda^{-2\chi-b}w$  since the sector that merges in at the corresponding intersection point is the lift of  $s$  at height  $-2\chi - b$ .



With these modifications, Equation (3.1) now reads

$$\begin{aligned}\lambda^{-2x} &\geq 2N + (a_1 - 1) + (a_2 - 1) + 2(\lambda^{-2x-b} - 1) \\ &\geq 2N - 4 + a_1 + a_2 + 2 \max\left\{\lambda^{-x} \frac{2}{\sqrt{a_1 a_2}}, \lambda^{-x}\right\}\end{aligned}$$

**Claim 5.8.** *If  $\lambda^{-x} \geq 2$ , the minimum of  $2N - 4 + a_1 + a_2 + 2 \max\{\lambda^{-x} \frac{2}{\sqrt{a_1 a_2}}, \lambda^{-x}\}$  over  $a_1, a_2 \geq 1$  is  $2N + 2\lambda^{-x}$ .*

Claim 5.8 will be shown in Appendix A.

This implies that

$$\begin{aligned}\lambda^{-2x} &\geq 2N + 2\lambda^{-x} \\ N &\leq \frac{1}{2}\lambda^{-2x} - \lambda^{-x}.\end{aligned}$$

□

We summarize the main argument of Proposition 5.7 in Table 7.

TABLE 7. The argument in Proposition 5.7

Vertices of $-c$	Quantity	Contribution
Vertex at $v_1^i$ where $t_i$ merges in	2	$a_i w$
Second-to-last vertex	1	$\lambda^{-2x-b} w$
Last vertex	1	$\lambda^{-2x-b} w$
Pairs of vertices that meet a B-resolved hook vertex	# hook vertices $- 1$	$2w$
Remaining non-hook vertices	$2N - 2(\# \text{ hook vertices}) - 3$	$w$

**Proposition 5.9.** *Let  $s$  be a sector of minimum weight. Suppose that there is an Eulerian circuit  $c$  containing the hook  $h_1$  of  $s$ , and suppose that:*

- $s$  is fan
- $s \neq s_1^1$  or  $s_1^2$
- $s$  satisfies (FRC) and (TBT)
- $h_1$  is not deep
- One side of the dual edge  $e$  of  $s$  (necessarily the  $\beta = 2$  side by the item above) is short

Then the number of tetrahedra in  $\Delta$  is  $\leq \min\{\frac{1}{2}(\lambda^{-2x} - \lambda^{-\frac{4}{3}x} - \lambda^{-\frac{2}{3}x}) + 1, \frac{1}{6\sqrt{3}}\lambda^{-2x} + \frac{3}{2}\}$ .

*Proof.* Let  $f$  be the fan sector that has  $e_1^2$  as a top edge. Let  $f_2^2$  be the other top edge of  $f$  and let  $f_1^2$  be the bottom side of  $f$  below  $f_2^2$ . See [Figure 28](#) left. By the second item in the hypothesis,  $f \neq s$ . Also notice that  $s$  satisfying (TBT) forces  $f$  to satisfy (TBT) as well, in particular  $(f_i^2)_{i \in \mathbb{Z}/2}$  is a  $\Gamma$ -cycle. The proof is divided into two cases depending on whether  $f_1^2 = f_2^2$ .

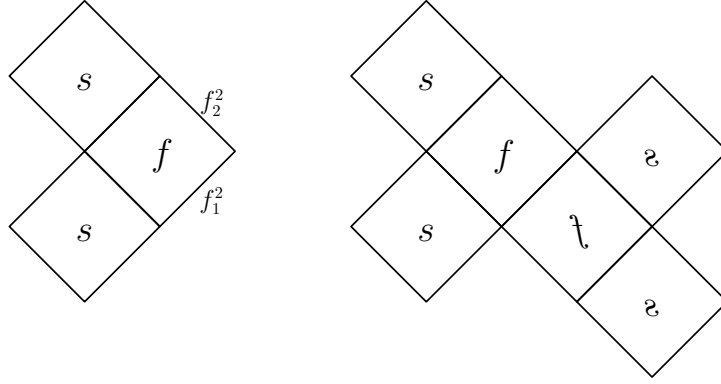


FIGURE 28. The set up in [Proposition 5.9](#). Left: when  $f_1^2 \neq f_2^2$ . Right: when  $f_1^2 = f_2^2$ .

Let us first deal with the case when  $f_1^2 \neq f_2^2$ . Let  $b$  be the number of arcs on  $s$ . This is equal to the intersection number of the cycle  $(e_i^2)_{i \in \mathbb{Z}/2}$  with  $S$ . But  $(e_i^2)$  is homotopic to  $(f_i^2)$  and  $(e_i^1)_{i \in \mathbb{Z}/\delta_1+1}$ , and under our assumptions, these cycles are simple and disjoint, so  $3b \leq -2\chi$ .

Let  $u$  and  $u'$  be the last vertex of  $-c$  and the last vertex of  $-c$  on  $(f_i^2)$  respectively. These are blue hence do not meet B-resolved hook vertices, so their original contributions to [Equation \(3.1\)](#) are both  $w$ . We replace the contribution of  $u$  by  $\lambda^{-2x-b}w$  since the corresponding intersection point has height  $-2\chi - b$ , and replace the contribution of  $u'$  by  $\lambda^b w$  since at that point  $-c$  would have traversed through  $(f_i^2)$ . [Equation \(3.1\)](#) then becomes

$$\begin{aligned} \lambda^{-2x} &\geq 2N + (\lambda^b - 1) + (\lambda^{-2x-b} - 1) \\ &\geq 2N - 2 + \lambda^{-\frac{4}{3}x} + \lambda^{-\frac{2}{3}x} \end{aligned}$$

Here we use the fact that  $\lambda^b + \lambda^{-2x-b}$  is decreasing on  $b \in [0, -\chi]$ . Hence we have

$$N \leq \frac{1}{2}(\lambda^{-2x} - \lambda^{-\frac{4}{3}x} - \lambda^{-\frac{2}{3}x}) + 1$$

We then deal with the case when  $f_1^2 = f_2^2$ . In this case,  $(f_i^2)_{i \in \mathbb{Z}/2}$  is not a simple cycle so the above argument fails. What we will do instead is modify the argument of [Proposition 4.3](#).

We first claim that  $\Gamma(h_1 \cup \{(v_0, \text{A resolution})\})$  has two components. This is because  $\Gamma(h_1)$  is connected and resolving an additional vertex at most creates one more component. Meanwhile  $\{e_1^2, e_2^2, f_1^2\}$  forms its own component, as can be inspected from [Figure 28](#) right.

Let  $c_1$  be a circuit that is the image of an Eulerian circuit of the component of  $\Gamma(h_1 \cup \{(v, A \text{ resolution})\})$  containing  $h_1$ . Let  $b$  be the number of arcs on  $s$  again. We claim that [Equation \(4.1\)](#) applied to  $c_1$  reads

$$\lambda^{-2\chi - \frac{3}{2}b} w \geq (2N - 3)w$$

This is because there are  $2N - 3$  vertices along  $c_1$  (missing the 3 in the other component),  $c_1$  intersects the fiber surface  $-2\chi - \frac{3}{2}b$  times (missing the  $\frac{3}{2}b$  times in the other component, noting that two times  $(f_1^2)$  is homotopic to  $(e_i^2)$ ), and all the hook vertices of  $h_1$  lie in the same component as  $c_1$  (so that the pairing trick works).

Meanwhile we have  $\lambda^b \geq 3$  by the same argument as in [Proposition 5.6](#), so putting these together, we have  $\lambda^{-2\chi} \geq 3\sqrt{3}(2N - 3)$  which implies the second bound in the proposition.  $\square$

We summarize the argument in the first case of [Proposition 5.9](#) in [Table 8](#).

TABLE 8. The argument in the first case of [Proposition 5.9](#)

Vertices of $-c$	Quantity	Contribution
Last vertex on $(f_i^2)_{i \in \mathbb{Z}/2}$	1	$\lambda^b w$
Last vertex	1	$\lambda^{-2\chi - b} w$
Pairs of vertices that meet a B-resolved hook vertex	$\#$ hook vertices $- 1$	$2w$
Remaining non-hook vertices	$2N - 2(\# \text{ hook vertices}) - 1$	$w$

**5.4. When the sector is toggle.** In this subsection, we lay out the final propositions we need. These will concern cases when  $s$  is toggle.

**Proposition 5.10.** *Let  $s$  be a sector of minimum weight. Suppose that there is an Eulerian circuit  $c$  containing the hook  $h_1$  of  $s$ , and suppose that:*

- $s$  is toggle
- $s$  satisfies (FRC)
- $s_1^1 \neq s \neq s_1^2$

*Then the number of tetrahedra in  $\Delta$  is  $\leq \min\{\frac{1}{4}\lambda^{-2\chi} + 1, \frac{1}{2}\lambda^{-2\chi} - \sqrt{\lambda^{-2\chi} + 4\lambda^{-\chi}} + 2\}$ .*

*Proof.* This proof is morally similar to that of [Proposition 5.7](#). Let  $t_i$  be the sector that has  $e_{\delta_i+1}^i$  along its bottom side. By the third item in the hypothesis,  $t_1$  and  $t_2$  are distinct from  $s$ .

If  $t_1 = t_2$ , then  $v_{\delta_1}^1 = v_{\delta_2}^2$ . By [Lemma 4.8](#),  $\Gamma(h_1 \cup h_2)$  is connected, hence [Proposition 4.4](#) and [Proposition 4.3](#) implies the first bound in the proposition.

If  $t_1 \neq t_2$ . Let the weight of  $t_i$  be  $a_i w$ , and let  $p_i$  be the number of times the bottom side of  $t_i$  not meeting  $s$  meets the fiber surface.  $\lambda^{p_i} \geq \frac{2}{a_i}$  by the same argument as in [Proposition 5.7](#).

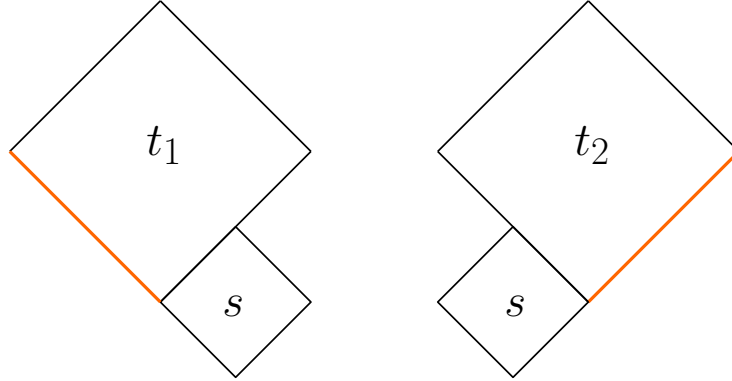


FIGURE 29. The set up in Proposition 5.10. We consider the weights of  $t_i$  and the highlighted bottom sides of  $t_i$  to improve the estimates in Equation (3.1).

Let  $b$  be the number of arcs in  $s$ . By the same reason as in Proposition 5.7,  $2b + p_1 + p_2 \leq -2\chi$ , which implies that  $\lambda^b \leq \min\{\lambda^{-\chi \frac{\sqrt{a_1 a_2}}{2}}, \lambda^{-\chi}\}$ .

Let  $u_i$  be the vertices of the Eulerian hook circuit  $c$  sitting at the top vertex of  $s$ , for which  $t_i$  merges in at the corresponding intersection point with the branch locus. By the third item in the hypothesis,  $u_i$  do not meet hook vertices, nor are they the last vertex of  $c$  on  $h_2$ . However, notice that one of  $u_i$  is the last vertex of  $-c$ .

For the sake of concreteness we assume that  $u_2$  is the last vertex of  $-c$ . Strictly speaking  $u_1$  and  $u_2$  do not have symmetric roles here, since we have broken the symmetry by assuming that  $c$  contains the hook  $h_1$ , but the reader can check that this will not matter for the bounds we use below.

Let  $u'$  be the last vertex of  $-c$  on  $h_2$ . We modify Equation (3.1) by replacing the contributions of  $u_1$ ,  $u_2$ , and  $u'$ . For  $u_1$ , we replace  $w$  with  $a_1 w$ . For  $u_2$ , we replace  $w$  with  $a_2 \lambda^{-2\chi-b} w$ . For  $u'$ , we replace  $w$  with  $\lambda^b w$ . Then Equation (3.1) becomes

$$\begin{aligned} \lambda^{-2\chi} &\geq 2N + (a_1 - 1) + (a_2 \lambda^{-2\chi-b} - 1) + (\lambda^b - 1) \\ &\geq 2N + (a_1 - 1) + (a_2 - 1) + (\lambda^{-2\chi-b} - 1) + (\lambda^b - 1) \\ &= 2N - 4 + a_1 + a_2 + \lambda^{-2\chi-b} + \lambda^b \end{aligned}$$

Here we use the fact that  $a_2, \lambda^{-2\chi-b} \geq 1$  thus  $(a_2 \lambda^{-2\chi-b} - 1) \geq (a_2 - 1) + (\lambda^{-2\chi-b} - 1)$ . As in Proposition 5.9, this last expression is minimized when  $b = \min\{\lambda^{-\chi \frac{\sqrt{a_1 a_2}}{2}}, \lambda^{-\chi}\}$ , since  $\lambda^{-2\chi-b} + \lambda^b$  is decreasing for  $b \in [0, -\chi]$ .

**Claim 5.11.** *The minimum of  $2N - 4 + a_1 + a_2 + \lambda^{-2\chi-b} + \lambda^b$ , where  $b = \min\{\lambda^{-\chi \frac{\sqrt{a_1 a_2}}{2}}, \lambda^{-\chi}\}$ , over  $a_1, a_2 \geq 1$  is  $2N - 4 + 2\sqrt{\lambda^{-2\chi} + 4\lambda^{-\chi}}$ .*

Claim 5.11 will be shown in Appendix A.

This implies that

$$\begin{aligned}\lambda^{-2x} &\geq 2N - 4 + 2\sqrt{\lambda^{-2x} + 4\lambda^{-x}} \\ N &\leq \frac{1}{2}\lambda^{-2x} - \sqrt{\lambda^{-2x} + 4\lambda^{-x}} + 2\end{aligned}$$

□

We summarize the argument of [Proposition 5.10](#) in [Table 9](#).

TABLE 9. The argument in [Proposition 5.10](#)

Vertices of $-c$	Quantity	Contribution
First vertex at top vertex of $s$	1	$a_1 w$
Second vertex at top vertex of $s$ = Last vertex	1	$a_2 \lambda^{2-b} w$
Last vertex of $c$ on $h_2$	1	$\lambda^b w$
Pairs of vertices that meet a B-resolved hook vertex	# hook vertices $- 1$	$2w$
Remaining non-hook vertices	$2N - 2(\# \text{ hook vertices}) - 1$	$w$

Similar to [Section 5.3](#), for the rest of the propositions we will assume that  $h_1$  is not deep. Depending on whether  $e_{\delta_1+1}^1 = e_1^1$  and  $e_{\delta_2+1}^2 = e_1^2$ , [Proposition 5.12](#) and [Proposition 5.13](#) will conclude our arguments in this subsection.

**Proposition 5.12.** *Let  $s$  be a sector of minimum weight. Suppose that there is an Eulerian circuit  $c$  containing the hook  $h_1$  of  $s$ , and suppose that:*

- $s$  is toggle
- $s$  satisfies (FRC)
- $e_{\delta_2+1}^2 = e_1^2$
- $h_1$  is not deep

Then the number of tetrahedra in  $\Delta$  is  $\leq \frac{1}{4}\lambda^{-2x} + 1$ .

*Proof.* Under the hypothesis,  $\Gamma(h_1 \cup h_2)$  satisfies the hypothesis of [Proposition 4.4](#) by [Lemma 4.11](#), so the bound follows from [Proposition 4.3](#). □

We come to the final proposition, whose proof contains the most modifications to [Proposition 3.3](#). To state the bounds in the proposition we need to define some auxiliary functions.

Let  $F_1(x)$  be the maximum of

$$f_1(x, u) = \frac{1}{2}x^2 - \frac{1}{2}x(u + u^{-1}) - \left(\frac{3}{2}\right)^{\frac{4}{3}}u^{\frac{2}{3}} + 2 - \frac{1}{2x}$$

over  $0 < u \leq 1$ .

Let  $F_2(x)$  be the maximum of

$$f_2(x, a) = \frac{1}{2}x^2 - \frac{1}{2}x\left(\sqrt{\frac{a}{a+1}} + \sqrt{\frac{a+1}{a}}\right) - \frac{1}{2}a - a^{-1} + 2 - \frac{1}{2x}$$

over  $a \geq 1$ .

**Proposition 5.13.** *Let  $s$  be a sector of minimum weight. Suppose that there is an Eulerian circuit  $c$  containing the hook  $h_1$  of  $s$ , and suppose that:*

- $s$  is toggle
- $s$  satisfies (FRC)
- $e_{\delta_1+1}^1 = e_1^1$  but  $s \neq s_1^2$

Then the number of tetrahedra in  $\Delta$  is  $\leq \max\{\frac{1}{4}\lambda^{-2x} + 1, F_1(\lambda^{-x}), F_2(\lambda^{-x})\}$ , provided that  $\lambda^{-x} \geq 4\sqrt{2}$ .

Like [Proposition 5.7](#), the assumption  $\lambda^{-x} \geq 4\sqrt{2}$  is used to simplify the statement and does not play a role in the main argument. Here this hypothesis is nontrivial, but it will not matter for our application to the fully-punctured normalized dilatation problem.

*Proof of [Proposition 5.13](#).* Notice that  $e_{\delta_1+1}^1 = e_1^1$  implies that  $h_1$  is not deep, otherwise  $\Gamma(h_1)$  cannot be connected. Since  $\Gamma(e_2^1, \dots, e_{\delta_1+1}^1)$  is connected by [Lemma 3.10](#), we can assume that  $-c$  starts with  $(-e_{\delta_1+1}^1, \dots, -e_2^1)$ . Then  $-c$  has to take an anti-branching turn at  $v_1^1$  otherwise it would not be an Eulerian circuit. Write  $t = s_1^2$ . Let  $t_1^2$  be the top edge of  $t$  other than  $e_1^2$ , let  $t_1^1$  be the bottom side of  $t$  below  $t_1^2$ , and let  $t_1^1$  be the other bottom side of  $t$ .

By [Lemma 4.7](#),  $\Gamma(h_1 \cup h_2)$  is connected unless  $e_{\delta_1+1}^1$  or  $e_{\delta_2+1}^2$  lies along  $t_1^1$ . If  $e_{\delta_1+1}^1$  lies along  $t_1^1$ , then by the hypothesis that  $e_{\delta_1+1}^1 = e_1^1$ , we have  $t = s$ , but this contradicts the hypothesis that  $s \neq s_1^2$ . So we either have the first bound in the proposition from [Proposition 4.4](#) and [Proposition 4.3](#) or  $e_{\delta_2+1}^2$  lies along  $t_1^1$ . See [Figure 30](#) left, where we also indicate the initial portion of the descending path (obtained from  $c$ ) in yellow then teal. The second and third bounds in the proposition will follow from splitting into cases when  $t_1^2$  is disjoint from  $t_2^2$  and when it is not.

We first tackle the case when  $t_1^2$  is disjoint from  $t_2^2$ . Let  $b$  be the number of arcs on  $s$ . Let  $b'$  be the number of times  $e_{\delta_2+1}^2$  intersects the fiber surface, and let  $b''$  be the total number of times  $e_i^2$  for  $i = 1, \dots, \delta_2$  intersects the fiber surface. Then  $b = b' + b''$ . Meanwhile let  $q$  be the number of arcs on  $t$  and let  $p + b'$  be the number of times  $t_1^1$  intersects the fiber surface. We label these variables on [Figure 30](#) left. Finally, let  $aw$  be the weight of  $t$ .

We have  $\lambda^q \geq \frac{3}{a}$  by the same argument as in [Proposition 5.6](#) but applied to  $t$ . Similarly,  $\lambda^{p+b'} \geq \frac{2}{a}$ . We claim that  $2b+p+q \leq -2\chi$ . This follows from the observation that  $t_1^1, t_1^2, t_2^2$  are disjoint from the sides of  $s$  except for  $e_{\delta_2+1}^2$  lying along  $t_1^1$ , and the fact that  $e_1^1$  does not meet

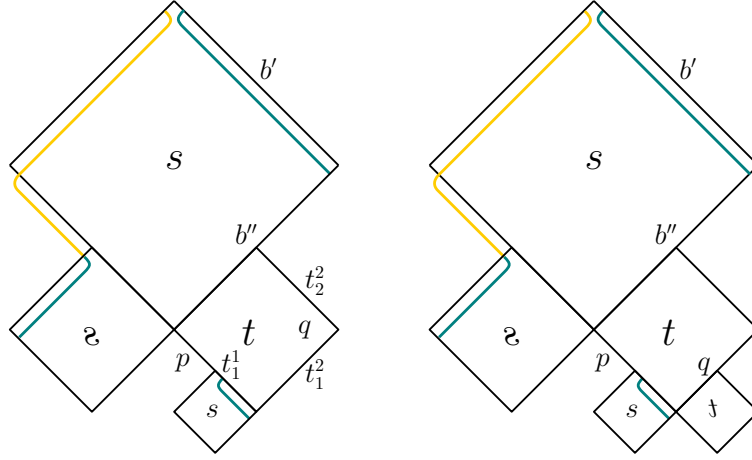


FIGURE 30. The set up in [Proposition 5.13](#). We can assume that  $-c$  first goes through  $(-e_{\delta_1+1}^1, \dots, -e_2^1)$  (in yellow) and takes an antibranching turn at  $v_1^1$  (in teal). Left: if  $t_1^2$  is disjoint from  $t_2^2$ . Right: if  $t_1^2 \subset t_2^2$ .

the fiber surface, since  $h_1$  is not deep. The claim implies that  $\lambda^b \leq \min\{\lambda^{-x-\frac{p}{2}}\sqrt{\frac{a}{3}}, \lambda^{-x}\}$ . We also note that we have  $\lambda^{b'} \geq \lambda^{-p\frac{2}{a}}$ .

Let  $u_1$  be the vertex of  $-c$  at the top vertex of  $s$  for which  $t$  merges in. Let  $u_2$  be the vertex of  $-c$  after it traverses  $e_{\delta_2+1}^2$ . In other words,  $u_1$  and  $u_2$  are the first two vertices of  $c$  after it traverses  $(-e_{\delta_1+1}^1, \dots, -e_2^1)$ . This implies that  $u_1$  and  $u_2$  are distinct from each other and distinct from the last vertex of  $-c$  on  $h_2$  and the last vertex of  $-c$ . Let us write  $u'$  and  $u$  for these last two vertices respectively. Since  $t = s_1^2 \neq s$ ,  $u'$  and  $u$  are distinct, so  $u_1, u_2, u', u$  are all distinct vertices of  $-c$ .

$u_1$  does not meet a B-resolved hook vertex since  $h_1$  is not deep.  $u_2$  does not meet a B-resolved hook vertex since it is blue.  $u'$  does not meet a B-resolved hook vertex since it is either blue or takes an anti-branching turn.  $u$  does not meet a B-resolved hook vertex since  $h_1$  is not deep.

Hence we can modify [Equation \(3.1\)](#) by replacing the contribution of  $u_1$  from  $w$  to  $aw$ , replacing the contribution of  $u_2$  from  $w$  to  $\lambda^{b'}w$ , replacing the contribution of  $u'$  from  $w$  to  $\lambda^b w$ , and replacing the contribution of  $u$  from  $w$  to  $\lambda^{-2x-b}$ . We remark that we could have replaced the contribution of  $u_1$  from  $w$  to  $a\lambda^{b'}w$  but it turns out that does not actually buy us any advantage, and would only complicate the arithmetic below.

Finally, we also estimate the first term of [Equation \(3.1\)](#), that is, the term corresponding to the A-resolved hook vertex, by  $\lambda^{-b}w$  instead of ignoring it. This estimate comes from the fact that in the proof of [Proposition 3.3](#), the vertex of  $-\hat{c}$  corresponding to the first term is at height  $\leq b$ .



Thus [Equation \(3.1\)](#) now reads

$$\begin{aligned}
 \lambda^{-2x} &\geq 2N + (a - 1) + (\lambda^{b'} - 1) + (\lambda^b - 1) + (\lambda^{-2x-b} - 1) + \lambda^{-b} \\
 &= 2N - 4 + \lambda^{-b} + \lambda^b + \lambda^{-2x-b} + a + \lambda^{b'} \\
 &\geq 2N - 4 + \lambda^x + \lambda^{-x}(\min\{\lambda^{-\frac{p}{2}}\sqrt{\frac{a}{3}}, 1\} + \min\{\lambda^{-\frac{p}{2}}\sqrt{\frac{a}{3}}, 1\}^{-1}) + a + \lambda^{-p}\frac{2}{a} \\
 N &\leq \frac{1}{2}\lambda^{-2x} - \frac{1}{2}\lambda^{-x}(\min\{\} + \min\{\}^{-1}) - \frac{1}{2}(a + \lambda^{-p}\frac{2}{a}) + 2 - \frac{\lambda^x}{2}
 \end{aligned}$$

where we write  $\min\{\} = \min\{\lambda^{-\frac{p}{2}}\sqrt{\frac{a}{3}}, 1\}$  to save space.

**Claim 5.14.** *For any  $a \geq 1, p \geq 0$ , we have*

$$a + \lambda^{-p}\frac{2}{a} \geq 3\left(\frac{3}{2}\right)^{\frac{1}{3}}\left(\lambda^{-\frac{p}{2}}\sqrt{\frac{a}{3}}\right)^{\frac{2}{3}}$$

[Claim 5.14](#) will be shown in [Appendix A](#).

This implies that

$$\begin{aligned}
 N &\leq \frac{1}{2}\lambda^{-2x} - \frac{1}{2}\lambda^{-x}(\min\{\} + \min\{\}^{-1}) - \left(\frac{3}{2}\right)^{\frac{4}{3}}\left(\lambda^{-\frac{p}{2}}\sqrt{\frac{a}{3}}\right)^{\frac{2}{3}} + 2 - \frac{\lambda^x}{2} \\
 &\leq \frac{1}{2}\lambda^{-2x} - \frac{1}{2}\lambda^{-x}(\min\{\} + \min\{\}^{-1}) - \left(\frac{3}{2}\right)^{\frac{4}{3}}\min\{\}^{\frac{2}{3}} + 2 - \frac{\lambda^x}{2} \\
 &= f_1(\lambda^{-x}, \min\{\}) \\
 &\leq F_1(\lambda^{-x})
 \end{aligned}$$

Now we tackle the case when  $t_1^2$  is contained in  $t_1^1$ . Let  $b$  be the number of arcs on  $s$ . Let  $b'$  be the number of times  $e_{\delta_2+1}^2$  intersects the fiber surface, and let  $b''$  be the total number of times  $e_i^2$  for  $i = 1, \dots, \delta_2$  intersects the fiber surface. Then  $b = b' + b''$ . Meanwhile let  $q$  be the times  $t_1^2$  intersects the fiber surface and let  $p + b'$  be the number of times  $t_1^1$  intersects the fiber surface. See [Figure 30](#) right. Finally, let  $aw$  be the weight of  $t$ .

Consider  $t_1^2$ , push it upwards in the direction of  $t$  and reverse its orientation to get a descending path. Using this path, we get the inequality  $\lambda^q \geq \frac{a+1}{a}$ . We reuse the same inequalities  $\lambda^{p+b'} \geq \frac{2}{a}$  and  $2b + p + q \leq 2$  as above. This implies that  $\lambda^b \leq \lambda^{-x-\frac{p}{2}}\sqrt{\frac{a}{a+1}}$ , and that  $\lambda^{b'} \geq \lambda^{-p}\frac{2}{a}$ .

We let  $u_1, u_2, u', u$  be the same vertices as above and apply the exact same modifications as above. Then [Equation \(3.1\)](#) reads

$$\begin{aligned}
\lambda^{-2x} &\geq 2N + (a-1) + (\lambda^{b'} - 1) + (\lambda^b - 1) + (\lambda^{-2x-b} - 1) + \lambda^{-b} \\
&= 2N - 4 + \lambda^{-b} + \lambda^b + \lambda^{-2x-b} + a + \lambda^{b'} \\
&\geq 2N - 4 + \lambda^x + \lambda^{-x} \left( \lambda^{-\frac{p}{2}} \sqrt{\frac{a}{a+1}} + \left( \lambda^{-\frac{p}{2}} \sqrt{\frac{a}{a+1}} \right)^{-1} \right) + a + \lambda^{-p} \frac{2}{a} \\
N &\leq \frac{1}{2} \lambda^{-2x} - \frac{1}{2} \left( \lambda^{-x} \left( \lambda^{-\frac{p}{2}} \sqrt{\frac{a}{a+1}} + \left( \lambda^{-\frac{p}{2}} \sqrt{\frac{a}{a+1}} \right)^{-1} \right) + a + \lambda^{-p} \frac{2}{a} \right) + 2 - \frac{\lambda^x}{2}
\end{aligned}$$

**Claim 5.15.** *If  $\lambda^{-x} \geq 4\sqrt{2}$ , then*

$$\lambda^{-x} \left( \lambda^{-\frac{p}{2}} \sqrt{\frac{a}{a+1}} + \left( \lambda^{-\frac{p}{2}} \sqrt{\frac{a}{a+1}} \right)^{-1} \right) + a + \lambda^{-p} \frac{2}{a} \geq \lambda^{-x} \left( \sqrt{\frac{a}{a+1}} + \sqrt{\frac{a+1}{a}} \right) + a + \frac{2}{a}$$

for all  $a \geq 1$ .

[Claim 5.15](#) will be shown in [Appendix A](#).

This implies that

$$\begin{aligned}
N &\leq \frac{1}{2} \lambda^{-2x} - \frac{1}{2} \left( \lambda^{-x} \left( \sqrt{\frac{a}{a+1}} + \sqrt{\frac{a+1}{a}} \right) + a + \frac{2}{a} \right) + 2 - \frac{\lambda^x}{2} \\
&= f_2(\lambda^{-x}, a) \\
&\leq F_2(\lambda^{-x})
\end{aligned}$$

□

We summarize the argument of [Proposition 3.3](#) in [Table 10](#).

TABLE 10. The argument in [Proposition 5.13](#)

Vertices of $-c$	Quantity	Contribution
Vertex at top vertex of $s$ where $t$ merges in	1	$aw$
Vertex after $-c$ traverses $e_{\delta_2+1}^2$	1	$\lambda^{b'}w$
Last vertex on $h_2$	1	$\lambda^b w$
Last vertex	1	$\lambda^{-2x-b}w$
Pairs of vertices that meet a B-resolved hook vertex	# hook vertices $- 1$	$2w$
Remaining non-hook vertices	$2N - 2(\# \text{ hook vertices}) - 3$	$w$
A-resolved hook vertex	1	$\lambda^{-b}w$

**5.5. Putting everything together.** By combining all the arguments we had in the previous subsections, we will prove the following theorem in this subsection.

**Theorem 5.16.** *Let  $f : S \rightarrow S$  be a fully-punctured pseudo-Anosov map with normalized dilatation  $\lambda^{-x}$ . Suppose the mapping torus of  $f$  has only one boundary component and suppose  $4\sqrt{2} \leq \lambda^{-x} < 8$ , then the mapping torus of  $f$  admits a veering triangulation with the number of tetrahedra less than or equal to*

$$\max\left\{\frac{1}{3}\lambda^{-2x} + \frac{1}{2}, \frac{1}{2}\lambda^{-2x} - \lambda^{-x}, \frac{1}{2}(\lambda^{-2x} - \lambda^{-\frac{4}{3}x} - \lambda^{-\frac{2}{3}x} + 3), \frac{1}{2}\lambda^{-2x} - \sqrt{\lambda^{-2x} + 4\lambda^{-x}} + 2, F_1(\lambda^{-x}), F_2(\lambda^{-x}), 8 \log_3 \lambda^{-x}\right\}$$

*Proof.* Suppose we are given  $f$  as in the statement. We first check if the number of branch cycles  $l$  is greater than  $\frac{\log \lambda^{-x}}{\log 2}$ . If so, we apply [Proposition 5.2](#), noting that

$$\frac{1}{4}\lambda^{-2x} + 1 \leq \frac{1}{3}\lambda^{-2x} + \frac{1}{2}$$

for  $\lambda^{-x} \geq 4\sqrt{2}$ , and

$$\frac{1}{2}(\lambda^{-2x} - \frac{\lambda^{-2x} - \lambda^{-\frac{2}{7}x}}{\lambda^{-\frac{2}{7}x} - 1} + l) \leq \frac{1}{2}(\lambda^{-2x} - \lambda^{-\frac{4}{3}x} - \lambda^{-\frac{2}{3}x} + 3)$$

for  $l > \frac{\log 4\sqrt{2}}{\log 2} = 2.5$ , i.e.  $l \geq 3$ , and we are done. If not, then by the hypothesis that  $\lambda^{-x} < 8$ , we have  $l = 1$  or  $2$ .

Suppose there exists some choice of fiber surface such that there is a minimum weight sector  $s$  that is not deep. Recall (from [Section 3.3](#)) that this means one of the hooks  $h_\beta$  of  $s$  is not deep. Without loss of generality we assume  $h_1$  is not deep. Notice by [Lemma 3.10](#),  $\Gamma(h_1)$  is connected, so there exists an Eulerian hook circuit containing  $h_1$ . If  $e_{\delta_1+1}^1 = e_1^2$  or  $e_{\delta_2+1}^2 = e_1^1$ , then we apply [Proposition 5.3](#) and we are done. If  $s$  does not satisfy (FRC), then we apply [Proposition 5.4](#), noting that

$$\frac{1}{2}(\lambda^{-2x} - \lambda^{-\frac{4}{3}x} - \lambda^{-x}) + 1 \leq \frac{1}{2}(\lambda^{-2x} - \lambda^{-\frac{4}{3}x} - \lambda^{-\frac{2}{3}x} + 3)$$

and we are done. Hence we assume that  $e_{\delta_1+1}^1 \neq e_1^2$ ,  $e_{\delta_2+1}^2 \neq e_1^1$ , and  $s$  satisfies (FRC) from this point onwards.

Suppose  $s$  is fan. If  $s = s_1^1$  or  $s_1^2$ , we apply [Proposition 5.5](#) and we are done, so we assume that  $s \neq s_1^1$  or  $s_1^2$  from this point onwards. If  $s$  does not satisfy (TBT), then we apply [Proposition 5.6](#) and we are done. If  $s$  satisfies (TBT), we apply [Proposition 5.7](#) and [Proposition 5.9](#), noting that

$$\frac{1}{6\sqrt{3}}\lambda^{-2x} + \frac{3}{2} \leq \frac{1}{3}\lambda^{-2x} + \frac{1}{2}$$

for  $\lambda^{-x} \geq 4\sqrt{2}$ , and we are done.

Suppose on the other hand that  $s$  is toggle. If  $s \neq s_1^1$  or  $s_1^2$  then we apply [Proposition 5.10](#). If  $s = s_1^2$ , then by the assumption that  $e_{\delta_1+1}^1 \neq e_1^2$ , we must have  $e_{\delta_2+1}^2 = e_1^2$ , and we can

apply [Proposition 5.12](#). So we can assume that  $s = s_1^1$  but  $s \neq s_1^2$ . By the assumption that  $e_{\delta_2+1}^2 \neq e_1^1$ , we must have  $e_{\delta_1+1}^1 = e_1^1$ , so we can apply [Proposition 5.13](#).

So we can assume now that for any choice of fiber surface, every minimum weight sector is deep. For a sector  $s$  of  $B$ , use [Proposition 3.13](#) to pick a fiber surface so that  $s$  is the only deep sector, thus the only minimum weight sector. If  $e_{\delta_1+1}^1 = e_1^2$  or  $e_{\delta_2+1}^2 = e_1^1$ , then we apply [Proposition 5.3](#). If  $s$  does not satisfy (FRC), then we apply [Proposition 5.4](#). Hence we assume that  $e_{\delta_1+1}^1 \neq e_1^2$ ,  $e_{\delta_2+1}^2 \neq e_1^1$ , and  $s$  satisfies (FRC) from this point onwards.

Suppose  $s$  is fan. We claim that either the theorem holds or  $s$  satisfies (TBT). If neither  $\Gamma(h_1)$  nor  $\Gamma(h_2)$  are connected, then by [Lemma 3.11](#),  $s$  satisfies (TBT) and we have proved the claim. Hence we can assume that one of  $\Gamma(h_\beta)$ , say  $\Gamma(h_1)$  is connected. If  $s = s_1^1$  or  $s_1^2$ , we apply [Proposition 5.5](#). If  $s \neq s_1^1$  or  $s_1^2$  and  $s$  does not satisfy (TBT), then we apply [Proposition 5.6](#). So the remaining case is if  $s$  satisfies (TBT), as claimed.

Repeating this argument for all fan sectors, we can assume that all fan sectors of  $B$  satisfy (TBT).

Suppose  $s$  is toggle. We claim that either the theorem holds or  $s$  satisfies (SBF) on some side. If neither  $\Gamma(h_1)$  nor  $\Gamma(h_2)$  are connected, then by [Lemma 3.14](#),  $s$  satisfies (BSBF) hence (SBF) and we have proved the claim. Hence we can assume that one of  $\Gamma(h_\beta)$ , say  $\Gamma(h_1)$  is connected. If  $s \neq s_1^1$  or  $s_1^2$  then we apply [Proposition 5.10](#) and the theorem holds. Hence we can assume that  $s = s_1^1$  or  $s_1^2$ . By the assumption that  $e_{\delta_1+1}^1 \neq e_1^2$  and  $e_{\delta_2+1}^2 \neq e_1^1$ , we must have  $e_{\delta_1+1}^1 = e_1^1$  or  $e_{\delta_2+1}^2 = e_1^1$  in the respective cases, that is,  $s$  satisfies (SBF).

Repeating this argument for all toggle sectors, we can assume that all toggle sectors of  $B$  satisfy (SBF).

Hence the proof of [Theorem 5.16](#) is completed by the following proposition.

**Proposition 5.17.** *Let  $\Delta$  be a veering triangulation and let  $B$  be its stable branched surface. Suppose that:*

- *For any fiber surface, every minimum weight sector is deep.*
- *Every fan sector satisfies (TBT) and every toggle sector satisfies (SBF) on some side.*

*Then the number of tetrahedra in  $\Delta$  is  $\leq 8 \log_3 \lambda^{-\chi}$ .*

*Proof.* For each blue sector  $s$  of  $B$ , we choose a branch cycle  $c_s$  as follows:

- If  $s$  is fan, take  $c_s = (e_i^\beta)_{i \in \mathbb{Z}/\delta_\beta+1}$  for some arbitrary choice of  $\beta$ . Since  $s$  satisfies (TBT),  $c_s$  is a  $\Gamma$ -cycle.
- If  $s$  is toggle,  $s$  satisfies (SBF) on some side, so  $e_1^\beta = e_{\delta_\beta+1}^\beta$  for some  $\beta$ . Take  $c_s = (e_i^\beta)_{i \in \mathbb{Z}/\delta_\beta}$ . If  $s$  satisfies (BSBF), we take some arbitrary choice of  $\beta$ .

The  $c_s$  for  $s$  toggle are disjoint from each other, and also disjoint from  $c_s$  for  $s$  fan. The  $c_s$  for  $s$  fan are not necessarily disjoint, but each edge meets at most two such

$c_s$ . Hence if we let  $p_s$  be the number of times  $c_s$  intersects a fiber surface, we have  $\sum_{s \text{ blue fan}} \frac{1}{2}p_s + \sum_{s \text{ blue toggle}} p_s \leq -2\chi$ .

Meanwhile, for each sector  $s$ , we can choose a fiber surface so that  $s$  is the only deep sector by [Proposition 3.13](#). By the first assumption,  $s$  must be the only minimum weight sector under this choice of fiber surface. We can then bound  $p_s$  as demonstrated in the previous subsections. Namely, if  $s$  is fan, then we have  $\lambda^{p_s} \geq 3$ ; if  $s$  is toggle, then we have  $\lambda^{p_s} \geq 2$ . Combining this with the inequality we have from the last paragraph, we get

$$\lambda^{-2\chi} \geq \prod_{s \text{ blue fan}} \lambda^{\frac{1}{2}p_s} \prod_{s \text{ blue toggle}} \lambda^{p_s} \geq \sqrt{3}^{\# \text{ blue sectors}}$$

$$\# \text{ blue sectors} \leq 4 \log_3 \lambda^{-\chi}$$

Similarly,  $\# \text{ red sectors} \leq 4 \log_3 \lambda^{-\chi}$ , so

$$\# \text{ tetrahedra} = \# \text{ sectors} \leq 8 \log_3 \lambda^{-\chi}$$

□

□

In [Figure 31](#), we provide a flowchart that illustrates the strategy of the proof of [Theorem 5.16](#).

Showing [Theorem 1.5](#) now essentially amounts to substituting  $\lambda^{-\chi} = 6.86$  in each of the bounds in [Theorem 5.16](#) and checking that they are all less than 17. We relegate this computation to [Appendix A](#).

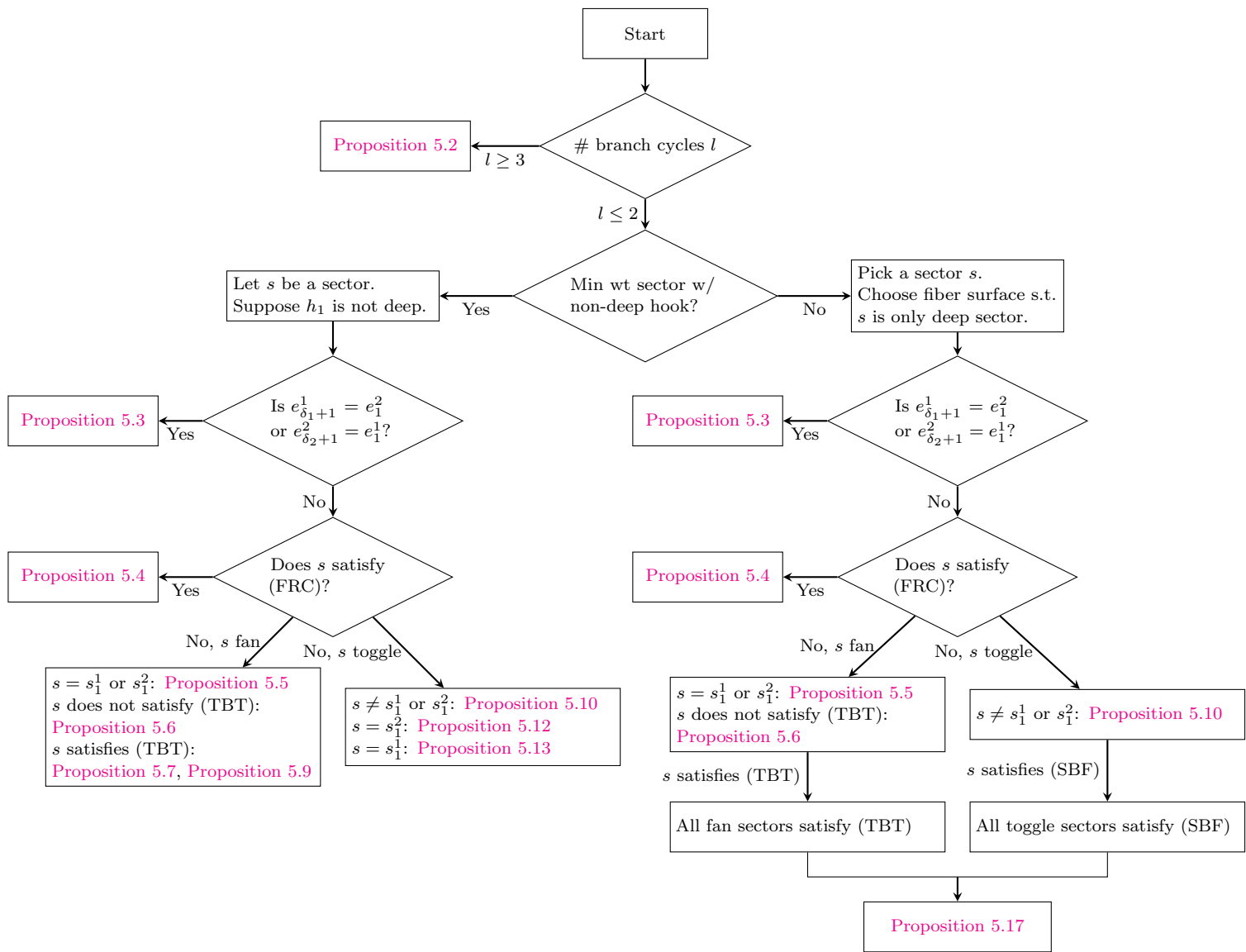


FIGURE 31. Flowchart for Theorem 5.16.

6. APPLICATION TO THE FULLY-PUNCTURED NORMALIZED DILATATION PROBLEM

In this section, we prove [Theorem 1.6](#). As explained in the introduction, with [Theorem 1.5](#), this amounts to running a computation on veering triangulations in the census [\[GSS\]](#). Our main task in this section is to explain how to run this computation using the Veering code [\[PSS23\]](#) written by Parlak, Schleimer, and Segerman, and SageMath scripts written by the author, and how to use these results to conclude [Theorem 1.6](#).

In [Section 6.1](#), we recall some basic facts about Thurston-Fried fibered face theory. In [Section 6.2](#), we classify the isolated points of  $\mathcal{D}$ , as well as the maps that attain such normalized dilatations. In [Section 6.3](#), we show that the minimum accumulation point of  $\mathcal{D}$  is  $\mu^4$  and classify the maps that attain this normalized dilatation.

**6.1. Thurston-Fried fibered face theory.** Let  $M$  be an orientable, irreducible, boundary incompressible, atoroidal, and acylindrical 3-manifold with torus boundary components. The *Thurston norm* of a homology class  $a \in H_2(M, \partial M)$  is defined to be  $\|a\| = \min\{-\chi(S)\}$  where the minimum is taken over all properly embedded surfaces  $S$  such that  $[S, \partial S] = a$ . Under our assumptions on  $M$ , the Thurston norm is a norm on  $H_2(M, \partial M) \cong H^1(M)$ , and its unit ball is a polyhedron.

If  $M$  can be fibered over  $S^1$ , the fibration defines a class  $a \in H^1(M)$ , which must lie in the interior of the cone over some top dimensional face  $F$ . In this case, we call  $F$  a *fibered face*. It is shown in [\[Thu86\]](#) that every primitive class  $a$  in the interior  $(\mathbb{R}^+ \cdot F)^\circ$  is realized uniquely (up to isotopy) by a fibration, hence we can consider the associated dilatation  $\lambda(a)$ . It is shown in [\[Fri82\]](#) that  $\lambda$  can be extended into a continuous function on  $(\mathbb{R}^+ \cdot F)^\circ$ . Moreover, it is shown in [\[McM00\]](#) that  $\frac{1}{\log \lambda}$  is strictly concave on  $F^\circ$ , which implies that  $\lambda$  is strictly convex on  $F^\circ$ .

We can normalize the function  $\lambda(a)$  by considering the function  $P(a) = \lambda(a)^{\|a\|}$  instead. Since  $\lambda(ta) = \lambda(a)^{\frac{1}{t}}$ ,  $P(a)$  is constant on rays. Together with the fact that  $P(a) = \lambda(a)$  on  $F^\circ$ , we see that the set of normalized dilatations of all the fibrations in  $(\mathbb{R}^+ \cdot F)^\circ$  form a dense subset among the values of  $P$  on  $F$ , and that  $P$  is strictly convex on  $F$ . We call the minimum value of  $P$  on  $F$  the *minimum normalized dilatation* of  $F$ .

Now, if  $b_1(M) = 1$ , then there are only two top dimensional faces, and one is the negative of the other. So if  $M$  fibers, then  $M$  fibers in a unique way, and the associated normalized dilatation is the unique, hence minimum normalized dilatation.

On the other hand, if  $b_1(M) \geq 2$ , then any fibered face has infinitely many points, hence if  $\lambda$  is the minimum normalized dilatation of  $F$ , then the set of normalized dilatations of all the fibrations in  $(\mathbb{R}^+ \cdot F)^\circ$  is a dense subset of  $[\lambda, \infty)$ .

**Remark 6.1.** In this latter case, the set of normalized dilatations of all the fibrations in  $(\mathbb{R}^+ \cdot F)^\circ$  contains the minimum  $\lambda$  if and only if  $\lambda$  is attained at a rational homology class. In [\[Sun15\]](#) it is shown that this might not be the case, and in fact the argument suggests that ‘generically’ this is not the case.

In [McM00], McMullen defines a polynomial invariant  $\Theta_F \in \mathbb{Z}H_1(M)$ , called the *Teichmüller polynomial*, associated to each fibered face  $F$ , such that when specialized to a rational class  $a \in F^\circ$ , the largest real root of  $\Theta_F^a$  is equal to the normalized dilatation  $P(a)$ .

**6.2. Isolated points.** We first classify the isolated points of  $\mathcal{D}$ , as well as the maps that attain such normalized dilatations. As pointed out in [Theorem 1.3](#), there are mapping tori with Betti number  $\geq 2$  and with minimum normalized dilatation given by  $\mu^4$ . Hence these isolated points must be strictly less than  $\mu^4 \approx 6.854$ .

Let  $f$  be a fully-punctured pseudo-Anosov map with normalized dilatation equal to one of these isolated points. The mapping torus  $T_f$  must have Betti number 1. By [Theorem 1.3](#), any fully-punctured pseudo-Anosov map  $f$  with normalized dilatation strictly less than  $\mu^4$  must have only one punctured orbit, that is, its mapping torus  $T_f$  has only one boundary component. By [Theorem 1.5](#),  $T_f$  has a layered veering triangulation with  $\leq 16$  tetrahedra.

The task now is to go through all the layered veering triangulation with  $\leq 16$  tetrahedra and with Betti number 1, of which there are 29698, and compute the normalized dilatations of the corresponding monodromies.

To do this we run the following code, included in the auxiliary file named `dilatation2.py`, in SageMath.

```
sage: dilatation2.dilatation_script_betti_one()
```

This outputs a list of the 29698 triangulations in the format

(number in census, isoSig, normalized dilatation, Euler characteristic of unique fiber)

This list is included as an auxiliary file named `betti_one_compile.txt`.

Since  $\mu^4 \approx 6.854$ , we look for entries of the output that have logarithm of normalized dilatation less than 6.86. There are 18 of these, namely:

```

cPcbbbdxm_10          cPcbbbiht_12          dLQbccchhsj_122
dLQaccjsnk_200        dLQbccchhfo_122        eLMkbcdddhhqqa_1220
eLMkbcdddhhhd_1221    eLMkbcdddhhml_1221    eLMkbcdddhxqlm_1200
eLMkbcdddhhqxh_1220   eLMkbcdddhxqdu_1200   eLPkbcdddhrvc_1200
eLPkaccddjnkaj_2002   eLPkbcdddhrvc_1200
fLLQcbeddeehhkh_21112 fLMPcbcdeehhkhkn_12211 fLMPcbcdeehhhvc_12211
gLmzQbcdeffhthhit_122112 gLmzQbcdeffhthhpe_122112

```

For each of these, we can then compute the exact normalized dilatation by calculating the Teichmüller polynomial as follows

```

sage: sig1='cPcbbbdxm_10'
sage: taut_polynomial.taut_polynomial_via_fox_calculus(sig1)
sage: sig2='cPcbbbiht_12'
sage: taut_polynomial.taut_polynomial_via_fox_calculus(sig2)
...

```

and computing the largest root.



5 of these triangulations have normalized dilatation  $\mu^4$  which is not an isolated point. The rest of them have normalized dilatation strictly less than  $\mu^4$ , hence do determine isolated points of  $\mathcal{D}$ . These 13 triangulations and their normalized dilatation are recorded in [Table 1](#).

The descriptions of the maps in [Table 1](#) follow by analyzing the structure of the veering triangulation and the topology of the underlying 3-manifold.

**6.3. The minimum accumulation point.** By [Theorem 1.3](#), to show that the minimum accumulation point of  $\mathcal{D}$  is  $\mu^4$ , one has to show that there are no fully-punctured pseudo-Anosov maps  $f$  with normalized dilatation strictly less than  $\mu^4$ , whose mapping torus  $T_f$  has only one boundary component but has Betti number  $\geq 2$ .

By [Theorem 1.5](#), such a mapping torus  $T_f$  would have a layered veering triangulation with  $\leq 16$  tetrahedra. So the task now is to go through all the layered veering triangulations with  $\leq 16$  tetrahedra and with one boundary component and Betti number  $\geq 2$ , of which there are 381, and compute the minimum normalized dilatations of the corresponding monodromies.

We wrote two scripts `dilatation_betti_two_fibred` and `dilatation_betti_two_fibred_eucl`, again included in the auxiliary file `dilatation2.py`, to carry out the computation for those triangulations with  $b_1 = 2$  (374 triangulations among the 381 fall into this class). The first script is in general faster but fails on a handful of triangulations; the second script is used for those triangulations. See [Appendix B](#) for an explanation of what it means for the first script to fail, and how the two scripts differ.

We first run

```
sage: dilatation2.dilatation_script_one_cusp_betti_two()
```

On the author's run of this line, the script failed on 8 triangulations:

```
pLLLPwLLMQQcegeehjmkonoomnnqhqxqvqcsqpqqsta_022210001222100
pLLvLAMPQAQbefgikjjimlnnooxxhvcqrfrhfjrmla_211120020212120
qLLLwzMAAQkacfighlmkmpopjkgllwlvbjkduajrc_2002121012100202
qLLLzLzLQwMQkbefgjlimkionnoppxmxxmwhdsephterr_1022101100112222
qLLvAALzQzQkbefghfilkmlnmpphxxagbqqokbjqagb_0111022020111020
qLLvLMvzQQQkdbdjgjminkloopmopdwbwbagpadbssrjos_210102222110001
qLLvMLzzAAQkbfegjkionmplnmpphhqqaqfxbawvbnha_0111022001111210
qLLvzzwPPQkcdkajnokljmpnnopphshepahphebgbvnn_1222011112220200
```

So we run

```
sage: sig1='pLLLPwLLMQQcegeehjmkonoomnnqhqxqvqcsqpqqsta_022210001222100'
sage: dilatation2.dilatation_betti_two_fibred_eucl(sig1)
sage: sig2='pLLvLAMPQAQbefgikjjimlnnooxxhvcqrfrhfjrmla_211120020212120'
sage: dilatation2.dilatation_betti_two_fibred_eucl(sig2)
...
```

We compile the result of these computations as a list in the format

(number in census, isoSig, min normalized dilatation, gcd of norms of spanning rays)

and include this list as an auxiliary file named `one_cusp_betti_two_compile.txt`.

The smallest value for the minimum normalized dilatation among these 374 triangulations is 17.9443. In particular all of them are strictly greater than  $\mu^4$ .

The remaining 7 triangulations out of the 381 have  $b_1 = 3$ . For these triangulations we did the computations entirely by hand. A fact that made these computations manageable was that the minimum normalized dilatation for all 7 triangulations are attained at the center of the fibered face.

Below we show the results of the computations. Similarly as above, each line records a triangulation as

(number in census, isoSig, min normalized dilatation, gcd of norms of spanning rays)

```
21390 ovLLLLPMQQceekjmlimnllnfssfjhhshhahhh_20110222222110 582.6871 3
21444 ovLLLLMPPPccdjfghlijnmnlmnnkqxnkavkaxhhcc_12020111111202 582.6871 3
42251 pvLLLLMPzPQQcdjfglhlinolmonnkqxnkavhaxhhccv_120201111112002 1124.3809 5
66862 qLLvLQwLQPMkbebigilnkmmnoppxxxgbrglheabnphwr_1022101010011222 1523.2123 5
80635 qLvVAMQvAQPkbhghhkjmnolmppopharrwarqqbbraxgh_2111220020111110 2867.8560 7
86454 qvLvVLPAAQQQkekjinlolnmpmpopongiwwvwaoflflfipmo_2100100211112211 1523.2123 5
86954 qvvLPAMzMQMkfhfghjlm lononmpppqh qxaxa qh h x h a _ 2100122222210102 1153.9991 4
```

Again, all of the minimum normalized dilatations are strictly greater than  $\mu^4$ .

As explained at the beginning of this subsection, this shows that  $\mu^4$  is the minimum accumulation point of  $\mathcal{D}$ .

We now classify the fully-punctured maps  $f$  that have normalized dilatation  $\mu^4$ . For such a map  $f$  whose mapping torus has only one boundary component, the computations in this and the last subsection show that the corresponding layered veering triangulation on the mapping torus must be one of the following 5 triangulations:

```
eLMkbcdddhxqdu_1200      eLMkbcdddhxqlm_1200
fLLQcbeddeehnkhh_21112
gLMzQbcdeffh h h h h i t _ 122112  gLMzQbcdeffh h h h h h p e _ 122112
```

The descriptions of the maps giving rise to these triangulations in [Table 2](#) follow by analyzing the structure of the veering triangulations.

For such a map  $f$  whose mapping torus has at least two boundary components, the statement of [Theorem 1.3](#) shows that  $f$  must be defined on a surface  $S$  with  $\chi(S) = -2$ . Now, there are only two such surfaces, namely the 4-punctured sphere  $S_{0,4}$  and the 2-punctured torus  $S_{1,2}$ .

For  $S_{0,4}$ , its mapping classes are well-understood. See, for example, the appendix of [\[Gué06\]](#). In particular, it is straightforward to check that the only pseudo-Anosov map with dilatation  $\mu^2$  is the one induced by  $\begin{bmatrix} 2 & 1 \\ 1 & 1 \end{bmatrix}$  as recorded in [Table 2](#).

For  $S_{1,2}$ , we can fill in one of the punctures to get a map on the once-punctured torus  $S_{1,1}$  with dilatation  $\mu^2$  as well. The mapping classes on  $S_{1,1}$  are well understood. See for example, [\[Gué06\]](#). In particular, it is straightforward to check that the only pseudo-Anosov

maps with dilatation  $\mu^2$  are the ones induced by  $\begin{bmatrix} 2 & 1 \\ 1 & 1 \end{bmatrix}$  and  $\begin{bmatrix} -2 & -1 \\ -1 & -1 \end{bmatrix}$ . (Alternatively, one can appeal to the results in the last subsection.) The filled-in puncture is some fixed point of this map on  $S_{1,1}$ . But one can check that the map induced by  $\begin{bmatrix} 2 & 1 \\ 1 & 1 \end{bmatrix}$  has no fixed points, so the map  $f$  must be that induced by  $\begin{bmatrix} -2 & -1 \\ -1 & -1 \end{bmatrix}$  as recorded in [Table 2](#).

The veering triangulations associated to these two maps can be recovered from the descriptions of  $S_{0,4}$ - and  $S_{1,1}$ -bundles in [\[Gué06\]](#). These are as recorded in [Table 2](#).

### 7. DISCUSSION AND FURTHER QUESTIONS

We first discuss some questions one can still ask about the set  $\mathcal{D}$ .

One can interpret the minimum accumulation point of  $\mathcal{D}$  as the minimum element of

$$\mathcal{D}_2 := \{\text{Normalized dilatations of fully-punctured maps } f \text{ with } b_1(T_f) \geq 2\}$$

where we write  $T_f$  for the mapping torus of  $f$ . Motivated by this, one can define

$$\mathcal{D}_k := \{\text{Normalized dilatations of fully-punctured maps } f \text{ with } b_1(T_f) \geq k\}$$

and ask

**Question 7.1.** What is the minimum element of  $\mathcal{D}_k$  for  $k \geq 3$ ? What are the maps that attain these normalized dilatations?

One should compare [Question 7.1](#) with [\[HT22, Question 8.3\]](#), which asks for the minimum normalized dilatations among fully-punctured maps  $f$  whose mapping torus has at least  $k$  boundary components.

Notice that these questions, at least in part, can be solved via the same approach of using veering triangulations, provided that one can improve [Theorem 1.4](#) or improve the technology in generating census of veering triangulations.

Next, we discuss the relevance of our work to the golden ratio conjecture, which we state again below in a slightly different form.

**Conjecture 7.2** ([\[Hir10, Question 1.12\]](#)). *The minimum dilatations  $\delta_{g,0}$  on the closed surfaces of genus  $g$  grow as*

$$\lim_{g \rightarrow \infty} \delta_{g,0}^{2g-2} = \mu^4.$$

One approach for proving [Conjecture 7.2](#) is to show that one can choose pseudo-Anosov maps realizing the minimum dilatations  $\delta_{g,0}$  that have a uniformly bounded number of singularities. If this is true, then [Conjecture 7.2](#) would follow from [Theorem 1.6](#) and the examples exhibited in [\[Hir10\]](#).

We remark that the examples in [Hir10] (and also those in [AD10] and [KT13]) do have a uniformly bounded number of singularities, giving some evidence that this approach is feasible.

Of course, one can consider using the approach of veering triangulations again. However, this approach generally becomes much weaker in the closed case. The reason is that veering triangulations can only exist on fully-punctured mapping tori, and so one has to fully puncture the pseudo-Anosov map before applying the notion. Without good knowledge of the number and types of singularities, one can in general only bound the Euler characteristic of the punctured surface by 3 times the Euler characteristic of the original closed surface, making the exponent on the bounds 3 times as worse thus computationally infeasible, as seen in [Corollary 3.19](#).

Finally, we discuss and speculate some possible sources of improvement to [Theorem 3.18](#) and [Theorem 5.16](#).

As remarked at the start of [Section 4](#), [Proposition 4.3](#) provides a bound better than [Proposition 3.3](#) by a factor of 2. Even though we are unable to show so, we suspect that [Proposition 4.3](#) can always be applied.

**Conjecture 7.3.** *For any veering triangulation on a mapping torus, there exists a fiber surface such that the hypothesis of [Proposition 4.3](#) is satisfied for some minimum weight sector.*

Another approach to improving the bound would be to find a way to bypass the cases when we have a minimum weight sector that is not deep. As seen in [Section 3.3](#) and [Section 5.5](#), when one can assume that all minimum weight sectors are deep, one can use the flexibility granted by [Proposition 3.13](#) to strongly constrain the triangulation.

That is, a positive answer to the following question would likely lead to sharper bounds.

**Question 7.4.** Let  $\Delta$  be a veering triangulation on a mapping torus. Is it true that for every sector  $s$ , there is a fiber surface such that  $s$  is a minimum weight sector?

It is useful to consider the particular case of veering triangulations on once-punctured torus bundles. As mentioned in the proof of [Proposition 3.16](#), these are very neatly described in [Gué06]. In these veering triangulations, the normalized dilatation grows at worst linearly in the number of tetrahedra.

Moreover, in this case, the normalized dilatation seems to behave differently with respect to the number of fan and toggle tetrahedra. Intuitively, it grows linearly with respect to the former and grows as an exponential function of the latter. This leads one to suspect that perhaps one can obtain bounds that treat the number of fan and toggle tetrahedra separately. These would be of a different nature than [Theorem 3.18](#), but we think they would be significantly sharper for applications.

Of course, it is interesting to know the best possible bound one can hope for at all.

**Question 7.5.** What is the smallest exponent  $\alpha$  such that the number of tetrahedra at worse grows as the  $\alpha^{\text{th}}$  power of the normalized dilatation, across all layered veering triangulations?

The triangulations on once-punctured torus bundles show that the smallest exponent is at least 1 and [Theorem 3.18](#) shows that it is at most 2.

#### APPENDIX A. CALCULUS EXERCISES

*Proof of Claim 5.8.* By symmetry, the minimum is attained when  $a_1 = a_2$ , so we have to calculate the minimum of  $2N - 4 + 2a + 2\lambda^{-x} \max\{\frac{2}{a}, 1\}$ .

Let

$$h(a) = 2N - 4 + 2a + \frac{4\lambda^{-x}}{a}.$$

Then

$$h'(a) = 2 - \frac{4\lambda^{-x}}{a^2} > 0 \Leftrightarrow a > \sqrt{2\lambda^{-x}}.$$

If  $\lambda^{-x} \geq 2$ , then  $\sqrt{2\lambda^{-x}} \geq 2$ , which is when the second term in the maximum takes over. So the minimum of the whole expression is  $2N + 2\lambda^{-x}$ .  $\square$

*Proof of Claim 5.11.* By symmetry, the minimum is attained when  $a_1 = a_2$ , so we have to calculate the minimum of  $2N - 4 + 2a + \lambda^{-x}(\min\{\frac{a}{2}, 1\}^{-1} + \min\{\frac{a}{2}, 1\})$ .

Let

$$\begin{aligned} h(a) &= 2N - 4 + 2a + \lambda^{-x}\left(\frac{2}{a} + \frac{a}{2}\right) \\ &= 2N - 4 + \left(2 + \frac{\lambda^{-x}}{2}\right)a + \frac{2\lambda^{-x}}{a}. \end{aligned}$$

Then

$$h'(a) = 2 + \frac{\lambda^{-x}}{2} - \frac{2\lambda^{-x}}{a^2} > 0 \Leftrightarrow a > \sqrt{\frac{4\lambda^{-x}}{\lambda^{-x} + 4}}.$$

Now  $\sqrt{\frac{4\lambda^{-x}}{\lambda^{-x} + 4}}$  is always less than 2, which is where the first term in the minimum in  $b$  takes over. So the minimum of the whole expression is  $2N - 4 + 2\sqrt{\lambda^{-2x} + 4\lambda^{-x}}$ .  $\square$

*Proof of Claim 5.14.* We perform a variable change  $t = \lambda^p, u = \sqrt{\frac{a}{3t}}$ , so that

$$a + \lambda^{-p}\frac{2}{a} = 3u^2t + \frac{2}{3}u^{-2}t^{-2}.$$

Letting  $h(u, t)$  be this last expression, we compute

$$\frac{\partial h}{\partial t} = 3u^2 - \frac{4}{3}u^{-2}t^{-3} > 0 \Leftrightarrow t > \left(\frac{2}{3}\right)^{\frac{2}{3}}u^{-\frac{4}{3}}.$$

Hence

$$\begin{aligned}
h(u, t) &\geq h(u, (\frac{2}{3})^{\frac{2}{3}} u^{-\frac{4}{3}}) \\
&= 3(\frac{3}{2})^{\frac{1}{3}} u^{\frac{2}{3}} \\
&= 3(\frac{3}{2})^{\frac{1}{3}} (\lambda^{-\frac{p}{2}} \sqrt{\frac{a}{3}})^{\frac{2}{3}}.
\end{aligned}$$

□

*Proof of Claim 5.15.* Let

$$h(t, a) = \lambda^{-x} (t^{-1} \sqrt{\frac{a}{a+1}} + t \sqrt{\frac{a+1}{a}}) + a + t^{-2} \frac{2}{a}$$

where  $t \geq 1$ . Then

$$\begin{aligned}
\frac{\partial h}{\partial t} &= \lambda^{-x} (-t^{-2} \sqrt{\frac{a}{a+1}} + \sqrt{\frac{a+1}{a}}) - 4t^{-3} a^{-1} \\
&\geq \lambda^{-x} (-\sqrt{\frac{a}{a+1}} + \sqrt{\frac{a+1}{a}}) - 4a^{-1} \\
&= \lambda^{-x} \sqrt{\frac{a}{a+1}} (-1 + \frac{a+1}{a}) - 4a^{-1} \\
&= (\lambda^{-x} \sqrt{\frac{a}{a+1}} - 4) a^{-1} \geq 0
\end{aligned}$$

for  $a \geq 1$  if  $\lambda^{-x} \geq 4\sqrt{2}$ .

Hence

$$\begin{aligned}
&\lambda^{-x} (\lambda^{-\frac{p}{2}} \sqrt{\frac{a}{a+1}} + (\lambda^{-\frac{p}{2}} \sqrt{\frac{a}{a+1}})^{-1}) + a + \lambda^{-p} \frac{2}{a} \\
&= h(\lambda^{\frac{p}{2}}, a) \\
&\geq h(1, a) \\
&= \lambda^{-x} (\sqrt{\frac{a}{a+1}} + \sqrt{\frac{a+1}{a}}) + a + \frac{2}{a}
\end{aligned}$$

□

*Proof of Theorem 1.5.* Let  $\Delta$  be the veering triangulation on the mapping torus of  $f$ . If  $\lambda^{-x} \leq 4\sqrt{2}$ , then by [Theorem 1.4](#),  $\Delta$  has less than or equal to  $\frac{1}{2}(4\sqrt{2})^2 = 16$  tetrahedra.

If  $\lambda^{-x} \geq 4\sqrt{2}$ , we can apply [Theorem 5.16](#) to  $\Delta$ . Our task is to show that each of the bounds in [Theorem 5.16](#) is strictly less than 17 when we substitute a value of  $\lambda^{-x}$  between  $4\sqrt{2}$  and 6.86.

We first claim that each of the bounds in [Theorem 5.16](#) that are not  $F_i(\lambda^{-x})$  is an increasing function in  $\lambda^{-x}$  for  $\lambda^{-x} \geq 4\sqrt{2}$ . This would imply that we only have to check that the bounds are strictly less 17 when  $\lambda^{-x} = 6.86$ .

The claim is clear for  $\frac{1}{3}\lambda^{-2x} + \frac{1}{2}$ ,  $\frac{1}{2}\lambda^{-2x} - \lambda^{-x}$ , and  $8 \log_3 \lambda^{-x}$ .

Let

$$h_1(x) = x^2 - x^{\frac{4}{3}} - x^{\frac{2}{3}} + 3.$$

Then

$$\begin{aligned} h_1'(x) &= 2x - \frac{4}{3}x^{\frac{1}{3}} - \frac{2}{3}x^{-\frac{1}{3}} \\ &\geq 2x - \frac{4}{3}x - \frac{2}{3}x = 0 \end{aligned}$$

for  $x \geq 1$ . This shows that  $\frac{1}{2}(\lambda^{-2x} - \lambda^{-\frac{4}{3}x} - \lambda^{-\frac{2}{3}x} + 3)$  is an increasing function in  $\lambda^{-x}$ .

Let

$$h_2(x) = \frac{1}{2}x^2 - \sqrt{x^2 + 4x} + 2.$$

Then

$$h_2'(x) = x - \frac{x+2}{\sqrt{x^2+4x}} \geq 0 \Leftrightarrow x^2(x^2+4x) \geq x^2+4x+4$$

which is evidently true for  $x \geq 2$ . This shows that  $\frac{1}{2}\lambda^{-2x} - \sqrt{\lambda^{-2x} + 4\lambda^{-x}} + 2$  is an increasing function in  $\lambda^{-x}$ .

Now substituting in  $\lambda^{-x} = 6.86$ , we have

$$\begin{aligned} \frac{1}{3}6.86^2 + \frac{1}{2} &\approx 16.187 \\ \frac{1}{2}6.86^2 - 6.86 &\approx 16.670 \\ \frac{1}{2}(6.86^2 - 6.86^{\frac{4}{3}} - 6.86^{\frac{2}{3}} + 3) &\approx 16.707 \\ \frac{1}{2}6.86^2 - \sqrt{6.86^2 + 4 \times 6.86} + 2 &\approx 16.898 \\ 8 \log_3 6.86 &\approx 14.023 \end{aligned}$$

each of which is strictly less than 17.

We now move on to  $F_1(\lambda^{-x})$  and  $F_2(\lambda^{-x})$ . The strategy is the same: We first show that these are increasing functions then evaluate them at  $\lambda^{-x} = 6.86$ .

We show that  $F_1(\lambda^{-x})$  is an increasing function for  $\lambda^{-x} \geq 4\sqrt{2}$ . Recall that  $F_1(x)$  is the maximum of

$$f_1(x, u) = \frac{1}{2}x^2 - \frac{1}{2}x(u + u^{-1}) - \left(\frac{3}{2}\right)^{\frac{4}{3}}u^{\frac{2}{3}} + 2 - \frac{1}{2x}$$

over  $0 < u \leq 1$ . We compute

$$\frac{\partial f_1}{\partial u} = -\frac{1}{2}x(1 - u^{-2}) - \left(\frac{3}{2}\right)^{\frac{1}{3}}u^{-\frac{4}{3}}.$$

Note that  $\frac{\partial f_1}{\partial u} \geq -\frac{1}{2}x + \left(\frac{1}{2}x - \left(\frac{3}{2}\right)^{\frac{1}{3}}\right)u^{-2} \geq \frac{3}{2}x - 4\left(\frac{3}{2}\right)^{\frac{1}{3}} > 0$  for  $u \leq \frac{1}{2}$ , and  $\frac{\partial f_1}{\partial u}$  is negative for  $u$  close to 1, so the maximum is attained in the interior of  $[\frac{1}{2}, 1]$ . If we let  $u(x)$  be the point where this maximum is attained for fixed  $x$ , then

$$\begin{aligned} \frac{df_1(x, u(x))}{dx} &= \frac{\partial f_1}{\partial x} + \frac{\partial f_1}{\partial u}u'(x) = \frac{\partial f_1}{\partial x} \\ &= x - \frac{1}{2}(u + u^{-1}) + \frac{1}{2x^2} \\ &\geq x - \frac{5}{4} + \frac{1}{2x^2} > 0 \end{aligned}$$

for  $x \geq 4\sqrt{2}$ . This shows that  $F_1(\lambda^{-x})$  is an increasing function for  $\lambda^{-x} \geq 4\sqrt{2}$ .

Using a computer algebra system, we check that  $F_1(6.86) \approx 16.966$ , which is strictly less than 17.

Similarly, we show that  $F_2(\lambda^{-x})$  is an increasing function for  $\lambda^{-x} \geq 4\sqrt{2}$ . Recall that  $F_2(x)$  is the maximum of

$$f_2(x, a) = \frac{1}{2}x^2 - \frac{1}{2}x\left(\sqrt{\frac{a}{a+1}} + \sqrt{\frac{a+1}{a}}\right) - \frac{1}{2}a - a^{-1} + 2 - \frac{1}{2x}$$

over  $a \geq 1$ . We compute

$$\frac{\partial f_2}{\partial a} = -\frac{1}{2}x\left(\frac{1}{2a^{\frac{1}{2}}(a+1)^{\frac{3}{2}}} - \frac{1}{2a^{\frac{3}{2}}(a+1)^{\frac{1}{2}}}\right) - \frac{1}{2} + a^{-2} \rightarrow \frac{1}{8\sqrt{2}}x + \frac{1}{2} \geq 0$$

as  $a \rightarrow 1^+$ , so the maximum is attained in the interior of  $(1, \infty)$ .

If we let  $a(x)$  be the point where this maximum is attained for fixed  $x$ , then

$$\begin{aligned} \frac{df_2(x, a(x))}{dx} &= \frac{\partial f_2}{\partial x} + \frac{\partial f_2}{\partial a}a'(x) = \frac{\partial f_2}{\partial x} \\ &= x - \frac{1}{2}\left(\sqrt{\frac{a}{a+1}} + \sqrt{\frac{a+1}{a}}\right) + \frac{1}{2x^2} \\ &\geq x - \frac{3}{2\sqrt{2}} + \frac{1}{2x^2} > 0 \end{aligned}$$

for  $x \geq 4\sqrt{2}$ . This shows that  $F_2(\lambda^{-x})$  is an increasing function for  $\lambda^{-x} \geq 4\sqrt{2}$ .

Using a computer algebra system, we check that  $F_2(6.86) \approx 16.975$ , which is strictly less than 17.  $\square$



APPENDIX B. EXPLANATION OF CODE USED FOR COMPUTATION

The scripts we use are included in `dilatation2.py` in the auxiliary files. Among these, the three main ones are `dilatation_betti_one_fibred`, `dilatation_betti_two_fibred`, and `dilatation_betti_two_fibred_eucl`.

`dilatation_betti_one_fibred` takes in a layered veering triangulation with  $b_1 = 1$  and outputs the associated normalized dilatation. The workings of this script are as follows:

- It computes the Alexander polynomial and the taut polynomial of the triangulation using Fox calculus. See [Par21, Proposition 5.7].
- It computes the Euler characteristic of the fiber surface as the span of the Alexander polynomial minus 1.
- It computes the dilatation of the monodromy as the largest root of the taut polynomial using the SageMath function `real_roots`. This uses the fact the taut polynomial equals the Teichmuller polynomial, see [LMT20, Theorem 7.1].

`dilatation_betti_two_fibred` takes in a layered veering triangulation with  $b_1 = 2$  and outputs the minimum normalized dilatation. The workings of this script are as follows:

- It computes the Alexander polynomial and the taut polynomial of the triangulation (as above).
- It computes two spanning vectors of the fibered cone.
- It computes the Euler characteristic of the surface corresponding to each spanning ray, using the fact that the Thurston norm equals the Alexander norm in a fibered cone, see [McM00, Theorem 7.1]. Using this information, it parametrizes the fibered face  $F$  by one parameter  $t$ .
- It removes some cyclotomic factors from the taut polynomial  $\Theta$  for simpler computations, and computes its derivative  $\frac{\partial \Theta}{\partial t}$  along  $F$ .
- It checks whether  $\frac{\partial \Theta}{\partial t} = 0$  at the midpoint of  $F$ .

If yes, then the minimum normalized dilatation occurs at the midpoint of  $F$ , so the script does the following:

- It computes the single-variable polynomial obtained by restricting the taut polynomial to the mid-ray of the fibered cone.
- It computes the minimum normalized dilatation as the largest root of this polynomial using the SageMath function `real_roots`.

Otherwise the script attempts to solve the system  $\begin{cases} \Theta = 0 \\ \frac{\partial \Theta}{\partial t} = 0 \end{cases}$  as follows:

- It performs variable changes such that  $\Theta$  and  $\frac{\partial \Theta}{\partial t}$  are polynomials with relatively prime exponents.

– It uses the SageMath function `solve` to solve the simplified system.

As mentioned in [Section 6.3](#), `dilatation_betti_two_fibred` works for most triangulations. The main problem with it, however, is that the SageMath function `solve` is not guaranteed to succeed; it might only simplify the system symbolically or might get stuck and show no sign of terminating.

On the author’s run of the script, this happens for the 8 triangulations mentioned in [Section 6.3](#). We remark that on a more powerful system, the script may terminate and succeed for some, if not all, of these triangulations.

For us to deal with these triangulations, we need a more robust way of solving the equation  $\begin{cases} \Theta = 0 \\ \frac{\partial \Theta}{\partial t} = 0 \end{cases}$ . For this we use the following simple algebraic fact.

**Lemma B.1.** *Suppose  $a, b \in \mathbb{R}[x, y], p, q \in \mathbb{R}[x]$ . Then any root of the system  $\begin{cases} a(x, y) = 0 \\ b(x, y) = 0 \end{cases}$*

*is a root of the system  $\begin{cases} a(x, y) = 0 \\ p(x)a(x, y) - q(x)b(x, y) = 0 \end{cases}$*

In the setting of the lemma, we can consider  $a$  and  $b$  as polynomials of  $y$  with coefficients in  $\mathbb{R}[x]$ . By taking  $p$  to be the leading coefficient of  $b$  and  $q$  to be the leading coefficient of  $a$ ,  $p(x)a(x, y) - q(x)b(x, y)$  will have a smaller  $y$ -degree and in passing from  $\begin{cases} a(x, y) = 0 \\ b(x, y) = 0 \end{cases}$

to  $\begin{cases} a(x, y) = 0 \\ p(x)a(x, y) - q(x)b(x, y) = 0 \end{cases}$  we have reduced the complexity of the system in terms

of its total  $y$ -degree. Repeating this procedure inductively, we eventually arrive at a system where one equation is only a polynomial in  $x$ . We can then compute the roots of this polynomial, substitute these back in the polynomial containing  $y$ , and compute the corresponding values for  $y$ . This process will of course produce many extraneous solutions, but we can substitute these into the original system to verify whether they are true solutions. We wrote the script `eucl_eq_solver` to exactly implement this process.

The script `dilatation_betti_two_fibred_eucl` differs from `dilatation_betti_two_fibred` by replacing `solve` by `eucl_eq_solver`. `dilatation_betti_two_fibred_eucl` works for the 8 triangulations that `dilatation_betti_two_fibred` fails on.

In general, `eucl_eq_solver` is very slow because of its iterative nature. Hence we have chosen to tackle most of the cases using the faster `dilatation_betti_two_fibred`.

## REFERENCES

- [Abi80] William Abikoff. *The real analytic theory of Teichmüller space*, volume 820 of *Lecture Notes in Mathematics*. Springer, Berlin, 1980.
- [AD10] John W. Aaber and Nathan Dunfield. Closed surface bundles of least volume. *Algebr. Geom. Topol.*, 10(4):2315–2342, 2010.

- [Ago11] Ian Agol. Ideal triangulations of pseudo-Anosov mapping tori. In *Topology and geometry in dimension three*, volume 560 of *Contemp. Math.*, pages 1–17. Amer. Math. Soc., Providence, RI, 2011.
- [AT22] Ian Agol and Chi Cheuk Tsang. Dynamics of veering triangulations: infinitesimal components of their flow graphs and applications, 2022.
- [BS09] Francis Bonahon and Larry Siebenmann. New geometric splittings of classical knots, and the classification and symmetries of arborescent knots. *Preprint*, 2009.
- [FG13] David Futer and François Guéritaud. Explicit angle structures for veering triangulations. *Algebr. Geom. Topol.*, 13(1):205–235, 2013.
- [FLM11] Benson Farb, Christopher J. Leininger, and Dan Margalit. Small dilatation pseudo-Anosov homeomorphisms and 3-manifolds. *Adv. Math.*, 228(3):1466–1502, 2011.
- [Fri82] David Fried. The geometry of cross sections to flows. *Topology*, 21(4):353–371, 1982.
- [Fri85] David Fried. Growth rate of surface homeomorphisms and flow equivalence. *Ergodic Theory Dynam. Systems*, 5(4):539–563, 1985.
- [GSS] Andreas Giannopolous, Saul Schleimer, and Henry Segerman. A census of veering structures. <https://math.okstate.edu/people/segerman/veering.html>.
- [Gué06] François Guéritaud. On canonical triangulations of once-punctured torus bundles and two-bridge link complements. *Geom. Topol.*, 10:1239–1284, 2006. With an appendix by David Futer.
- [Gué16] François Guéritaud. Veering triangulations and Cannon-Thurston maps. *J. Topol.*, 9(3):957–983, 2016.
- [Hir10] Eriko Hironaka. Small dilatation mapping classes coming from the simplest hyperbolic braid. *Algebr. Geom. Topol.*, 10(4):2041–2060, 2010.
- [HS07] Ji-Young Ham and Won Taek Song. The minimum dilatation of pseudo-Anosov 5-braids. *Experiment. Math.*, 16(2):167–179, 2007.
- [HT22] Eriko Hironaka and Chi Cheuk Tsang. Standardly embedded train tracks and pseudo-anosov maps with minimum expansion factor, 2022.
- [KKT13] Eiko Kin, Sadayoshi Kojima, and Mitsuhiro Takasawa. Minimal dilatations of pseudo-Anosovs generated by the magic 3-manifold and their asymptotic behavior. *Algebr. Geom. Topol.*, 13(6):3537–3602, 2013.
- [KT13] Eiko Kin and Mitsuhiro Takasawa. Pseudo-Anosovs on closed surfaces having small entropy and the Whitehead sister link exterior. *J. Math. Soc. Japan*, 65(2):411–446, 2013.
- [Lan23] Michael Landry. Stable loops and almost transverse surfaces. *Groups Geom. Dyn.*, 17(1):35–75, 2023.
- [LMT20] Michael Landry, Yair N. Minsky, and Samuel J. Taylor. A polynomial invariant for veering triangulations, 2020.
- [LMT21] Michael P. Landry, Yair N. Minsky, and Samuel J. Taylor. Flows, growth rates, and the veering polynomial, 2021.
- [LT11a] Erwan Lanneau and Jean-Luc Thiffeault. On the minimum dilatation of braids on punctured discs. *Geom. Dedicata*, 152:165–182, 2011. Supplementary material available online.
- [LT11b] Erwan Lanneau and Jean-Luc Thiffeault. On the minimum dilatation of pseudo-Anosov homeomorphisms on surfaces of small genus. *Ann. Inst. Fourier (Grenoble)*, 61(1):105–144, 2011.
- [LT23] Michael P. Landry and Chi Cheuk Tsang. Endperiodic maps, splitting sequences, and branched surfaces, 2023.
- [McM00] Curtis T. McMullen. Polynomial invariants for fibered 3-manifolds and Teichmüller geodesics for foliations. *Ann. Sci. École Norm. Sup. (4)*, 33(4):519–560, 2000.
- [McM15] Curtis T. McMullen. Entropy and the clique polynomial. *J. Topol.*, 8(1):184–212, 2015.
- [Par21] Anna Parlak. Computation of the taut, the veering and the teichmüller polynomials. *Experimental Mathematics*, 0(0):1–26, 2021.
- [Pen91] R. C. Penner. Bounds on least dilatations. *Proc. Amer. Math. Soc.*, 113(2):443–450, 1991.
- [PSS23] Anna Parlak, Saul Schleimer, and Henry Segerman. Veering, code for studying taut and veering ideal triangulations. <https://github.com/henryseg/Veering>, 2023.

- [SS19] Saul Schleimer and Henry Segerman. From veering triangulations to link spaces and back again, 2019.
- [Sun15] Hongbin Sun. A transcendental invariant of pseudo-Anosov maps. *J. Topol.*, 8(3):711–743, 2015.
- [Thu86] William P. Thurston. A norm for the homology of 3-manifolds. *Mem. Amer. Math. Soc.*, 59(339):i–vi and 99–130, 1986.

UNIVERSITY OF CALIFORNIA, BERKELEY, 970 EVANS HALL #3840, BERKELEY, CA 94720-3840

*Email address:* `chicheuk@math.berkeley.edu`